MODEL FITTING AND METHODS OF RESPONSE DATA ANALYSIS FOR LIQUID MIXING ON DISTILLATION TRAYS

by

YIE-SHON WU

B.S., NATIONAL TAIWAN UNIVERSITY, TAIWAN, CHINA, 1963

A MASTER'S THESIS

submitted in partial fulfillment of the

requirements for the degree

MASTER OF SCIENCE

DEPARTMENT OF CHEMICAL ENGINEERING

KANSAS STATE UNIVERSITY

Manhattan, Kansas

1968

Approved by

Liang-Tang Fan

Major Professor

TABLE OF CONTENTS

CHAPTER 1

INTRODUCTION

A chemical reaction is always coupled with physical phenomena in a chemical process. Coupling of the transport phenomena and chemical reactions makes the chemical process very complex to analyze and design. Recently, considerable success has been achieved in systematizing the process analysis as shown in Fig. 1-1 (1,2).

The fundamental physical variables such as flow rate, temperature, pressure, liquid level, weir height, free area, recycle ratio, etc., which are directly measurable and thus can be expressed in explicit form, are treated as the first level variables. In the classical method of process analysis, these first level variables and chemical kinetics are jointly analyzed, and an experimental study is carried out to verify the results of the analysis. Actually, a process design based on such an analysis is often very tedious, because the analysis provides incomplete information. The knowledge of macromixing (1,2,3), i.e. the residence time distribution function which indicates the length of stay of various fractions of the fluid in the vessel, should also be a major item to be determined in the process analysis (specifically the analysis of flow pattern). This macromixing information is, of course, implicitly a function of the first level variables and is treated as the second level variable. Recently, a tracer method has generally been used to obtain the macromixing information. Today, owing to the availability of modern high speed computers, either on-line or off-line analysis of a process is feasible (4). For the process with

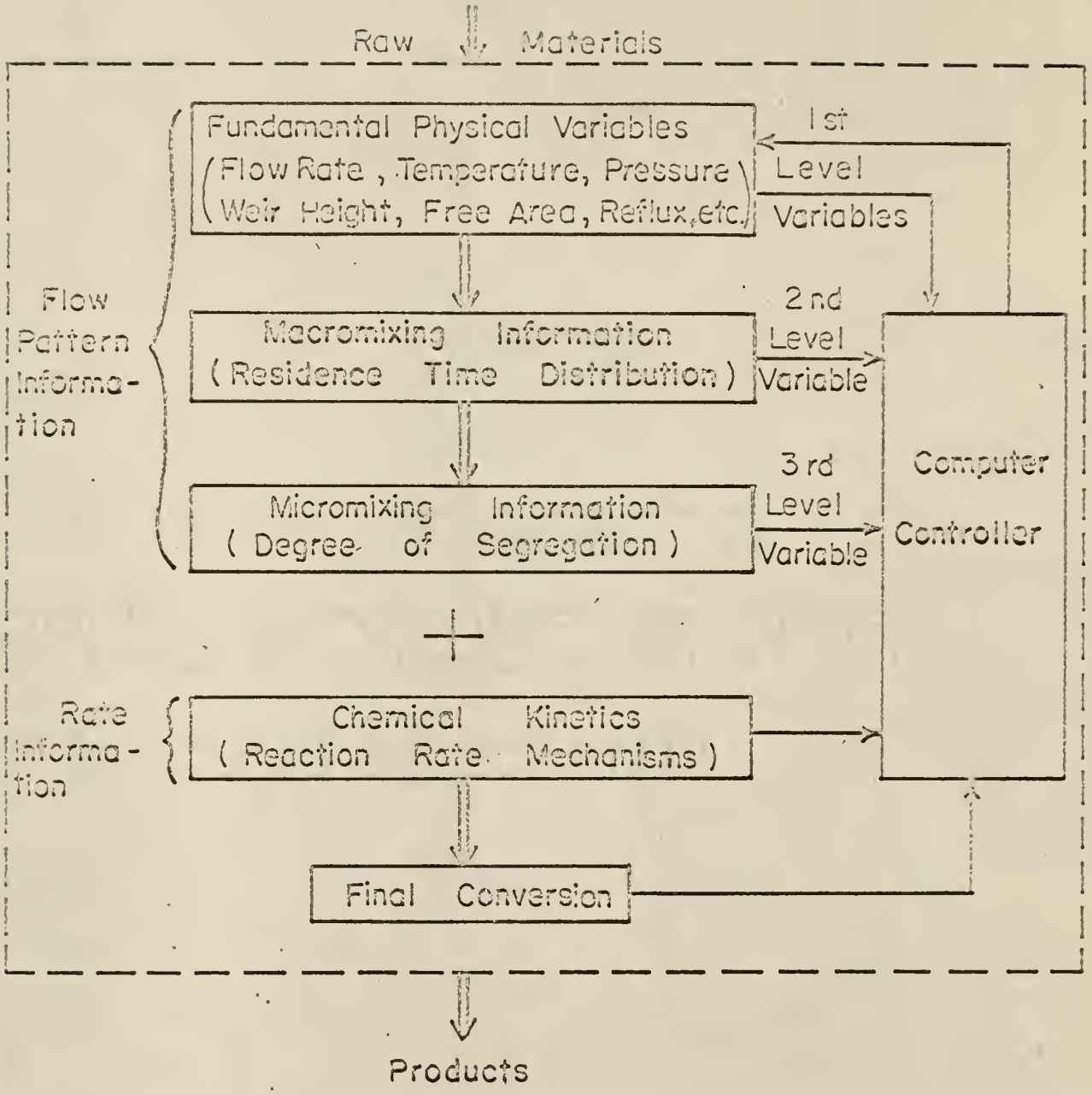

Fig. 1-1. General schematic diagram for chemical process analysis and feed-forward control

first-order or decay type of kinetics, the equipment performance can be predicted solely from the response to tracer excitation (macromixing information) and known kinetics. For all other cases, further detail about the fluid mixing is required. Additional information concerning the point to point action of the fluid is the knowledge of micromixing (1,2,3), and as may be expected, it requires much more effort to measure than the macromixing. It is treated as the third level variable. Though the experimental measurement of micromixing is very difficult as compared to the measurement of macromixing, it can be shown how bounds can be put on the micromixing (2,3), which are the two extremes of complete segregation and maximum mixedness, without knowing exact details. These bounds are often narrow enough so that prediction and design methods based on the macromixing information prove to be practical. The micromixing is only important for processes accompanying high order, nonlinear reactions.

In other words, the flow pattern and the kinetics are the essential information required to predict the performance of process equipment. The step by step information analysis of the process variables and the correlation among them give rise to the so-called performance equations which are required in the design and optimization of the system.

The research described herein is concerned with the first and second level variables. The investigation emphasizes analysis of the dynamic characteristics of a system in which fluid mixing takes place. The general approach is as follows:

1. Select the system to be studied.
2. Select the tracer to be used.

3. Carry out the experimental work.

4. Select a physical model or mathematical model (or models) to describe the flow pattern of the system.

5. Use a suitable method to analyze the response data.

Since the design of a distillation column is very important in many industries, the understanding of fluid mixing on distillation trays is essential. An extensive experimental system was carried out by Johnson (5) to study the characteristics of liquid mixing on distillation trays. This work emphasizes the selection of methods in analyzing experimental data for the purpose of fitting a model to the data.

Chapter 2 is devoted to describing the general pulse testing method, which has been proved to be practical in determining the dynamic behavior of a system. Various questions such as selection of a tracer, the pulse height and width, and the detection and recording systems will also be discussed. The notion of age distribution will be briefly discussed and methods for the response data reduction in formulating the transfer function of the experimental system will also be examined.

Chapter 3 is concerned with the general notion of model selection and the description of the gamma distribution model (6). The gamma distribution model with bypassing will be fitted to the experimental data. The characteristics of this model will be revealed by using several types of response curves.

Chapter 4 presents three methods of response data analysis. Each method is followed by an example in which the model described in Chapter 3 is used.

Chapter 5 contains the results obtained by applying the schemes

of response data analysis to the liquid mixing system on distillation trays. The results verify the reliability of the experimental work and the proper model selection. It is indicated that the required computing time and the goodness of the quantitative results are major factors which must be considered in selecting a method for analyzing response data.

In summary, this research is concerned with the development of what appears to be a rapid, reliable, simple procedure for procuring knowledge of a flow pattern for liquid mixing on distillation trays. The model selected here and the analysis method used can be applied to other systems.

CHAPTER 2

PULSE TESTING METHOD

In detecting the dynamic characteristics of a system, the general approach is to purposely excite the system (introduce a forcing disturbance) and to observe and analyze its response. One of the common methods of exciting a system is the use of the sinusoidal forcing method. The steady state response to the sinusoidal forcing is termed the frequency response of the system. This method has many disadvantages. First, the test must be sustained long enough to reach a steady state. It is thus time consuming. Second, the oscillations may induce unstable operation and off-specification products when the method is directly applied to a process plant. Third, it may be difficult to build and operate the apparatus required to induce the desired sinusoidal disturbance. It is thus clear that this direct method has serious limitations as a means of obtaining dynamic data for many of the systems in a plant operation or a laboratory study (7). The impulse response and the step response methods have also been used widely (1,24,25).

Recently, the pulse testing method has been devised, which makes it possible to obtain the needed information about the dynamic characteristics of a system. This method employs a single pulse to excite the system with all frequencies at once. By employing appropriate computational techniques, the frequency response information can be extracted from the resulting response (7).

In studying mixing of fluid in a flow system, a tracer is injected

into the system in a pulse-manner. The response also appears as a pulse. Both the input and output signals can be subjected to various methods of analysis. The mixing characteristics of the system can be extracted from the response data, which in turn can be used in constructing a model of the system. It appears that the pulse test is a practical method.

Pulse testing (3). Now consider that a certain amount of tracer M is injected into a system containing fluid volume V, through which a fluid flows at a steady rate of Q. Let $C_i(t)$ be the concentration in the influent stream and $C_e(t)$ be the concentration in the effluent stream. If there is no dead space in the system, the tracer injected will sooner or later come out in the exit stream. Thus a material balance gives

$$\int_0^\infty C_i(t)Qdt = M = \int_0^\infty C_e(t)Qdt \quad . \tag{2-1}$$

Dividing this by Q yields

$$\int_0^\infty C_i(t)dt = \frac{M}{Q} = \int_0^\infty C_e(t)dt \quad . \tag{2-2}$$

We can see that if $C_i(t)$ and $C_e(t)$ are plotted against t, the areas underneath both curves are the same. This, of course, follows the law of conservation of mass. Nevertheless, the response, $C_e(t)$, to that of $C_i(t)$ has a characteristic distribution which depends only on the flow pattern of the system. We can thus obtain considerable information about the flow pattern in the system from the characteristic features

of $C_e(t)$.

Let $\langle C \rangle$ be the average concentration of tracer if it were uniformly distributed throughout the system and $\bar{t}$ be the mean residence time. Then the following relations hold,

$$\langle C \rangle = \frac{M}{V}$$

$$\bar{t} = \frac{V}{Q}$$

$$A_c = \frac{M}{Q} = \frac{MV}{QV} = \frac{MV}{VQ} = \langle C \rangle \bar{t} \quad ,$$

or

$$A_c = \int_0^\infty C_i(t)dt = \int_0^\infty C_e(t)dt = \langle C \rangle \bar{t} \quad ,$$

where A_c is the area under the concentration distribution curve. Suppose that the tracer is injected in an impulsive manner. Then all the molecules of the tracer have a zero initial age and the inlet concentration can be expressed as

$$C_i(t) = \frac{M}{Q}\delta(t) = \langle C \rangle \bar{t}\,\delta(t) \quad ,$$

where $\delta(t)$ is the Dirac distribution with its spike at $t = 0$ and has the following mathematical properties:

$$\delta(t) = 0, \text{ if } t \neq 0,$$

$$\int_{-\infty}^{\infty} \delta(t)dt = 1 \quad .$$

If the flow pattern in the system is an ideal plug flow, all the

molecules of the tracer spend the same period of time (mean residence time) in the system. The exit concentration distribution is thus given by

$$C_e(t) = \frac{M}{Q}\,\delta(t - \overline{t}) = \langle C \rangle\, \overline{t}\, \delta(t - \overline{t}) \quad , \qquad (2\text{-}3)$$

where $\delta(t - \overline{t})$ is the Dirac distribution with its spike at $t = \overline{t}$. If the fluid in the system is completely mixed, all the molecules of the tracer in the system are also completely mixed throughout the system at any instant. This in turn means that all the molecules of the tracer in the system have an equal probability of exiting from the system. The exit concentration distribution thus has the form of the exponential decay expressed as

$$C_e(t) = \langle C \rangle\, e^{-t/\,\overline{t}} \quad . \qquad (2\text{-}4)$$

These are the ideal cases, as shown in Fig. 2-1-a. These ideal cases, of course, seldom occur in reality. The tracer injected is usually in an arbitrary shape and the response is also in an arbitrary shape with a certain degree of spread, as shown in Fig. 2-1-b. The degree of spread of the exit signal, $C_e(t)$, in relation to the spread of the inlet signal reveals the behavior of mixing in the system (14).

Data normalization. In order to carry out a statistical treatment of response data, the concentration distribution is transformed into a probability distribution by dividing equation (2-2) by M/Q. This yields

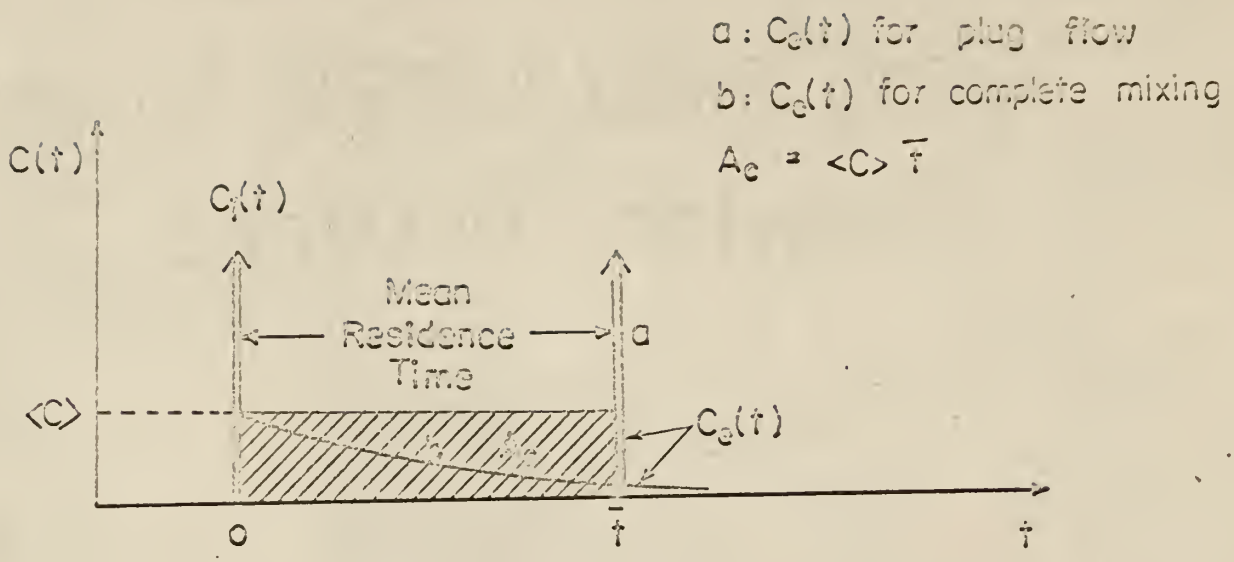

Fig. 2-1-a. Response of an ideal system to an impulse tracer injection.

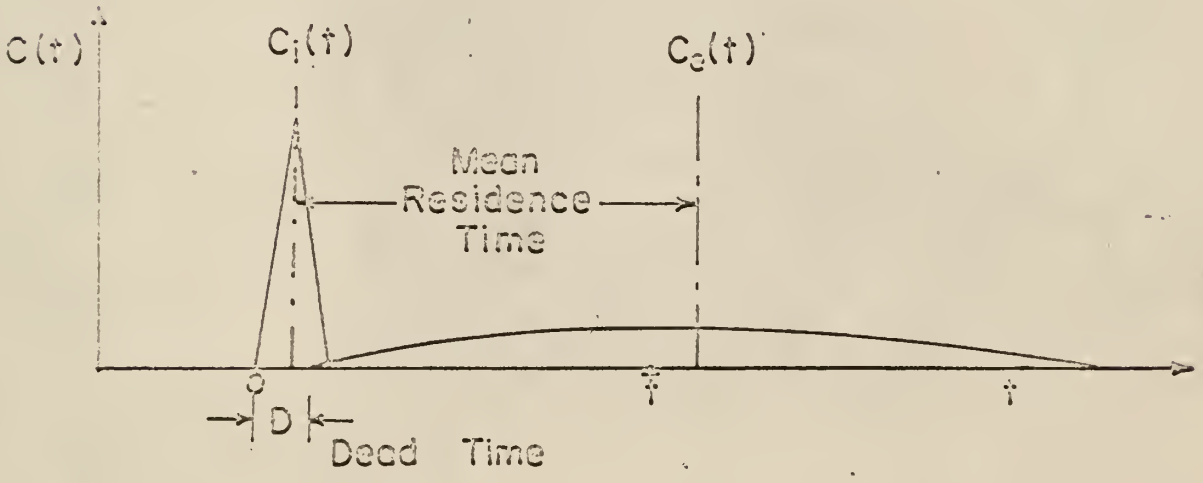

Fig. 2-1-b. Response of a nonideal system to an arbitrary trace injection.

$$\int_0^\infty \frac{C_i(t)}{M/Q}\,dt = 1 = \int_0^\infty \frac{C_e(t)}{M/Q}\,dt \quad . \tag{2-5}$$

Let

$$X(t) = \frac{C_i(t)}{M/Q} = \frac{C_i(t)}{\int_0^\infty C_i(t)dt} \tag{2-6}$$

and

$$Y(t) = \frac{C_e(t)}{M/Q} = \frac{C_e(t)}{\int_0^\infty C_e(t)dt} \quad . \tag{2-7}$$

Then

$$\int_0^\infty X(t)dt = 1 = \int_0^\infty Y(t)dt \quad . \tag{2-8}$$

The functions, X(t) and Y(t), so obtained are the probability density functions associated with the inlet stream and the exit stream respectively. X(t)dt is the fraction of tracer in the inlet stream which enters the system between time t and t+dt, while Y(t)dt is the fraction of the tracer in the outlet stream which leaves the system between time t and t+dt. Response data are usually analyzed by using the probability distribution instead of using the concentration distribution, because of its convenience. If Y(t) is the impulse response, it corresponds to the so-called residence time distribution (RTD) which characterizes the macromixing in the system. The exit age distribution is a different name for the same function as RTD (2,3).

The scheme for measuring signals for an experimental system is shown in Fig. 2-2-a. Both the inlet and outlet concentration signals

are transformed into the electrical signals in the final recording. To assure the identity of the information of RTD, the final recording must hold a linear relationship with respect to the concentration throughout the detecting range. Otherwise, difficulties arise out of the final data correction. Let K_i be the proportionality factor for the input signal recording, $R_i(t)$, and K_e be the proportionality factor for the output signal recording, $R_e(t)$. Then

$$R_i(t) = K_i C_i(t)$$

and

$$R_e(t) = K_e C_e(t) \quad .$$

The block diagrams for both input and output signal transformations are shown in Fig. 2-2-b and Fig. 2-2-c respectively. Generally, K_i and K_e are nearly the same but it is not always so. Frequently the output pulse decays very slowly. It is thus better to amplify K_e a little higher than K_i in order to reduce the noise effect. The area under $R_i(t)$ is now equal to

$$\frac{K_i M}{Q} = \int_0^\infty R_i(t)dt = \int_0^\infty K_i C_i(t)dt \quad , \qquad (2\text{-}9)$$

while the area under $R_e(t)$ is equal to

$$\frac{K_e M}{Q} = \int_0^\infty R_e(t)dt = \int_0^\infty K_e C_e(t)dt \quad . \qquad (2\text{-}10)$$

Dividing equation (2-9) by $K_i M/Q$ yields

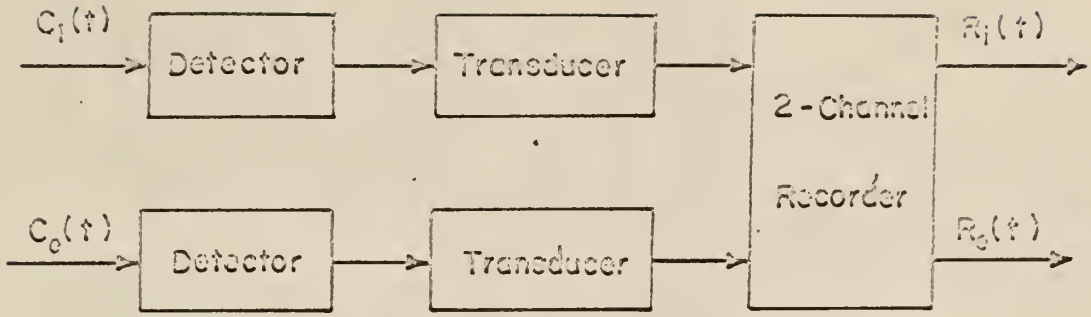

Fig. 2-2-a. General scheme of instrumentation.

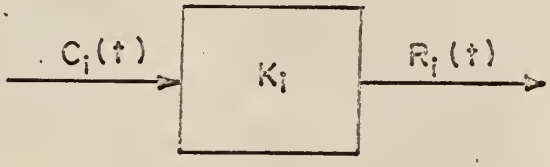

Fig. 2-2-b. Block diagram for input signal.

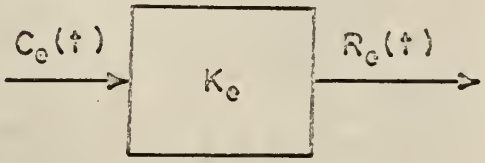

Fig. 2-2-c. Block diagram for output signal.

$$1 = \int_0^\infty \frac{R_i(t)}{K_i M/Q}\,dt = \int_0^\infty \frac{C_i(t)}{M/Q}\,dt \quad ,$$

i.e.

$$X(t) = \frac{R_i(t)}{K_i M/Q} = \frac{R_i(t)}{\int_0^\infty R_i(t)dt} \quad . \tag{2-11}$$

Dividing equation (2-10) by $K_e M/Q$ yields

$$1 = \int_0^\infty \frac{R_e(t)}{K_e M/Q}\,dt = \int_0^\infty \frac{C_e(t)}{M/Q}\,dt \quad ,$$

i.e.

$$Y(t) = \frac{R_e(t)}{K_e M/Q} = \frac{R_e(t)}{\int_0^\infty R_e(t)dt} \quad . \tag{2-12}$$

In other words, the probability density functions of both the input, $X(t)$, and the output, $Y(t)$, are directly obtainable from the final recording of $R_i(t)$ and $R_e(t)$ regardless of how the signals are transformed and how they are amplified. The probability density functions, $X(t)$ and $Y(t)$, can be further transformed into the dimensionless time domain as follows:

$$\int_0^\infty X(t)dt = \int_0^\infty \bar{t}\,X(t)\,d\left(\frac{t}{\bar{t}}\right) = \int_0^\infty X(\theta)d\theta = 1 \tag{2-13}$$

and

$$\int_0^\infty Y(t)dt = \int_0^\infty \bar{t}\,Y(t)\,d\left(\frac{t}{\bar{t}}\right) = \int_0^\infty Y(\theta)d\theta = 1 \quad , \tag{2-14}$$

where

$$\theta = \frac{t}{\bar{t}} = \text{dimensionless time;}$$

$$X(\theta) = \bar{t}X(t) \quad ; \quad Y(\theta) = \bar{t}Y(t) \quad .$$

These notations will be used consistently throughout this writing.

Mathematical treatment. Once the probability density functions of $X(t)$ and $Y(t)$ have been obtained, they can be treated further mathematically.

The kth moment of the exit age distribution, $Y(t)$, is defined as (15)

$$m_{tyk} = \int_0^\infty t^k Y(t)dt \quad , \quad k = 1,2,3 \ldots \tag{2-15}$$

where the subscript tyk in m_{tyk} refers to the kth moment of $Y(t)$ in the time domain. When $k = 1$, the resulting expression gives the mean of $Y(t)$ or the first moment of $Y(t)$, i.e.

$$\mu_{ty} = m_{ty1} = \int_0^\infty tY(t)dt \quad . \tag{2-16}$$

The second moment about the mean, μ_{ty}, commonly called the variance, σ^2_{ty}, is defined as

$$\sigma^2_{ty} = \int_0^\infty (t - \mu_{ty})^2 Y(t)dt$$

$$= m_{ty2} - \mu^2_{ty} \quad , \tag{2-17}$$

where

$$m_{ty2} = \int_0^\infty t^2 Y(t)dt \quad .$$

Likewise, the third moment about the mean, μ_{ty}, commonly called the skewness, σ^3_{ty}, is defined as

$$\sigma^3_{ty} = \int_0^\infty (t - \mu_{ty})^3 \, Y(t)dt$$

$$= m_{ty3} - 3\mu_{ty}\sigma^2_{ty} - \mu^3_{ty} \quad , \tag{2-18}$$

where

$$m_{ty3} = \int_0^\infty t^3 Y(t)dt \quad .$$

By the same method, the kth moment of the inlet age distribution, X(t), is defined as

$$m_{txk} = \int_0^\infty t^k X(t)dt \quad , \qquad k = 1,2,3 \ . \ . \ . \tag{2-19}$$

The mean of X(t) is defined as

$$\mu_{tx} = m_{txl} = \int_0^\infty tX(t)dt \quad . \tag{2-20}$$

The variance of X(t) is defined as

$$\sigma^2_{tx} = \int_0^\infty (t - \mu_{tx})^2 X(t)dt$$

$$= m_{tx2} - \mu^2_{tx} \quad , \tag{2-21}$$

where

$$m_{tx2} = \int_0^\infty t^2 X(t)dt \quad .$$

The skewness of X(t) is defined as

$$\sigma_{tx}^3 = \int_0^\infty (t - \mu_{tx})^3 X(t)dt$$

$$= m_{tx3} - 3\mu_{tx}\sigma_{tx}^2 - \mu_{tx}^3 \quad , \qquad (2\text{-}22)$$

where

$$m_{tx3} = \int_0^\infty t^3 X(t)dt \quad .$$

The difference between the means is defined as

$$\Delta\mu_{tyx} = \mu_{ty} - \mu_{tx} \quad , \qquad (2\text{-}23)$$

the difference between the variances as

$$\Delta\sigma_{tyx}^2 = \sigma_{ty}^2 - \sigma_{tx}^2 \quad , \qquad (2\text{-}24)$$

and the difference between the skewnesses as

$$\Delta\sigma_{tyx}^3 = \sigma_{ty}^3 - \sigma_{tx}^3 \quad . \qquad (2\text{-}25)$$

Values of $\Delta\mu_{tyx}$, $\Delta\sigma_{tyx}^2$ and $\Delta\sigma_{tyx}^3$ are dependent on the structure and operating condition of the system. If they are correlated to the model parameters of the system, this gives rise to the so-called moments method of analysis. In general, the information of n+1 moments are required for fitting of an n-parameter model to experimental data.

In another method of correlating response data to the model parameters, the Laplace transform is applied to both Y(t) and X(t). By taking the ratio of the transformed response gives

$$H(s) = \frac{\int_0^\infty e^{-st} Y(t)dt}{\int_0^\infty e^{-st} X(t)dt} \quad , \qquad (2\text{-}26)$$

which is the system transfer function in the s-domain. The s-plane analysis fits this experimental transfer function to that of the model.

If a Fourier transformation is applied to both Y(t) and X(t), the transfer function in the frequency domain,

$$H(j\omega) = \frac{\int_0^\infty e^{-j\omega t} Y(t)dt}{\int_0^\infty e^{-j\omega t} X(t)dt} \quad , \qquad (2\text{-}27)$$

can be obtained. Since both Y(t) and X(t) are continuous functions of a bounded variation which return to their initial values after a finite time and remain so as time progresses, the integrals exist and they may be evaluated for each value of ω. We then obtain the amplitude ratio and phase angle from $H(j\omega)$. Theoretically, they are identical to those obtained by directly analyzing the response to the sinusoidal forcing signal of the tracer. In other words, fitting this experimental transfer function to that of the model is equivalent to the frequency response analysis.

Tracer injection. Tracers such as radioisotopes, dyestuffs and salt solutions are generally used. A tracer which is harmful to the human body is of course not suitable for use in the food industry. Some chemical processes may be conducted at high temperatures and high pressures. A tracer which is evaporated or destroyed during testing is of course not adopted; otherwise, the exit age distribution will

be meaningless. The general requirements for the tracer are that it should be stable (does not react with the main stream) and easily be detected. The most interesting question is the optimum pulse shape for the input. Ideally, it appears that the smaller the magnitude of the input pulse the better. However, the presence of noise necessitates producing a response which is discernible from the interference. To reduce the uncertainty, an increase in the pulse height is suggested (but not exceeding the response capacity of the system). If the width of the input is long compared with the response, the dynamics of the system are only moderately excited; hence, high frequency responses are suppressed, obscured, or non-existent (7). In practice, an impulse injection function is a physical impossibility. However, the injection time should not last too long; otherwise the high frequency response information can not be recovered from the response data. A nearly exact impulse injection was carried out by Williams by the arrangement of solenoid valves and a timer (9). Fitting of the model with experimental data is then based solely on the exit response which corresponds to the exit age distribution.

CHAPTER 3

GAMMA DISTRIBUTION MODEL

Constructing a model to describe mixing characteristics of a flow system is similar to deriving a rate expression for a chemical reaction. Although construction of a model for a flow system is tedious work, it is essential to designing reactors for new processes and improving performances of existing reactors. It is desirable to establish a fairly general model which is applicable to a variety of systems rather than to derive specific models for individual systems separately. Elements such as plug flow, backmix flow, dead space, bypass flow, recycle flow, cross flow, etc. are taken into consideration for constructing a general model. The general model then contains a number of parameters which make it flexible in fitting it to a wide variety of situations. However, the complexity of the accompanying mathematics may give rise to difficulties in the fitting procedure. Furthermore, it is possible that more than one set of parameters fit the experimental data equally well. This may make the model very unrealistic and unable to represent reality. To obtain the best flexibility, simplicity and reliability, we should construct the simplest model which closely represents reality and whose various flow regions resemble those of the real system (19).

An optimum way may be to subgroup the similar systems and describe these subgroups by suitable individual models. This way, a model will have a simple form and yet it can describe the mixing characteristics of a certain number of similar systems.

To construct a model, two approaches are adopted, namely, the model-prescribed method and the response-analysis method. In the model-prescribed method, a model is constructed from an imaginary physical picture of the system. It may simply be a mathematical one. In the response-analysis method, the response of a system is examined before any model is specified with the hope that the analysis of the response will shed some light on the proper choice of a model. In theory, the response-analysis approach is more reasonable than the model-prescribed approach because the former involves less bias in the choice of the model than the latter. Nevertheless, owing to the rather unsatisfactory methods of analysis available at the present time, the response-analysis approach has not been widely accepted. Cha (6) has discussed this approach but its practical usage has not been established.

Gamma distribution model (GDM). The gamma distribution model is essentially a mathematical model. Mathematically it corresponds to the following probability density function (6,10).

$$f(t) = \frac{1}{\nu^p \Gamma(p)} (t - D)^{p-1} e^{-(t-D)/\nu} \qquad (3\text{-}1)$$

$$p \geq 1, \qquad \infty > t > D \geq 0, \qquad \nu > 0 ,$$

where t is a continuous variable in the time domain, p, ν and D are parameters, and Γ denotes the gamma function defined as

$$\Gamma(p) = \int_0^\infty x^{p-1} e^{-x} dx \quad .$$

However, the parameter D may be considered the dead (or delay) time of the system while p may be considered as the parameter related to the extent of fluid mixing in the direction of flow. From appearance curves of f(t), we can see that the exit age distributions, E(t), of some flow systems can be represented by the typical unimodal Γ-distribution curves. For example, by letting

$$p = 1, \quad D = 0,$$

equation (3-1) is reduced to

$$f(t) = \frac{1}{\nu} e^{-t/\nu} \quad ,$$

which has the same form as the exit age distribution of the completely mixed system, i.e.

$$E(t) = \frac{1}{\bar{t}} e^{-t/\bar{t}} \quad .$$

Note that E(t) has a dimension of time^{-1}. Comparing these two forms, we can interpret ν as the mean residence time of the system. As the value of p is further increased beyond one, as shown later, the peak of the Γ-distribution gradually moves from the left to the right. Physically this means that the flow pattern gradually deviates from the completely mixed type. In general, various physical interpretations can be imposed on the parameters of the Γ-distribution model, although it is essentially a pure mathematical model.

If the exit age distribution of a flow system is approximated by the Γ-distribution as represented by equation (3-1), f(t) is equivalent

to the response at the exit of the system to the impulse tracer excitation at the inlet, i.e.

$$f(t) = E(t) = Y(t).$$

The system transfer function is equivalent to the Laplace transformation of f(t), i.e.

$$H(s) = \frac{Y(s)}{X(s)} = Y(s) = E(s) = f(s) \quad ,$$

because X(s) = 1 for the (unit) impulse input.

The mean of f(t) can be shown to be (6)

$$\mu_t = \nu p + D \quad . \tag{3-2}$$

If consideration is restricted to closed systems, the mean of the exit age distribution is equal to the mean residence-time, $\bar{t}$ (2), i.e.

$$\mu_t = \bar{t} = \frac{V}{Q} \quad , \tag{3-3}$$

and, therefore,

$$\nu = \frac{\mu_t - D}{p} = \frac{\bar{t} - D}{p} \quad . \tag{3-4}$$

Substituting equation (3-4) into equation (3-1) and noting that the exit age distribution of a flow system is represented by the gamma distribution, we have

$$E(t) = \frac{p^p}{(\bar{t} - D)^p \, \Gamma(p)} (t - D)^{p-1} \, e^{-p\left(\frac{t-D}{\bar{t}-D}\right)} \quad . \tag{3-5}$$

If the normalized age is used, the normalized exit age distribution of such a system is

$$E(\theta) = E(t)\bar{t} = \frac{p^p}{(1-\tau)^p\,\Gamma(p)}(\theta-\tau)^{p-1}\,e^{-p\left(\frac{\theta-\tau}{1-\tau}\right)}, \quad (3\text{-}6)$$

where

$$\theta = \frac{t}{\bar{t}} = \text{dimensionless time,}$$

$$\tau = \frac{D}{\bar{t}} = \text{dimensionless dead time.}$$

Note that $E(\theta)$ is dimensionless. Taking the Laplace transform of equation (3-6) yields the transfer function of the gamma distribution model, i.e.

$$H(s) = E(s) = \left[\frac{p}{(1-\tau)s+p}\right]^p e^{-\tau s} \quad . \quad (3\text{-}7)$$

Gamma distribution model with bypassing (GDMWB). This model is a structural modification of the original Γ-distribution. It is depicted in Fig. 3-1 (5). It consists of a gamma mixing section (or unit) in series with a plug flow section. However, a portion of the inlet stream bypasses the Γ-mixing unit and the by-pass stream goes directly from the inlet of the system to the inlet pulg flow unit.

The exit age distribution, $E(t)_\Gamma$, of the Γ-mixing section of the model is then given by

$$E(t)_\Gamma = \frac{1}{\nu^p\,\Gamma(p)}\,t^{p-1}\,e^{-t/\nu} \quad , \quad (3\text{-}8)$$

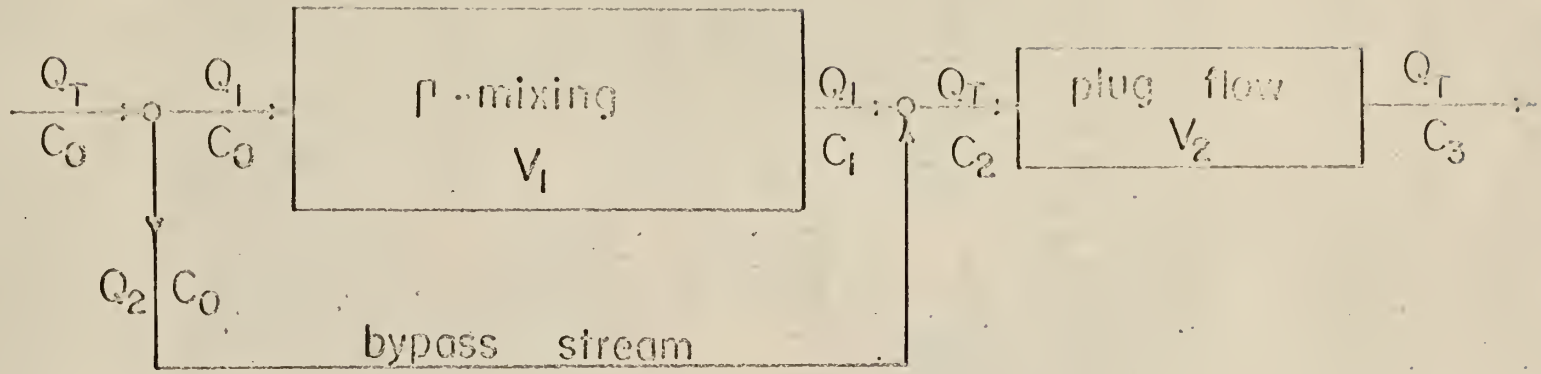

Q_1 = volumetric flow rate through the Γ-mixing section.

Q_2 = volumetric flow rate of the bypass stream.

Q_T = total volumetric flow rate.

V_1 = volume of the Γ-mixing section.

V_2 = volume of the plug flow section.

V_T = total volume of the whole system.

C_i = tracer concentration, a function of time.

Fig. 3-1. The Γ-distribution model with bypassing (5).

and the mean of $E(t)_\Gamma$ is

$$\bar{t}_\Gamma = \nu p \quad .$$

Let

$$\beta = \frac{Q_1}{Q_T} \quad \text{and} \quad \tau = \frac{V_2}{V_T} = 1 - \frac{V_1}{V_T} \quad ,$$

where β is the fraction of flow entering the Γ-mixing section and τ is the dimensionless residence time in the plug flow section. Again considering only a closed system, we can write

$$\bar{t} = \frac{V_T}{Q_T} \quad ,$$

where $\bar{t}$ is the mean residence time of the entire system. Then we can also write

$$\bar{t}_\Gamma = \nu p = \frac{V_1}{Q_1} = \frac{V_T V_1}{\beta Q_T V_T} = \frac{\bar{t}(1 - \tau)}{\beta} \quad .$$

Thus

$$\nu = \frac{\bar{t}(1 - \tau)}{p\beta} \quad . \qquad (3\text{-}9)$$

Substituting equation (3-9) into equation (3-8), and noting that $E(\theta)_\Gamma = \bar{t}E(t)_\Gamma$, we can show that the exit age distribution of the Γ-mixing section is given in terms of reduced time θ by

$$E(\theta)_\Gamma = \frac{(p\beta)^p}{(1 - \tau)^p \, \Gamma(p)} \theta^{p-1} e^{-\frac{p\beta}{1-\tau}\theta} \quad . \qquad (3\text{-}10)$$

Taking the Laplace transform of equation (3-10) gives the transfer function for the Γ-mixing section, i.e.

$$H(s)_\Gamma = E(s)_\Gamma = \frac{C_1(s)}{C_0(s)} = \left[\frac{p\beta}{(1-\tau)s + p\beta}\right]^p \quad . \qquad (3\text{-}11)$$

The transfer function for the plug flow section is

$$H(s)_p = \frac{C_3(s)}{C_2(s)} = e^{-\tau s} \quad . \qquad (3\text{-}12)$$

The material balance at the point where the bypass stream joins the outlet stream of the Γ-mixing section is

$$C_2 Q_T = Q_1 C_1 + Q_2 C_0 \quad .$$

Dividing by Q_T gives

$$C_2 = \beta C_1 + (1-\beta) C_0 .$$

Taking the Laplace transform yields

$$C_2(s) = \beta C_1(s) + (1-\beta) C_0(s) \quad . \qquad (3\text{-}13)$$

By combining equations (3-11) through (3-13), it can be shown that the transfer function of the entire system is given by

$$H(s) = \frac{C_3(s)}{C_0(s)} = \left\{\beta \left[\frac{p\beta}{(1-\tau)s + p\beta}\right]^p + (1-\beta)\right\} e^{-\tau s}, \qquad (3\text{-}14)$$

where p, β, and τ are the three parameters to be determined experimentally. In case there is no bypassing, i.e. β = 1, equation (3-14) reduces to

equation (3-7), which is the transfer function of the Γ-distribution model. By letting

$$\beta = 1,\ p = 1,\ \tau = 0,$$

equation (3-14) is reduced to

$$H(s) = \frac{1}{s + 1}$$

which corresponds to the transfer function of the completely mixed system. If

$$\beta = 0,\ \tau = 1,$$

equation (3-14) reduces to

$$H(s) = e^{-s}$$

which corresponds to the transfer function of the plug flow system.

Physically this means that an increase in the value of β tends to emphasize the effect of mixing (Γ-mixing). An increase in the value of p tends to increase the order of the transfer function of the Γ-mixing section or to reduce the effect of mixing in the axial direction. Recall that the Γ-mixing section is similar to a sequence of completely mixed tanks in series but the value of p is not restricted to an integer number (5). An increase in the value of τ tends to empahsize the effect of plug flow.

In summary, the three parameters play the major roles in describing the flow pattern which generally falls between the two ideal extremes of complete mixing and plug flow. This modified model appears to be flexible as useful and will be used to fit Johnson's experimental data (5). The characteristics of this model will further be revealed by

considering three types of transient responses of the model.

Impulse response. The impulse response is the response to the input in form of the unit impulse response,

$$X(\theta) = \delta(\theta)$$

The Laplace transform of the input is

$$X(s) = 1 \quad .$$

The Laplace transform of the output signal is then equal to

$$Y(s) = X(s)H(s) = H(s) = E(s) \quad .$$

This implies that the impulse response, $Y(\theta)$, of GDMWB in dimensionless form is identical to the dimensionless exit age distribution of the model, which can be obtained by taking the inverse transform of equation (3-14), i.e.

$$Y(\theta) = E(\theta)$$

$$= \frac{\beta(p\beta)^p}{(1-\tau)^p\,\Gamma(p)}(\theta-\tau)^{p-1}\, e^{-\frac{p\beta}{1-\tau}(\theta-\tau)} + (1-\beta)\delta(\theta-\tau) \quad . \tag{3-15}$$

The impulse responses of two typical systems, one without bypassing and one with bypassing, are illustrated in Figs. 3-2 and 3-3.

Equation (3-15) can be reduced to that for the response of well-known or idealized systems. For example, by letting

$\beta = 1$, $\tau = 0$ and p = a positive integer,

equation (3-15) reduces to

$$Y(\theta) = \frac{p^p}{(p-1)!}\theta^{p-1}\, e^{-p\theta} \quad , \tag{3-16}$$

which corresponds to the impulse response of p - completely stirred

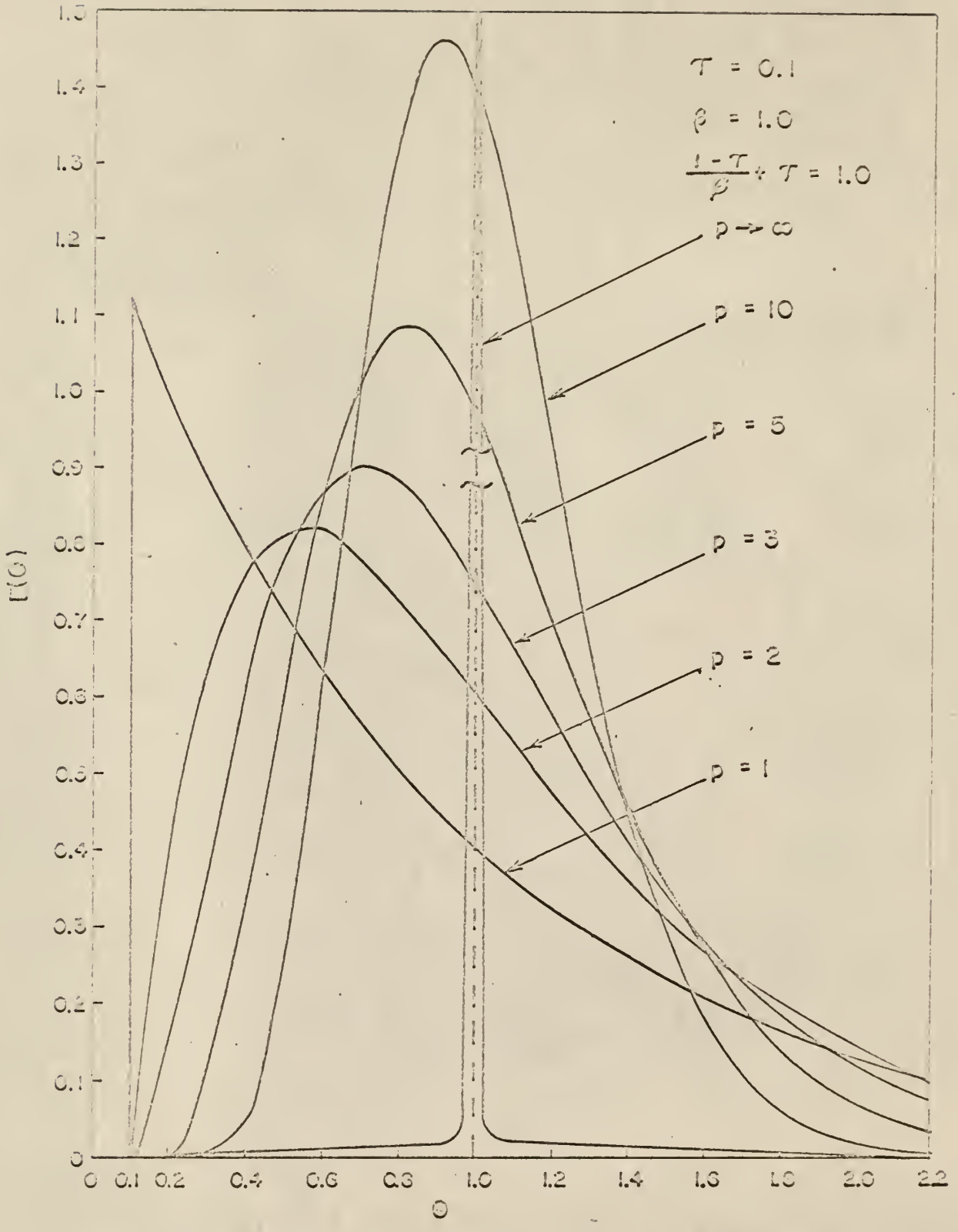

Fig. 3-2. Impulse response of the Γ-distribution model without bypassing.

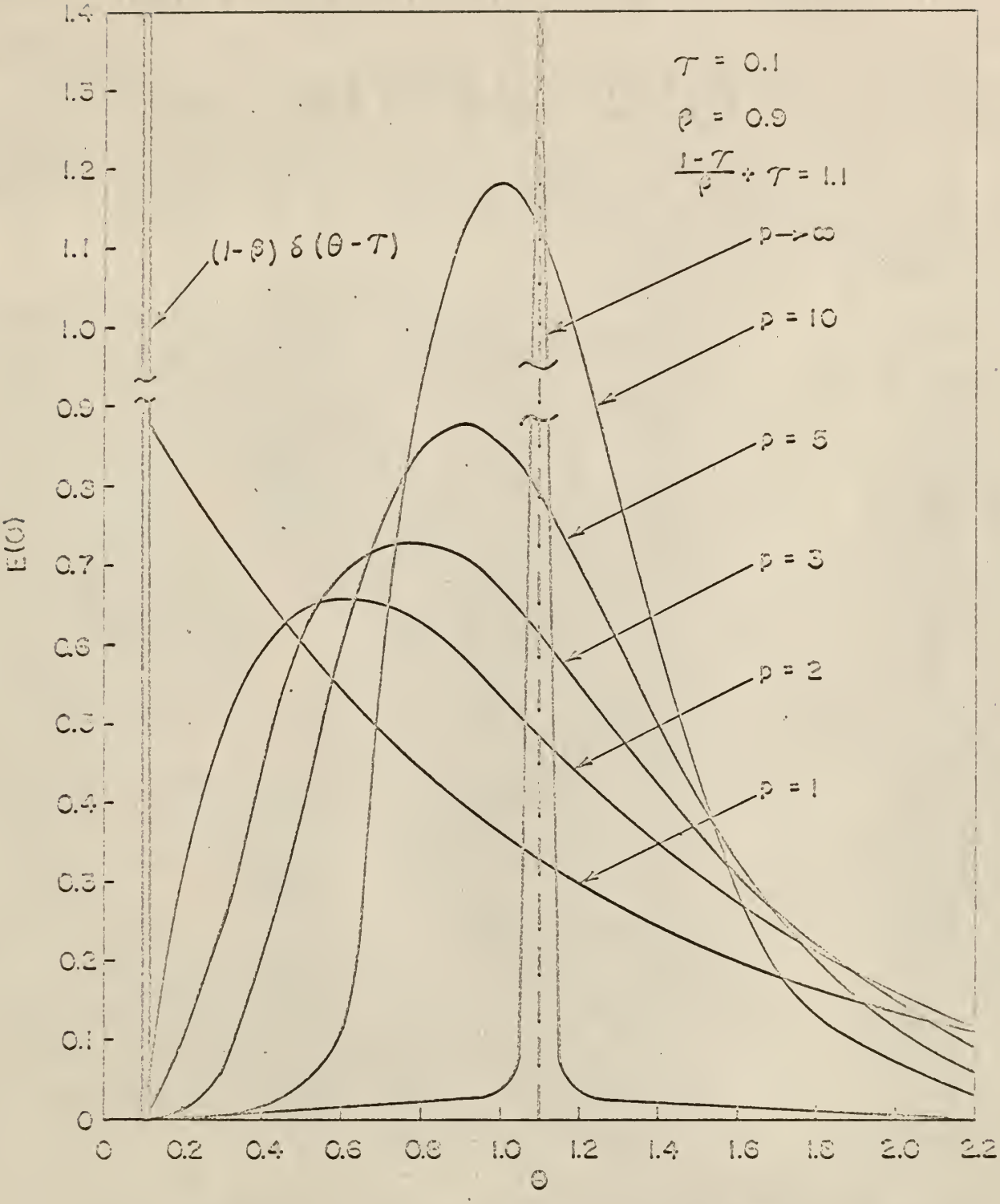

Fig. 3-3. Impulse response of the Γ-distribution model with bypassing. (β = 0.9)

tanks in series (p-CSTR). Equation (3-16) is identical to the C curve for the tanks-in-series model given by (19)

$$C(\theta) = \frac{j^j}{(j-1)!}\,\theta^{j-1}\,e^{-j\theta} \quad . \tag{3-17}$$

Comparing equation (3-16) with equation (3-17), we can see that

$j = p$ = no. of completely mixed tanks in series.

If

$p = 1$,

equation (3-16) reduces to

$$Y(\theta) = e^{-\theta}$$

which corresponds to the impulse response of the completely mixed system.

If

$\beta = 0, \tau = 1$,

equation (3-15) reduces to

$$Y(\theta) = \delta(\theta - 1)$$

which corresponds to the impulse response of the plug flow system.

Step response. A step response means that the input is

$X(\theta) = U(\theta)$ = unit step function .

The Laplace transform of this input function is

$$X(s) = \frac{1}{s} \quad .$$

Hence the Laplace transform of the output signal is

$$Y(s) = X(s)H(s) = \left\{\beta\left(\frac{p\beta}{1-\tau}\right)^p \frac{1}{s\left(s+\frac{p\beta}{1-\tau}\right)^p} + \frac{1-\beta}{s}\right\} e^{-\tau s} \quad . \tag{3-18}$$

Let

$$K = \beta\left(\frac{p\beta}{1-\tau}\right)^{p} \qquad \text{and} \qquad A = \frac{p\beta}{1-\tau} \quad .$$

Equation (3-18) can then be written as

$$Y(s) = \left\{K \frac{1}{s(s+A)^{p}} + \frac{1-\beta}{s}\right\} e^{-\tau s} \quad . \tag{3-19}$$

Letting

$$Y_1(s) = K \frac{1}{s(s+A)^{p}} + \frac{1-\beta}{s} \quad .$$

and writing its inverse Laplace transform as

$$\mathcal{L}^{-1} Y_1(s) = Y_1(\theta) \quad ,$$

the inverse Laplace transform of $Y(s)$ can be expressed as

$$\mathcal{L}^{-1} Y(s) = Y_1(\theta - \tau) \quad .$$

$Y_1(\theta)$ can be obtained by means of the Heaviside partial fractions theorem and the expression can be shown to be (11)

$$Y_1(\theta) = K\left\{\frac{1}{A^{p}} + \sum_{\gamma=0}^{p-1} \frac{\varphi^{p-1-\gamma}(-A)}{(p-1-\gamma)!\,\gamma!}\theta^{\gamma} e^{-A\theta}\right\} + (1-\beta)U(\theta) \quad ,$$

where

$$\varphi(s) = \frac{1}{s}$$

and

$$\varphi^{p-1-\gamma}(-A) = \frac{d^{p-1-\gamma}}{ds^{p-1-\gamma}}\varphi(s)\Bigg|_{s=-A}$$

The evaluation is feasible for integer values of p greater than unity by using this theorem. But it should be remembered that p in this model is not restricted to integer values. The step response is equal to

$$Y(\theta) = Y_1(\theta - \tau)$$

$$= K\left\{\frac{1}{A^p} + \sum_{\gamma=0}^{p-1} \frac{\varphi^{p-1-\gamma}(-A)}{(p-1-\gamma)!\,\gamma!}(\theta - \tau)^{\gamma} e^{-A(\theta-\tau)}\right\}$$

$$+ (1 - \beta)U(\theta - \tau) \quad . \tag{3-20}$$

By setting

$$J_p(\theta) = \sum_{\gamma=0}^{p-1} \frac{\varphi^{p-1-\gamma}(-A)}{(p-1-\gamma)!\,\gamma!}(\theta - \tau)^{\gamma} \quad , \tag{3-21}$$

$$p = 1,2,3 \ldots$$

Equation (3-21) can be illustrated for a few cases, for example

$$J_1(\theta) = \frac{\varphi(-A)}{0!\;0!}(\theta - \tau)^0 = \frac{-1}{A} \quad ,$$

$$J_2(\theta) = \frac{\varphi'(-A)}{1!\;0!}(\theta - \tau)^0 + \frac{\varphi(-A)}{0!\;1!}(\theta - \tau)$$

$$= \frac{-1}{A^2} + \frac{-1}{A}(\theta - \tau)$$

$$= \frac{1}{A}\left\{J_1(\theta) - \frac{(\theta - \tau)^{2-1}}{(2-1)!}\right\} \quad ,$$

$$J_3(\theta) = \frac{\varphi''(-A)}{2!\;0!}(\theta - \tau)^0 + \frac{\varphi'(-A)}{1!\;1!}(\theta - \tau) + \frac{\varphi^0(-A)}{0!\;2!}(\theta - \tau)^2$$

$$= \frac{-1}{A^3} + \frac{-1}{A^2}(\theta - \tau) + \frac{-1}{2!\;A}(\theta - \tau)^2$$

$$= \frac{1}{A}\left\{J_2(\theta) - \frac{(\theta - \tau)^{3-1}}{(3-1)!}\right\} \quad .$$

and so on. We thus obtain the recurrence relation as

$$J_p(\theta) = \frac{1}{A}\left\{J_{p-1}(\theta) - \frac{(\theta - \tau)^{p-1}}{(p-1)!}\right\} \quad .$$

Once the value of p is selected, $J_p(\theta)$ can be calculated by using this relation.

Unfortunately, the computational scheme based on this recurrence relation easily induces an error due to the loss of significant digits by the digital computer at a low value of θ. The calculated step response, $Y(\theta)$, often fails to show its monotone increasing characteristic at the initial stage as it should throughout the interval of θ from a mathematical viewpoint. The reason is briefly explained below by a specific example.

For example, at p = 2, the numerical value based on the recurrence relation is

$$J_2(\theta) = \frac{1}{A}\left[\frac{-1}{A} - \frac{(\theta - \tau)}{1!}\right]$$

which differs slightly from that calculated by the original relation

$$J_2(\theta) = \frac{-1}{A^2} + \frac{-1}{A}\frac{(\theta - \tau)}{1!} \quad .$$

The step response is computed by another approach in the present work. Recalling that the integration of the impulse response is equivalent to the step response, we can obtain the step response or the so-called F-curve by

$$Y(\theta) = F(\theta) = \int_0^\theta E(\theta)d\theta$$

Hence, integrating equation (3-15) yields the step response

$$Y(\theta) = \int_0^\theta \frac{\beta(p\beta)^p}{(1-\tau)^p\Gamma(p)} (\theta - \tau)^{p-1} e^{-\frac{p\beta}{1-\tau}(\theta-\tau)} d\theta$$

$$+ (1 - \beta)U(\theta - \tau) \qquad (3\text{-}22)$$

which can be evaluated by a straightforward numerical integration. The step response curves of two typical systems are shown in Figs. 3-4 and 3-5.

Frequency response. Letting

$$s = j\omega$$

in equation (3-14) yields the transfer function in the frequency domain as

$$H(j\omega) = \left\{\beta^{p+1} p^p \left[\frac{1}{(1 - \tau)j\omega + p\beta}\right]^p + (1-\beta)\right\}e^{-j\tau\omega} \quad . \qquad (3\text{-}23)$$

This may be rearranged and simplified to

$$H(j\omega) = \left\{\beta \left[\frac{1}{1 + j\frac{(1-\tau)\omega}{p\beta}}\right]^p + (1-\beta)\right\} e^{-j\tau\omega}$$

$$= \left\{\beta \left[\frac{1}{\sqrt{1 + \left[\frac{(1-\tau)\omega}{p\beta}\right]^2}} (\cos Z + j \sin Z)\right]^p + (1-\beta)\right\}e^{-j\tau\omega},$$

(3-24)

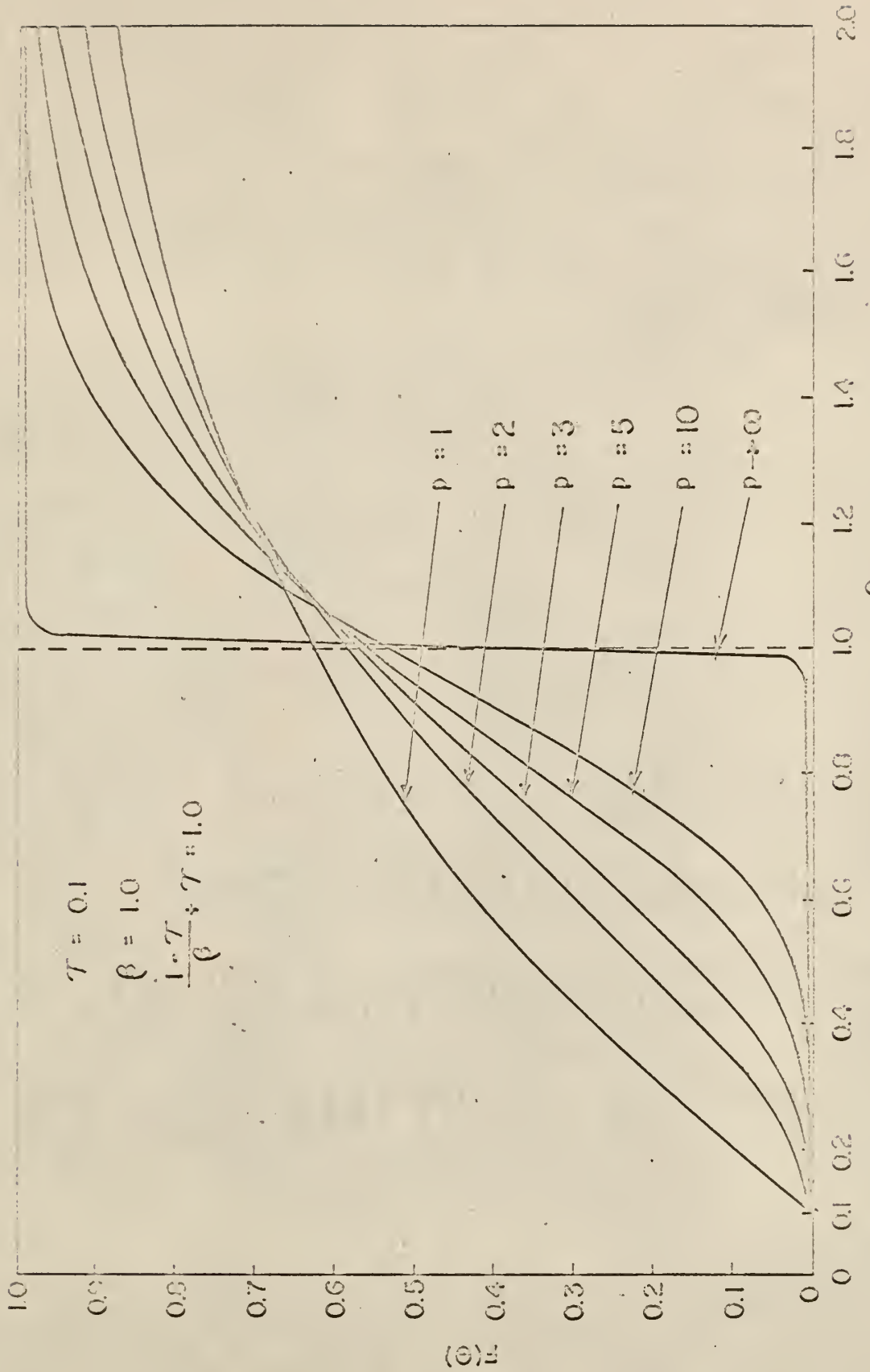

Fig. 3-4. Step response of the β-distribution model without bypassing.

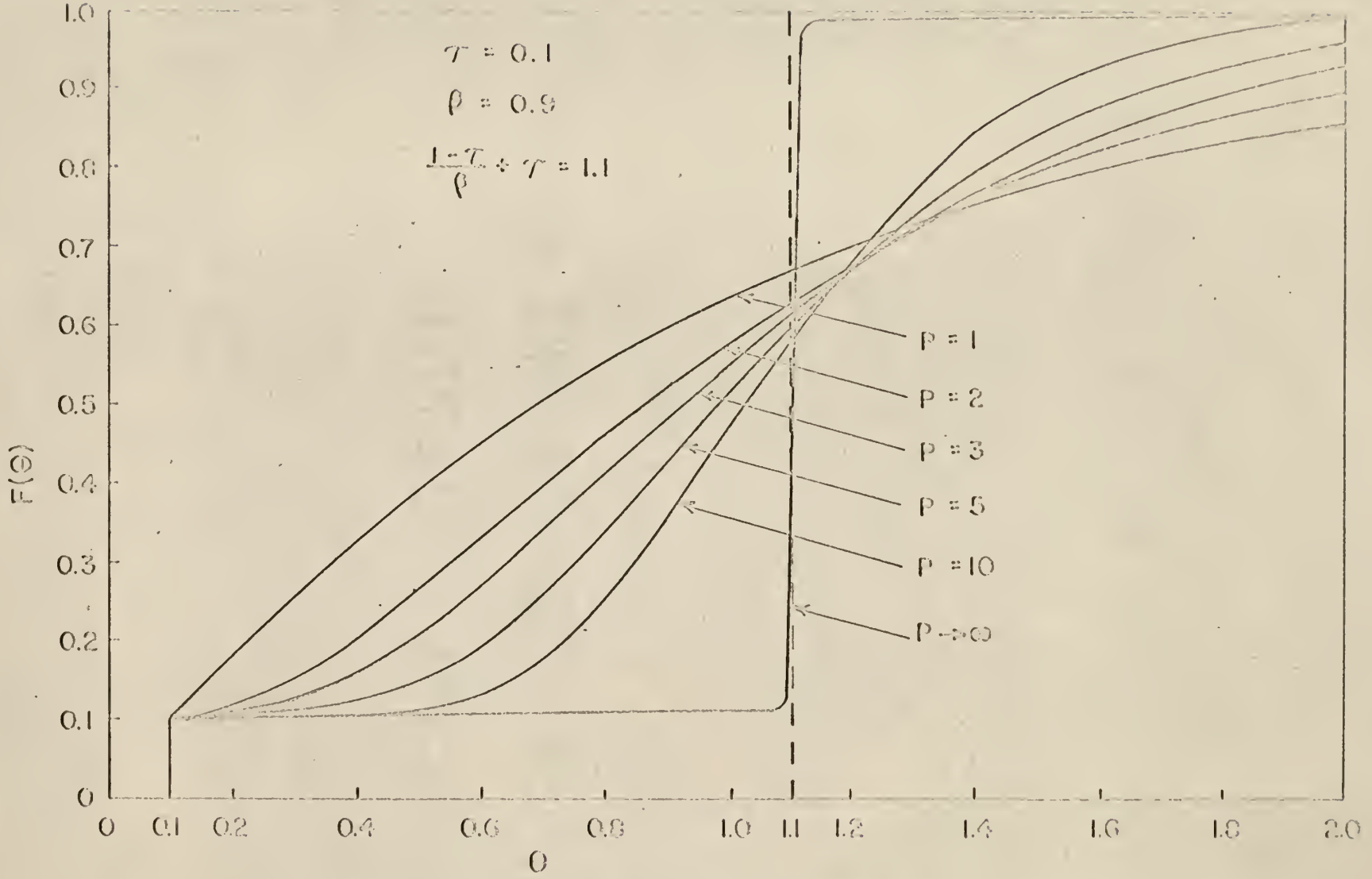

Fig. 3-5. Step response of the P-distribution model with bypassing.

where

$$Z = \tan^{-1}\left(-\frac{1-\tau}{p\beta}\,\omega\right)$$

$$j = \sqrt{-1}$$

ω = frequency, rad./unit dimensionless time.

Applying the Euler formula, i.e.

$$(\gamma e^{j\theta})^n = \gamma^n e^{jn\theta} = \gamma^n(\cos n\theta + j \sin n\theta) \quad ,$$

equation (3-24) is further simplified to

$$H(j\omega) = \beta\left\{1 + \left[\frac{(1-\tau)\omega}{p\beta}\right]^2\right\}^{-\frac{p}{2}} e^{j(pZ-\tau\omega)} + (1-\beta)e^{-j\tau\omega}. \quad (3\text{-}25)$$

Recalling that

$$e^{j(pZ-\tau\omega)} = \cos(pZ-\tau\omega) + j \sin(pZ-\tau\omega)$$

and

$$e^{-j\tau\omega} = \cos\tau\omega - j \sin\tau\omega \quad ,$$

equation (3-25), by expansion and rearranging, is reduced to a standard form for a complex variable, i.e.

$$H(j\omega) = R(\omega) + jI(\omega) \quad , \qquad (3\text{-}26)$$

where the real part is

$$R(\omega) = \beta\left\{1 + \left[\frac{(1-\tau)\omega}{p\beta}\right]^2\right\}^{-\frac{p}{2}} \cos(pZ-\tau\omega) + (1-\beta)\cos\tau\omega$$

and the imaginary part is

$$I(\omega) = \beta\left\{1 + \left[\frac{(1-\tau)\omega}{p\beta}\right]^2\right\}^{-\frac{p}{2}} \sin(pZ-\tau\omega) - (1-\beta)\sin\tau\omega \quad .$$

The amplitude ratio and phase angle are then given by

$$\text{A.R.} = \left| H(j\omega) \right| = \sqrt{R^2(\omega) + I^2(\omega)} \quad , \tag{3-27}$$

$$\text{Phase Angle} = \measuredangle H(j\omega) = \tan^{-1} \frac{I(\omega)}{R(\omega)} \quad . \tag{3-28}$$

Again the frequency response curves for two typical systems are illustrated in Figs. 3-6 and 3-7.

The frequency response given by this model again can be reduced to the responses of idealized systems. For example, by letting

$$\beta = 1, \ \tau = 0 \text{ and } p = \text{a positive integer,}$$

the expression given in equation (3-25) reduces to

$$H(j\omega) = \left\{ 1 + \left(\frac{\omega}{p}\right)^2 \right\}^{-\frac{p}{2}} e^{jpZ}$$

which corresponds to the frequency response of p-CSTR. The amplitude ratio and phase angle are then given by

$$\left.\begin{aligned} \text{A.R.} &= \left\{ 1 + \left(\frac{\omega}{p}\right)^2 \right\}^{-\frac{p}{2}} \\ \text{Phase Angle} &= pZ = p \tan^{-1} \frac{-\omega}{p} \end{aligned}\right\} \tag{3-29}$$

or say

$$\text{Phase Lag} = p \tan^{-1} \frac{\omega}{p} \quad .$$

The frequency response of m-CSTR is given by Nakanishi (22) as

$$\left.\begin{aligned} \text{A.R.} = G_m &= \frac{1}{\left\{ \left(\frac{\overline{F}}{m}\right)^2 + 1 \right\}^{\frac{m}{2}}} \\ \text{Phase Lag} = \Psi_m &= m \tan^{-1} \frac{\overline{F}}{m} \end{aligned}\right\} \tag{3-30}$$

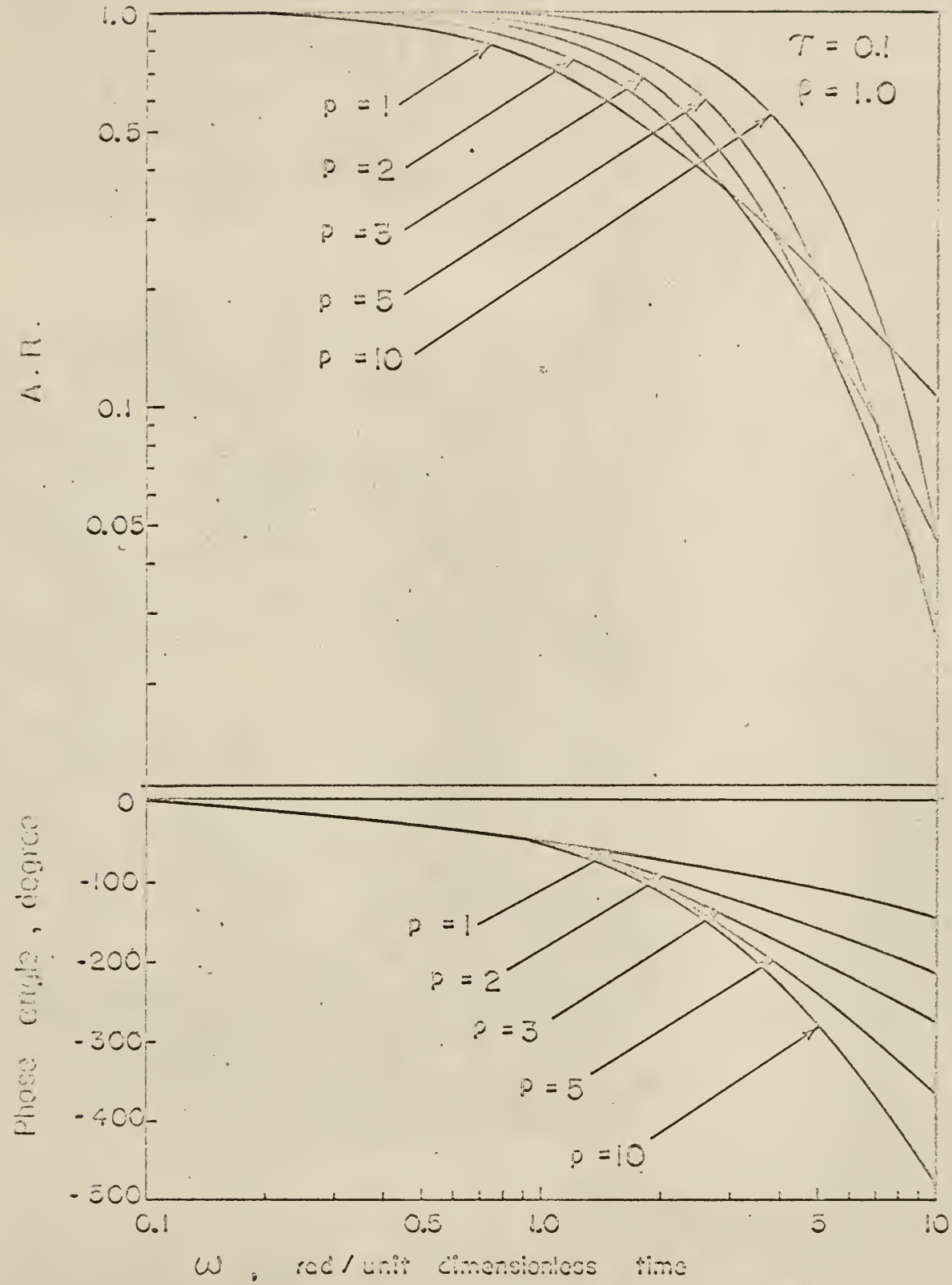

Fig. 3-6. Frequency response of the τ-distribution model without bypassing.

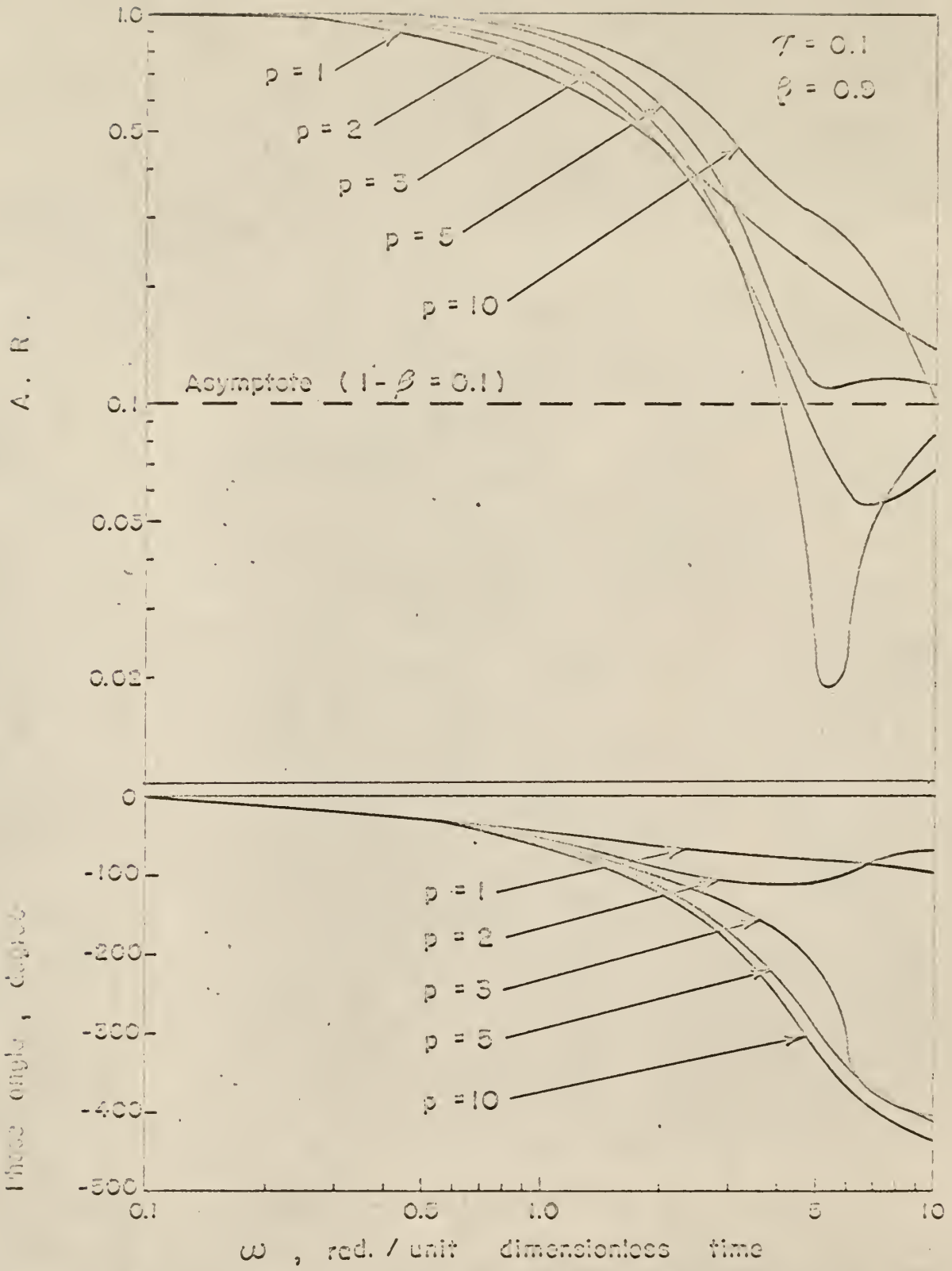

Fig. 3-7. Frequency response of the Γ-distribution model with bypassing .

Comparing equation (3-29) with equation (3-30), it is obvious that

$p = m$ = no. of completely mixed tanks in series

$\omega = \overline{F}$ = frequency.

Thus the expression in equation (3-29) is identical with that in equation (3-30).

Moments of the impulse response curve for GCMWB. Let $Y(\theta)$ denote the impulse response of GDMWB in the dimensionless time domain θ. The kth moment of $Y(\theta)$ is then defined as

$$m_{\theta yk} = \int_0^\infty \theta^k Y(\theta) d\theta \quad , \qquad k = 1, 2, 3, \ldots$$

where the subscript θyk in $m_{\theta yk}$ refers to the kth moment of $Y(\theta)$ in the θ-domain. The Laplace transform of $Y(\theta)$ is given by

$$Y(s) = \int_0^\infty e^{-s\theta} Y(\theta) d\theta$$

which by successive differentiation with respect to s and taking the limit as s approaches zero yields (8,23)

$$\lim_{s \to 0} \frac{dY^k(s)}{ds^k} = \lim_{s \to 0} \frac{dH^k(s)}{ds^k} = (-1)^k \int_0^\infty \theta^k Y(\theta) d\theta$$

or

$$m_{\theta yk} = (-1)^k \lim_{s \to 0} \frac{dH^k(s)}{ds^k} \quad . \qquad (3\text{-}31)$$

This means that the moments of $Y(\theta)$ can be generated from the derivatives of $H(s)$ by taking the limit as s approaches zero. Using the expression of $H(s)$ given in equation (3-14), it can be shown that

$$\lim_{s\to 0} \frac{dH(s)}{ds} = -1$$

$$\lim_{s\to 0} \frac{d^2H(s)}{ds^2} = -\tau^2 + 2\tau + (1-\tau)^2(p+1)(p\beta)^{-1}$$

$$\lim_{s\to 0} \frac{d^3H(s)}{ds^3} = 2\tau^3 - 3\tau^2 - 3\tau(1-\tau)^2(p+1)(p\beta)^{-1} - (1-\tau)^3(p+2)(p+1)(p\beta)^{-2} \quad .$$

The first three moments of $Y(\theta)$ are thus given by

$$m_{\theta y1} = \mu_{\theta y} = -\lim_{s\to 0} \frac{dH(s)}{ds} = 1$$

$$m_{\theta y2} = \lim_{s\to 0} \frac{d^2H(s)}{ds^2} = -\tau^2 + 2\tau + (1-\tau)^2(p+1)(p\beta)^{-1}$$

$$m_{\theta y3} = -\lim_{s\to 0} \frac{d^3H(s)}{ds^3} = -2\tau^3 + 3\tau^2 + 3\tau(1-\tau)^2(p+1)(p\beta)^{-1} + (1-\tau)^3(p+2)(p+1)(p\beta)^{-2} \quad .$$

With these first three moments in hand, we can obtain the (relative) variance and skewness of the impulse response $Y(\theta)$ which is equivalent to the dimensionless exit age distribution $E(\theta)$ as follows:

$$\sigma^2_{\theta y} = \int_0^\infty (\theta - \mu_{\theta y})^2 Y(\theta)d\theta$$

$$= m_{\theta y2} - \mu^2_{\theta y}$$

$$= \lim_{s\to 0} \left\{ \frac{d^2H(s)}{ds^2} - \left(\frac{dH(s)}{ds}\right)^2 \right\}$$

$$= -(1-\tau)^2 + (1-\tau)^2(p+1)(p\beta)^{-1} \qquad (3\text{-}32)$$

and

$$\sigma^3_{\theta y} = \int_0^\infty (\theta - \mu_{\theta y})^3 \, Y(\theta) d\theta$$

$$= m_{\theta y 3} - 3\mu_{\theta y}\sigma^2_{\theta y} - \mu^3_{\theta y}$$

$$= -\lim_{s \to 0} \left\{ \frac{d^3 H(s)}{ds^3} - 3 \frac{dH(s)}{ds} \frac{d^2 H(s)}{ds^2} + 2\left(\frac{dH(s)}{ds}\right)^3 \right\}$$

$$= (1-\tau)^3 \left[2 - 3(p+1)(p\beta)^{-1} + (p+2)(p+1)(p\beta)^{-2} \right] \quad . \quad (3\text{-}33)$$

If

$$\beta = 1, \ \tau = 0, \ p = \text{a positive integer,}$$

equations (3-32) and (3-33) reduce to

$$\sigma^2_{\theta y} = -1 + \frac{p+1}{p} = \frac{1}{p}$$

$$\sigma^3_{\theta y} = 2 - \frac{3(p+1)}{p} + \frac{(p+2)(p+1)}{p^2} = \frac{2}{p^2} \quad . \qquad (3\text{-}34)$$

These are the (relative) variance and skewness of the impulse response curve (the dimensionless exit age distribution) for p completely stirred tanks in series. They are identical to the values given for cell model by Ahn (15)

$$\sigma^2_{\theta y} = \frac{1}{n}$$

$$\sigma^3_{\theta y} = \frac{2}{n^2} \quad . \qquad (3\text{-}35)$$

Comparing equation (3-34) with equation (3-35), we can again see that

$$p = n = \text{no. of completely mixed tanks in series.}$$

Moreover, the (relative) variance given in equation (3-34) is identical to the value given for the C curve of j stirred tanks-in-series model by Levenspiel and Bischoff (19)

$$\sigma^2_{\theta y} = \frac{1}{j} \quad .$$

If $Y(\theta)$ is referred to the pulse response to the input pulse, $X(\theta)$, for GDMWB, the difference between the variances of output and input curves and the difference between the skewnesses of output and input curves are defined as

$$\Delta\sigma^2_{\theta yx} = \sigma^2_{\theta y} - \sigma^2_{\theta x} \quad ,$$

$$\Delta\sigma^3_{\theta yx} = \sigma^3_{\theta y} - \sigma^2_{\theta x} \quad .$$

The r.h.s. of equations (3-32) and (3-33) are, indeed, representing $\Delta\sigma^2_{\theta yx}$ and $\Delta\sigma^3_{\theta yx}$ respectively. More general meanings contained in the r.h.s. of equations (3-32) and (3-33) for GDMWB will be further clarified in Chapter 4.

Gamma distribution model with overall-cross bypassing. This represents another modification of the original gamma distribution model and is depicted in Fig. 3-8. It differs from the previous one (Fig. 3-1) only in that the bypass stream is now across the whole system and joins the outlet stream of the plug flow section. To formulate the transfer function for this model, the procedure used for the preceeding model (GDMWB) can be employed. The transfer function for the Γ-mixing section is the same as equation (3-11), i.e.

$$H(s)_\Gamma = \frac{C_1(s)}{C_0(s)} = \left[\frac{p\beta}{(1-\tau)s + p\beta}\right]^p \quad , \qquad (3\text{-}36)$$

where

$$\beta = \frac{Q_1}{Q_T} \quad \text{and} \quad \tau = \frac{V_2}{V_T} \quad .$$

The transfer function for the plug flow section is

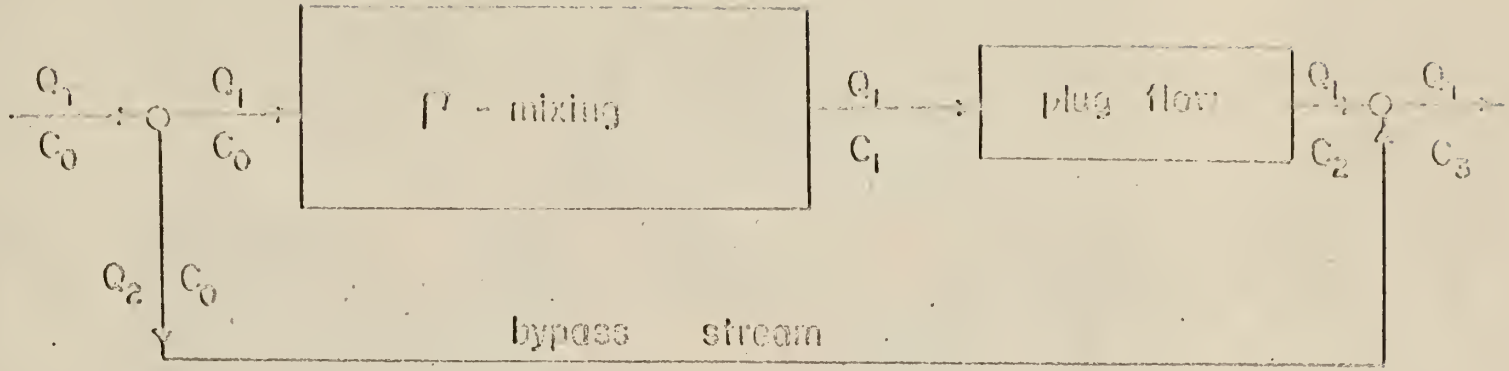

Q_1 = volumetric flow rate through the Γ - mixing section.

Q_2 = volumetric flow rate of bypass stream.

Q_T = total volumetric flow rate.

V_1 = volume of the Γ - mixing section.

V_2 = volume of the plug flow section.

V_T = total volume of the whole system.

C = tracer concentration, a function of time.

Fig. 3-8. The Γ - distribution model with overall - cross bypassing.

$$H(s)_p = \frac{C_2(s)}{C_1(s)} = e^{-\tau s} \quad . \qquad (3\text{-}37)$$

The material balance at the point where the bypass stream joins the outlet stream of the plug flow section is

$$C_3 Q_T = Q_1 C_2 + Q_2 C_0 \quad .$$

Dividing by Q_T gives

$$C_3 = \beta C_2 + (1 - \beta) C_0 \quad .$$

Taking the Laplace transform of the both sides of the equation yields

$$C_3(s) = \beta C_2(s) + (1 - \beta) C_0(s) \quad . \qquad (3\text{-}38)$$

By combining equations (3-36) through (3-38), it can be shown that the transfer function for the entire system is given by

$$H(s) = \frac{C_3(s)}{C_0(s)} = \beta \left[\frac{p\beta}{(1 - \tau)s + p\beta} \right]^p e^{-\tau s} + (1 - \beta) \quad , \qquad (3\text{-}39)$$

where p, β, and τ are the parameters and have the same physical significance described previously. In case there is no bypassing, i.e. when $\beta = 1$, equation (3-39) reduces to equation (3-7), which is the transfer function of the original Γ-distribution model.

CHAPTER 4

METHODS OF RESPONSE DATA ANALYSIS

Three methods for analyzing response data will be discussed in this chapter. The major purpose is to fit a model to the experimental data in order to determine its parameters. Although the curve fitting can be accomplished in the time domain, this is not always feasible due to the practical limitations imposed. In practice, the data are often transformed into other domains for analysis. Three methods for mathematically analyzing the response data have been briefly introduced in Chapter 2. The methods will be treated in detail in this chapter. Each method will be illustrated by an example in which the gamma distribution model with bypassing, described previously, will be used. The general flow chart of the data processing involved in the three methods is shown in Fig. 4-1.

Adjustment of the raw normalized data. It is generally recognized that the response of the pulse testing exhibits a slow decay, especially in industrial processes. In such cases data reduction becomes time consuming. Furthermore, the data in the tail part of the response curve may not be sufficiently reliable due to the error introduced in detecting and recording low tracer concentration. A general approach is to truncate the output at a certain finite value (9) and to approximate the tail from that point on by an exponential decay (12). In this work (5), another method as suggested and tested by Rooze (13) is used. This is to assume the input, $X(\theta)$, is fairly correct, while the output,

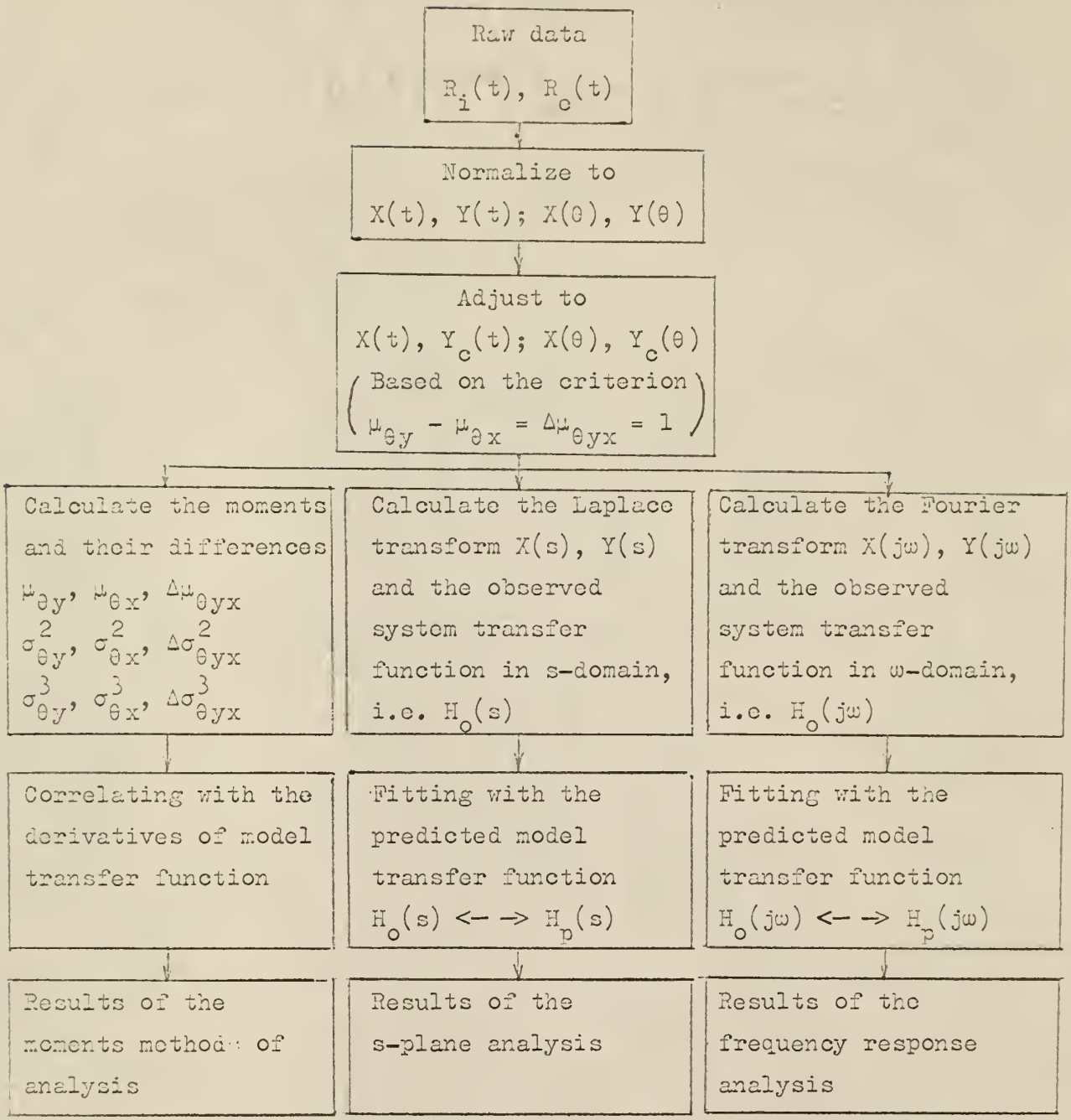

Fig. 4-1. Flow chart of the data processing involved in the three methods of response data analysis.

$Y(\theta)$, is corrected with an empirical correction formula as follows:

$$Y_c(\theta) = PY(\theta)(1 - Q\theta) \quad , \tag{4-1}$$

where θ = dimensionless time domain, $Y_c(\theta)$ represents the adjusted data, and P and Q are the correction factors. If the data are good, the values of P and Q should be close to one and zero respectively. P and Q can be computed by noting two properties of pulse testing data.

The first property as shown by equations (2-13) and (2-14) is:

$$\int_0^\infty X(\theta)d\theta = \int_0^\infty Y(\theta)d\theta = 1 \quad . \tag{4-2}$$

The second property is that for a closed system the mean of $Y(\theta)$, $\mu_{\theta y}$, minus the mean of $X(\theta)$, $\mu_{\theta x}$, is equal to unity (normalized mean residence time), which has been shown by Zwietering (2), i.e.

$$\mu_{\theta y} - \mu_{\theta x} = \Delta\mu_{\theta yx} = 1 \quad . \tag{4-3}$$

From equations (4-1) and (4-2), we have

$$\int_0^\infty Y_c(\theta)d\theta = P\int_0^\infty Y(\theta)d\theta - PQ\int_0^\infty \theta\, Y(\theta)d\theta = 1 \quad . \tag{4-4}$$

From equations (4-1) and (4-3), we have

$$\int_0^\infty \theta\, Y_c(\theta)d\theta - \int_0^\infty \theta\, X(\theta)d\theta$$

$$= P\int_0^\infty \theta Y(\theta)d\theta - PQ\int_0^\infty \theta^2 Y(\theta)d\theta - \int_0^\infty \theta X(\theta)d\theta = 1 \quad . \tag{4-5}$$

If we let

$$A = \int_0^\infty \theta Y(\theta)d\theta \ ; \ B = \int_0^\infty \theta X(\theta)d\theta \ ; \ M = \int_0^\infty \theta^2 Y(\theta)d\theta \quad ,$$

the solution of equations (4-4) and (4-5) for P and Q is given respectively by

$$P = \frac{A(1 + B) - M}{A^2 - M} \quad , \qquad Q = \frac{1 + B - A}{A(1 + B) - M} \quad .$$

Moments method of analysis (8,26). Let $Y(\theta)$ be the adjusted exit probability density function in the dimensionless time domain (here the subscript c is omitted). Then its kth moment is defined as

$$m_{\theta yk} = \int_0^\infty \theta^k Y(\theta)d\theta \quad , \qquad k = 1, 2, \ldots \tag{4-6}$$

and its Laplace transform is given by

$$Y(s) = \int_0^\infty e^{-s\theta} Y(\theta)d\theta \quad . \tag{4-7}$$

By differentiating equation (4-7) successively with respect to s and taking the limit as s approaches zero, it can be shown that

$$\lim_{s\to 0} \frac{d^k Y(s)}{ds^k} = (-1)^k m_{\theta yk} \quad , \quad k = 1, 2, \ldots \tag{4-8}$$

The mean of $Y(\theta)$ is then equal to

$$\mu_{\theta y} = \int_0^\infty \theta Y(\theta)d\theta = m_{\theta y1} = -\lim_{s\to 0} \frac{dY(s)}{ds} \quad , \tag{4-9}$$

its variance is

$$\sigma^2_{\theta y} = \int_0^\infty (\theta - \mu_{\theta y})^2 \, Y(\theta) d\theta$$

$$= m_{\theta y 2} - \mu^2_{\theta y}$$

$$= \lim_{s \to 0} \left[\frac{d^2 Y(s)}{ds^2} - \left(\frac{dY(s)}{ds} \right)^2 \right] \qquad (4\text{-}10)$$

and its skewness is

$$\sigma^3_{\theta y} = \int_0^\infty (\theta - \mu_{\theta y})^3 \, Y(\theta) d\theta$$

$$= m_{\theta y 3} - 3\mu_{\theta y} \sigma^2_{\theta y} - \mu^3_{\theta y}$$

$$= - \lim_{s \to 0} \left[\frac{d^3 Y(s)}{ds^3} - 3 \frac{dY(s)}{ds} \frac{d^2 Y(s)}{ds^2} + 2 \left(\frac{dY(s)}{ds} \right)^3 \right] . \qquad (4\text{-}11)$$

Similarly, it can be shown that the mean of $X(\theta)$ is

$$\mu_{\theta x} = - \lim_{s \to 0} \frac{dX(s)}{ds} , \qquad (4\text{-}12)$$

its variance is

$$\sigma^2_{\theta x} = \lim_{s \to 0} \left[\frac{d^2 X(s)}{ds^2} - \left(\frac{dX(s)}{ds} \right)^2 \right] , \qquad (4\text{-}13)$$

and its skewness is

$$\sigma^3_{\theta x} = - \lim_{s \to 0} \left[\frac{d^3 X(s)}{ds^3} - 3 \frac{dX(s)}{ds} \frac{d^2 X(s)}{ds^2} + 2 \left(\frac{dX(s)}{ds} \right)^3 \right] , \qquad (4\text{-}14)$$

where

$$X(s) = \int_0^\infty e^{-s\theta} X(\theta)d\theta \quad . \tag{4-15}$$

Now consider the system transfer function, which is given by

$$H(s) = \frac{Y(s)}{X(s)} \quad . \tag{4-16}$$

As shown by Otto (8), successive differentiation of equation (4-16) yields

$$\frac{H'(s)}{H(s)} = \frac{Y'(s)}{Y(s)} - \frac{X'(s)}{X(s)} \tag{4-17}$$

$$\frac{H''(s)}{H(s)} - \frac{H'^2(s)}{H^2(s)} = \left[\frac{Y''(s)}{Y(s)} - \frac{Y'^2(s)}{Y^2(s)}\right] - \left[\frac{X''(s)}{X(s)} - \frac{X'^2(s)}{X^2(s)}\right] \tag{4-18}$$

$$\frac{H'''(s)}{H(s)} - 3\,\frac{H''(s)H'(s)}{H^2(s)} + 2\,\frac{H'^3(s)}{H^3(s)}$$

$$= \left[\frac{Y'''(s)}{Y(s)} - 3\,\frac{Y''(s)Y'(s)}{Y^2(s)} + 2\,\frac{Y'^3(s)}{Y^3(s)}\right]$$

$$- \left[\frac{X'''(s)}{X(s)} - 3\,\frac{X''(s)X'(s)}{X^2(s)} + 2\,\frac{X'^3(s)}{X^3(s)}\right] \quad . \tag{4-19}$$

From the properties of the probability density functions, $X(\theta)$ and $Y(\theta)$, we can show that

$$\lim_{s\to 0} X(s) = \lim_{s\to 0} \int_0^\infty e^{-s\theta} X(\theta)d\theta = \int_0^\infty X(\theta)d\theta = 1 \tag{4-20}$$

and

$$\lim_{s\to 0} Y(s) = \lim_{s\to 0} \int_0^\infty e^{-s\theta} Y(\theta)d\theta = \int_0^\infty Y(\theta)d\theta = 1 \quad . \tag{4-21}$$

Hence

$$\lim_{s\to 0} H(s) = \lim_{s\to 0} \frac{Y(s)}{X(s)} = 1 \quad . \tag{4-22}$$

By taking the limit of equations (4-17) through (4-19) as s approaches zero and by making use of the relations derived in equations (4-9) through (4-14) and equations (4-20) through (4-22), it can be shown that:

$$\lim_{s\to 0} \frac{dH(s)}{ds} = -(\mu_{\theta y} - \mu_{\theta x}) = -\Delta\mu_{\theta yx} = -1 \quad , \tag{4-23}$$

$$\lim_{s\to 0} \left[\frac{d^2H(s)}{ds^2} - \left(\frac{dH(s)}{ds}\right)^2\right] = \sigma^2_{\theta y} - \sigma^2_{\theta x} = \Delta\sigma^2_{\theta yx} \quad , \tag{4-24}$$

$$\lim_{s\to 0} \left[\frac{d^3H(s)}{ds^3} - 3\,\frac{dH(s)}{ds}\,\frac{d^2H(s)}{ds^2} + 2\left(\frac{dH(s)}{ds}\right)^3\right]$$

$$= -(\sigma^3_{\theta y} - \sigma^3_{\theta x}) = -\Delta\sigma^3_{\theta yx} \quad . \tag{4-25}$$

These equations, equations (4-23) through (4-25), are the relationships required in fitting a 2-parameter model to experimental data. Equation (4-23), however, is an invariant for a closed flow system and is independent of the variation of model parameters and only equations (4-24) and (4-25) are actually used. The far right hand sides of equations (4-24) and (4-25) are evaluated from experimental data, while the far left hand sides are derived from the transfer function of the model which contains two parameters. In general, n + 1 moments are required for an n-parameter model.

The moments method described above seems to provide a simple means of fitting models to the experimental data since this method generally requires less computational time than other methods. However, a serious

fault of this method is that too much weight is placed on the tail part of $Y(\theta)$ corresponding to large values of θ. As has been stated, the tail of $Y(\theta)$ may not be reliable due to the difficulties of measuring tracer concentration accurately at low concentrations. In case it becomes necessary to use higher moments for fitting a model, this method tends to become less reliable. Another disadvantage is that the results of analysis provide no information on how well a particular model fits the data, unless we choose to compare the response of the model with the experimental response in the time domain after the parameters have been computed.

An illustration using GDMWB. The transfer function of the model as given in equation (3-14) is

$$H(s) = \left\{\beta \left[\frac{p\beta}{(1-\tau)s + p\beta}\right]^p + (1-\beta)\right\} e^{-\tau s} \quad . \tag{4-26}$$

By differentiating this equation successively with respect to s and taking the limits of the derivatives as s approaches zero, it can be shown that

$$\lim_{s\to 0} \frac{dH(s)}{ds} = -1 \quad , \tag{4-27}$$

$$\lim_{s\to 0} \frac{d^2H(s)}{ds^2} = -\tau^2 + 2\tau + (1-\tau)^2(p+1)(p\beta)^{-1} \quad , \tag{4-28}$$

$$\lim_{s\to 0} \frac{d^3H(s)}{ds^3} = 2\tau^3 - 3\tau^2 - 3\tau(1-\tau)^2(p+1)(p\beta)^{-1} - (p+2)(p+1)(1-\tau)^3(p\beta)^{-2} \quad . \tag{4-29}$$

Note that equation (4-27) verifies an invariant of a closed flow system mentioned previously (2). If equations (4-27) through (4-29) are substituted into equations (4-24) and (4-25), it can be shown that

$$(1-\tau)^2\left[-1 + (p+1)(p\beta)^{-1}\right] = \Delta\sigma^2_{\theta yx} \quad , \tag{4-30}$$

$$(1-\tau)^3\left[2 - 3(p+1)(p\beta)^{-1} + (p+2)(p+1)(p\beta)^{-2}\right] = \Delta\sigma^3_{\theta yx} \quad , \tag{4-31}$$

where τ is the dimensionless dead time and $\Delta\sigma^2_{\theta yx}$ and $\Delta\sigma^3_{\theta yx}$ are evaluated from the experimental data.

If the experimentally observed τ is used, the model parameters, p and β, can be determined by solving simultaneously equations (4-30) and (4-31), which are obviously non-linear. Linearization of the equations over a limited range by using the Taylor series expansion and truncating all but the linear terms will be used to solve this problem. By rearranging equations (4-30) and (4-31) and setting

$$F(p,\beta) = (1-\tau)^2\left[-1 + (p+1)(p\beta)^{-1}\right] - \Delta\sigma^2_{\theta yx} = 0 \quad , \tag{4-32}$$

$$G(p,\beta) = (1-\tau)^3\left[2 - 3(p+1)(p\beta)^{-1} + (p+2)(p+1)(p\beta)^{-2}\right] - \Delta\sigma^3_{\theta yx} = 0 \quad , \tag{4-33}$$

the Taylor series expansion around the initial guess p_o, β_o gives

$$F(p_o+\Delta p,\beta_o+\Delta\beta) = F(p_o,\beta_o) + \Delta p \left.\frac{\partial F}{\partial p}\right|_{p_o,\beta_o} + \Delta\beta \left.\frac{\partial F}{\partial \beta}\right|_{p_o,\beta_o} = 0 \quad ,$$

$$G(p_o+\Delta p,\beta_o+\Delta\beta) = G(p_o,\beta_o) + \Delta p \left.\frac{\partial G}{\partial p}\right|_{p_o,\beta_o} + \Delta\beta \left.\frac{\partial G}{\partial \beta}\right|_{p_o,\beta_o} = 0 \quad ,$$

where the higher order terms in $\Delta p = p-p_o$ and $\Delta\beta = \beta-\beta_o$ are neglected. The solution for Δp and $\Delta\beta$ are then given by

$$\Delta p = \frac{G(p_o,\beta_o)\left.\frac{\partial F}{\partial \beta}\right|_{p_o,\beta_o} - F(p_o,\beta_o)\left.\frac{\partial G}{\partial \beta}\right|_{p_o,\beta_o}}{\left.\frac{\partial F}{\partial p}\right|_{p_o,\beta_o}\left.\frac{\partial G}{\partial \beta}\right|_{p_o,\beta_o} - \left.\frac{\partial F}{\partial \beta}\right|_{p_o,\beta_o}\left.\frac{\partial G}{\partial p}\right|_{p_o,\beta_o}} \quad , \tag{4-34}$$

$$\Delta\beta = \frac{F(p_o,\beta_o)\left.\frac{\partial G}{\partial p}\right|_{p_o,\beta_o} - G(p_o,\beta_o)\left.\frac{\partial F}{\partial p}\right|_{p_o,\beta_o}}{\left.\frac{\partial F}{\partial p}\right|_{p_o,\beta_o}\left.\frac{\partial G}{\partial \beta}\right|_{p_o,\beta_o} - \left.\frac{\partial F}{\partial \beta}\right|_{p_o,\beta_o}\left.\frac{\partial G}{\partial p}\right|_{p_o,\beta_o}} \quad . \quad (4\text{-}35)$$

These are used to determine magnitudes for increments to obtain improved values of the parameters, p and β. The computing procedure is as follows (20,21).

1. Guess initial values of parameters as p^i and β^i.
2. Calculate the increments of p and β by using equations (4-34) and (4-35).
3. Obtain the new values of the parameters as

$$p^{i+1} = p^i + \Delta p^i$$

$$\beta^{i+1} = \beta^i + \Delta\beta^i \quad .$$

4. Repeat 2 and 3 until no further significant improvement is achieved.

For practical purposes, the correction is initiated by taking Δp and Δβ as one fifth of the step sizes given in equations (4-34) and (4-35) in order to assure the success of convergence.

The partial differential terms required for computation in equations (4-34) and (4-35) are given below.

$$\frac{\partial F}{\partial \beta} = \frac{-(1-\tau)^2}{\beta p^2} \quad ,$$

$$\frac{\partial F}{\partial p} = \frac{-(1-\tau)^2\,(p+1)}{p\beta^2} \quad ,$$

$$\frac{\partial G}{\partial p} = (1-\tau)^3\,\frac{3p(\beta-1)-4}{\beta^2 p^3} \quad ,$$

$$\frac{\partial G}{\partial \beta} = (1 - \tau)^3 \frac{3p\beta(p + 1) - 2(p + 2)(p + 1)}{\beta^3 p^2} \quad .$$

The values of $\Delta\sigma^2_{\theta yx}$ and $\Delta\sigma^3_{\theta yx}$ can be obtained from the experimental data as follows:

$$\Delta\sigma^2_{\theta yx} = \sigma^2_{\theta y} - \sigma^2_{\theta x} \quad ,$$

$$\Delta\sigma^3_{\theta yx} = \sigma^3_{\theta y} - \sigma^3_{\theta x} \quad ,$$

where

$$\sigma^2_{\theta y} = m_{\theta y2} - \mu^2_{\theta y} = m_{\theta y2} - m^2_{\theta y1} \quad ,$$

$$\sigma^2_{\theta x} = m_{\theta x2} - \mu^2_{\theta x} = m_{\theta x2} - m^2_{\theta x1} \quad ,$$

$$\sigma^3_{\theta y} = m_{\theta y3} - 3m_{\theta y1}\,\sigma^2_{\theta y} - m^3_{\theta y1} \quad ,$$

$$\sigma^3_{\theta x} = m_{\theta x3} - 3m_{\theta x1}\,\sigma^2_{\theta x} - m^3_{\theta x1} \quad .$$

It can be seen that the quantities required for evaluation of $\Delta\sigma^2_{\theta yx}$ and $\Delta\sigma^3_{\theta yx}$ are essentially the moments of both $Y(\theta)$ and $X(\theta)$. In the present case, the first through the third moment must be found. The moments for both $Y(\theta)$ and $X(\theta)$ are numerically evaluated by

$$m_{\theta yk} = \int_0^\infty \theta^k Y(\theta)\,d\theta = \sum_{i=1}^{N} \theta_i^k Y(\theta_i)\Delta\theta_i \quad ,$$

$$m_{\theta xk} = \int_0^\infty \theta^k X(\theta)\,d\theta = \sum_{i=1}^{M} \theta_i^k X(\theta_i)\Delta\theta_i \quad ,$$

where

$k = 1, 2, 3$

Another method for evaluating $\Delta\sigma^2_{\theta yx}$ and $\Delta\sigma^3_{\theta yx}$ is by

$$\Delta\sigma^2_{\theta yx} = \frac{\sigma^2_{ty} - \sigma^2_{tx}}{\bar{t}^2} \quad ,$$

$$\Delta\sigma^3_{\theta yx} = \frac{\sigma^3_{ty} - \sigma^3_{tx}}{\bar{t}^3} \quad ,$$

where

$\bar{t}$ = mean residence time,

and σ^2_{ty}, σ^2_{tx}, σ^3_{ty} and σ^3_{tx} are the variances and skewnesses of $Y(t)$ and $X(t)$ respectively in the (real) time domain. σ^2_{ty}, σ^3_{ty}, σ^2_{tx} and σ^3_{tx} can be evaluated by equations (2-17), (2-18), (2-21) and (2-22), which in turn can be obtained from the few fundamental moments of both $Y(t)$ and $X(t)$. Recalling that

$$\int_0^\infty Y(t)dt = 1 \quad ,$$

we can write the kth moment of $Y(t)$ as

$$m_{tyk} = \frac{\int_0^\infty t^k Y(t)dt}{\int_0^\infty Y(t)dt} \quad , \qquad k = 1, 2, 3$$

Actually, this is true even if $Y(t)$ is not normalized. If values $Y(t)$ are read at N equidistant points on the time axis, m_{tyk} can be numerically computed as

$$m_{tyk} = \frac{\sum_{i=1}^{N} t_i^k Y(t_i)}{\sum_{i=1}^{N} Y(t_i)} \quad , \qquad k = 1, 2, 3$$

σ_{ty}^2 and σ_{ty}^3 are then obtained by

$$\sigma_{ty}^2 = m_{ty2} - m_{ty1}^2 = m_{ty2} - \mu_{ty}^2 \quad ,$$

$$\sigma_{ty}^3 = m_{ty3} - 3m_{ty1}\sigma_{ty}^2 - m_{ty1}^3 \quad .$$

σ_{tx}^2 and σ_{tx}^3 are obtained similarly. The mean residence time, $\bar{t}$, can be measured from the experimental condition as

$$\bar{t} = \frac{V}{Q} \quad ,$$

where

V = total fluid volume of the system,

Q = steady flow rate.

s-plane analysis (9,27). This method in essence consists of fitting the model to the experimental data in the Laplace (s) domain. The Laplace transform of $Y(\theta)$, by definition, is

$$Y(s) = \int_0^\infty e^{-s\theta} Y(\theta) d\theta \qquad (4\text{-}36)$$

and the Laplace transform of $X(\theta)$ is

$$X(s) = \int_0^\infty e^{-s\theta} X(\theta) d\theta \qquad (4\text{-}37)$$

where

s = real and positive values.

The numerical calculation of Y(s), as given by Johnson (5), is to approximate it by a staircase integration, i.e.

$$Y(s) = \sum_{n=1}^{N} Y(s)_n$$

$$= \sum_{n=1}^{N} \left(\frac{Y(\theta)_{n-1} + Y(\theta)_n}{2}\right) \int_{\theta_{n-1}}^{\theta_n} e^{-s\theta}\, d\theta$$

$$= \sum_{n=1}^{N} \frac{-1}{2s}\left[Y(\theta)_{n-1} + Y(\theta)_n\right](e^{-s\theta_n} - e^{-s\theta_{n-1}})$$

$$= \frac{1}{2s}\left\{(Y(\theta)_0 + Y(\theta)_1)e^{-s\theta_0} + \sum_{n=1}^{N-1}(Y(\theta)_{n+1} - Y(\theta)_{n-1})e^{-s\theta_n}\right.$$

$$\left. -(Y(\theta)_{N-1} + Y(\theta)_N)e^{-s\theta_N}\right\} \quad . \qquad (4\text{-}38)$$

The numerical calculation of X(s) is carried out similarly. The observed transfer function of the system is then given by

$$H_o(s) = \frac{Y(s)}{X(s)} \quad . \qquad (4\text{-}39)$$

If the model selected is good enough to describe the system, there must be a set of parameter values in the (predicted) transfer function of the model, $H_p(s)$, such that

$$H_p(s_i) \cong H_o(s_i) \quad , \quad \text{for} \quad i = 1, 2, \ldots, N \, .$$

The criterion for selecting such a set of parameter values is that the (squared) error function, φ, is a minimum, i.e.

$$\varphi = \sum_{i=1}^{N}\left[H_p(s_i) - H_o(s_i)\right]^2 = \text{minimum}, \qquad (4\text{-}40)$$

where φ is the sum of the squared deviations between the data points

and the corresponding points predicted by the model. The goodness of fit is expressed by the value of φ. Theoretically, it is best to fit the data over the entire range of s domain, i.e. $0 \leq s < \infty$. In practice, the use of integer values of s ranging from 1 to 10 may lead to acceptable results. This can be visualized through the Laplace transform equations (4-36) and (4-37), where the term $e^{-s\theta}$ acts as a weighting function for both $Y(\theta)$ and $X(\theta)$. Generally, the response, $Y(\theta)$, has the properties of small amplitude, wide dispersion and slow decay as compared to the input, $X(\theta)$. The numerical value of $H_o(s)$ becomes smaller as s becomes larger. On the other hand, the transfer function predicted from the model, $H_p(s)$, such as given by equation (4-26), also approaches zero as s becomes larger. This is to say that a large value of s tends to reduce the effect of variation of the parameters of the model. Since fitting the model with too large a value of s gives no sensible results, it is desirable to select s = 10 as an upper bound to replace $s = \infty$. On the other hand, it is true that

$$\lim_{s\to 0} H_o(s) = \lim_{s\to 0} \frac{\int_0^\infty e^{-s\theta}\, Y(\theta)\, d\theta}{\int_0^\infty e^{-s\theta}\, X(\theta)\, d\theta} = \frac{\int_0^\infty Y(\theta)\, d\theta}{\int_0^\infty X(\theta)\, d\theta} = 1$$

and

$$\lim_{s\to 0} H_p(s) = 1 \quad .$$

This means that small values of s also tend to reduce the effect of variation of the parameters in the model. This is why s = 1 is selected as a lower bound of fit instead of starting from s = 0.

By using the same argument, it can be seen from equation (4-36)

that at large value of θ, the term $e^{-s\theta}$, acting as a weighting function for $Y(\theta)$, becomes very small as θ becomes large. This is why numerically transforming the $Y(\theta)$ data into the s-domain tends to reduce the errors in the tail portion of the response curve (9). Response curves of the model can be compared with experimental curves in the $H(s)$ vs. s plane and the goodness of fit can be expressed in terms of the error function, φ. These are the advantages associated with the s-plane analysis. The disadvantage is that the fit obtained does not guarantee the best in the least squares sense in the time domain.

An illustration using GDMWB. In this case the predicted transfer function of the model as given by equation (3-14) is

$$H_p(s) = \left\{\beta\left[\frac{p\beta}{(1-\tau)s + p\beta}\right]^p + (1-\beta)\right\} e^{-\tau s} \quad . \qquad (4\text{-}41)$$

The criterion of fitting the model to the experimental data is then to minimize

$$\varphi = \sum_{i=1}^{N}\left[H_p(s_i) - H_o(s_i)\right]^2 = \varphi(p,\beta) \quad . \qquad (4\text{-}42)$$

By using the observed dimensionless dead time τ and evaluating $H_o(s_i)$ from the experimental data by means of equation (4-39), the two parameters, p and β, can be determined from equation (4-44).

The Taylor series expansion of φ in the neighborhood of first guess, p_o and β_o, and truncating all but the linear terms yields

$$H_p(s_i) = H_p(s_i)\Big|_{p_o,\beta_o} + (\Delta p)\frac{\partial H_p(s_i)}{\partial p}\Big|_{p_o,\beta_o} + (\Delta\beta)\frac{\partial H_p(s_i)}{\partial \beta}\Big|_{p_o,\beta_o} \quad , \quad i = 1, 2, \ldots N \qquad (4\text{-}43)$$

where

$$\Delta p = p - p_o, \quad \Delta\beta = \beta - \beta_o \quad .$$

Let

$$H_p(s_i)\Big|_{p_o,\beta_o} - H_o(s_i) = Q_i \quad ,$$

$$\frac{\partial H_p(s_i)}{\partial p}\Bigg|_{p_o,\beta_o} = \left\{\beta^{p+1}\left(\frac{p}{(1-\tau)s_i + p\beta}\right)^p \left[\frac{(1-\tau)s_i}{(1-\tau)s_i + p\beta} + \ln\left(\frac{p\beta}{(1-\tau)s_i + p\beta}\right)\right] e^{-\tau s_i}\right\}_{p_o,\beta_o} = A_i \quad ,$$

$$\frac{\partial H_p(s_i)}{\partial \beta}\Bigg|_{p_o,\beta_o} = \left\{\left[\beta^{p+1}\left(\frac{p}{(1-\tau)s_i + p\beta}\right)^p \left(\frac{p+1}{\beta} - \frac{p^2}{(1-\tau)s_i + p\beta}\right) - 1\right] e^{-\tau s_i}\right\}_{p_o,\beta_o} = B_i \quad ,$$

then we have the error function as

$$\varphi = (Q_i + A_i\,\Delta p + B_i\,\Delta\beta)^2 \quad .$$

The method of least squares states that we should seek an unrestricted minimum of φ. This requires that

$$\frac{\partial \varphi}{\partial(\Delta p)} = \frac{\partial \varphi}{\partial p} = 0 \quad , \quad \frac{\partial \varphi}{\partial(\Delta\beta)} = \frac{\partial \varphi}{\partial \beta} = 0 \quad ,$$

or

$$\sum_{i=1}^{N} (Q_i + A_i\,\Delta p + B_i\,\Delta\beta)A_i = 0 \quad , \tag{4-44}$$

$$\sum_{i=1}^{N} (Q_i + A_i\,\Delta p + B_i\,\Delta\beta)B_i = 0 \quad . \tag{4-45}$$

Solving simultaneously equations (4-44) and (4-45) gives the magnitudes of increments for obtaining improved values of p and β as

$$\Delta p = \frac{\sum_{i=1}^{N} B_i Q_i \sum_{i=1}^{N} A_i B_i - \sum_{i=1}^{N} A_i Q_i \sum_{i=1}^{N} B_i^2}{\sum_{i=1}^{N} A_i^2 \sum_{i=1}^{N} B_i^2 - \left(\sum_{i=1}^{N} A_i B_i\right)^2} , \qquad (4\text{-}46)$$

$$\Delta \beta = \frac{\sum_{i=1}^{N} A_i Q_i \sum_{i=1}^{N} A_i B_i - \sum_{i=1}^{N} B_i Q_i \sum_{i=1}^{N} A_i^2}{\sum_{i=1}^{N} A_i^2 \sum_{i=1}^{N} B_i^2 - \left(\sum_{i=1}^{N} A_i B_i\right)^2} . \qquad (4\text{-}47)$$

The computing logic is the same as that used previously in the moments method. An iterative computation is performed until the values of increments converge to the desired tolerance.

Frequency response analysis (16,17,28). In this method we try to fit the model in the frequency (ω) domain. The first step is to calculate the observed transfer function of the system in the ω-domain from the experimental response data. This is done by applying the Fourier transformations to both $Y(\theta)$ and $X(\theta)$ and taking their ratio as follows:

$$H_o(j\omega) = \frac{\int_0^\infty e^{-j\omega\theta} Y(\theta) d\theta}{\int_0^\infty e^{-j\omega\theta} X(\theta) d\theta} , \qquad (4\text{-}48)$$

or

$$H_o(j\omega) = \frac{\int_0^\infty Y(\theta)\cos\omega\theta\, d\theta - j\int_0^\infty Y(\theta)\sin\omega\theta\, d\theta}{\int_0^\infty X(\theta)\cos\omega\theta\, d\theta - j\int_0^\infty X(\theta)\sin\omega\theta\, d\theta} , \qquad (4\text{-}49)$$

where

$$j = \sqrt{-1}$$

ω = frequency, rad./unit dimensionless time,

θ = dimensionless time.

Let

$$\left.\begin{aligned} A &= \int_0^\infty Y(\theta)\cos \omega\theta \, d\theta \\ B &= \int_0^\infty Y(\theta)\sin \omega\theta \, d\theta \\ C &= \int_0^\infty X(\theta)\cos \omega\theta \, d\theta \\ D &= \int_0^\infty X(\theta)\sin \omega\theta \, d\theta \end{aligned}\right\} , \tag{4-50}$$

then we can simplify equation (4-49) into a standard form of complex variable as

$$H_o(j\omega) = \frac{A - jB}{C - jD} = \frac{AC + BD}{C^2 + D^2} + j\,\frac{AD - BC}{C^2 + D^2} \quad . \tag{4-51}$$

The real part of $H_o(j\omega)$ is then

$$R_o(\omega) = \frac{AC + BD}{C^2 + D^2} \tag{4-52}$$

and the imaginary part is

$$I_o(\omega) = \frac{AD - BC}{C^2 + D^2} \quad . \tag{4-53}$$

The amplitude ratio and phase angle are then given by

$$A.R. = \left| H_o(j\omega) \right| = \left(\frac{A^2 + B^2}{C^2 + D^2} \right)^{\frac{1}{2}} \quad , \tag{4-54}$$

$$\text{Phase Angle} = \angle H_o(j\omega) = \tan^{-1} \frac{AD - BC}{AC + BD} \quad . \qquad (4\text{-}55)$$

It can be seen that A, B, C and D are the essential terms needed for evaluating equations (4-51) through (4-55). Since analytical expressions for $X(\theta)$ and $Y(\theta)$ are not known, these terms must be evaluated numerically. In order to illustrate the numerical technique which has been used in this investigation, consider the integral A of equation (4-50). As suggested by Huss and Donegan (16), $Y(\theta)$ is approximated by a staircase type function having equal dimensionless time intervals and of such height that the area under each step of the staircase function equals the area under that portion of the $Y(\theta)$ curve within the interval. Thus A can be expressed as

$$A = \sum_{n=1}^{N} \overline{Y}(\theta)_n \int_{\theta_{n-1}}^{\theta_n} \cos \omega\theta \, d\theta \quad , \qquad (4\text{-}56)$$

where $\overline{Y}(\theta)_n$ is the amplitude of the staircase approximation in the interval between θ_{n-1} and θ_n. $\overline{Y}(\theta)_n$ can be obtained by a parabolic approximation as (5)

$$\overline{Y}(\theta)_n = \frac{1}{12} \left\{ 5Y(\theta_{n-1}) + 8Y(\theta_n) - Y(\theta_{n+1}) \right\} \quad , \qquad (4\text{-}57)$$

or simply by a straight line approximation as

$$\overline{Y}(\theta)_n = \frac{1}{2} \left\{ Y(\theta)_{n-1} + Y(\theta)_n \right\} \quad . \qquad (4\text{-}58)$$

If the dimensionless time interval, $\Delta\theta_n = \theta_n - \theta_{n-1}$, is taken small enough, the approximation given by equation (4-58) is satisfactory. If the experimental data are read with fairly large intervals, approximation by equation (4-57) is preferred.

Now consider the right hand side of equation (4-56), which, upon completion of integration, can be further simplified to

$$A = \sum_{n=1}^{N} \bar{Y}(\theta)_n \frac{1}{\omega} (\sin \omega\theta_n - \sin \omega\theta_{n-1})$$

$$= \sum_{n=1}^{N} \bar{Y}(\theta)_n \frac{2}{\omega} \sin \frac{\omega}{2} (\theta_n - \theta_{n-1}) \cos \frac{\omega}{2} (\theta_n + \theta_{n-1}) \quad .$$

If the dimensionless time interval is fixed at a constant value of $\Delta\theta_y$ we have

$$\theta_n - \theta_{n-1} = \Delta\theta_y$$

and

$$\theta_n + \theta_{n-1} = (2n - 1)\Delta\theta_y \quad .$$

Thus, we finally obtain

$$A = \sum_{n=1}^{N} \bar{Y}(\theta)_n \frac{2}{\omega} \sin(\frac{\omega}{2} \Delta\theta_y) \cos \left[\frac{\omega}{2} (2n-1) \Delta\theta_y\right] \quad . \qquad (4\text{-}59)$$

In a similar manner, we can obtain the expressions for B, C, and D as follows:

$$B = \sum_{n=1}^{N} \bar{Y}(\theta)_n \frac{2}{\omega} \sin(\frac{\omega}{2} \Delta\theta_y) \sin \left[\frac{\omega}{2} (2n-1) \Delta\theta_y\right] \quad , \qquad (4\text{-}60)$$

$$C = \sum_{m=1}^{M} \bar{X}(\theta)_m \frac{2}{\omega} \sin(\frac{\omega}{2} \Delta\theta_x) \cos \left[\frac{\omega}{2} (2m-1) \Delta\theta_x\right] \quad , \qquad (4\text{-}61)$$

$$D = \sum_{m=1}^{M} \bar{X}(\theta)_m \frac{2}{\omega} \sin(\frac{\omega}{2} \Delta\theta_x) \sin \left[\frac{\omega}{2} (2m-1) \Delta\theta_x\right] \quad . \qquad (4\text{-}62)$$

where $\Delta\theta_x$ is the equal dimensionless time interval of the input data,

$X(\theta)$ and M is the number of steps in the staircase approximating the input data. In general, $\Delta\theta_x$ is not necessarily equal to $\Delta\theta_y$, and more steps are required to approximate the output, $Y(\theta)$, than the input, $X(\theta)$, i.e., usually

$$N > M \quad .$$

Consider now the transfer function of the model, which is expressed in the frequency domain as

$$H_p(j\omega) = R_p(\omega) + j\, I_p(\omega) \quad , \tag{4-63}$$

where $R_p(\omega)$ is the real part and $I_p(\omega)$ is the imaginary part. If the model selected is good enough to describe the flow pattern, there must be a corresponding set of parameters contained in $H_p(j\omega)$ such that

$$H_p(j\omega_i) \cong H_o(j\omega_i) \quad , \quad \text{for } i = 1, 2, \ldots, J$$

Again, the criterion of fit is to select a set of parameters such that the (squared) error function, φ, is a minimum, i.e.

$$\varphi = \sum_{i=1}^{J} \left\{ \left[R_p(\omega_i) - R_o(\omega_i) \right]^2 + \left[I_p(\omega_i) - I_o(\omega_i) \right]^2 \right\} \tag{4-64}$$

$$= \text{Minimum.}$$

Note that J is the total number of frequencies selected for fitting, which is not related to N in equation (4-59) or M in equation (4-61).

A careful consideration must be given to the range of the value of ω to be adopted for fitting the model. According to Schnelle (17), the reliability of the real and imaginary part of $H_o(j\omega)$ and also the amplitude ratio and phase angle decreases as ω is increased. This can be visualized through the numerical calculation of A, B, C and D. They all become very small at high frequency, which in turn gives the

evaluation in equations (4-52) through (4-55) as a small numerator divided by a small denominator. As the truncating errors are already imposed on the experimental data and A, B, C and D are all obtained by the staircase approximation, the significant digits lost in the data processing lead to serious errors in the high frequency evaluation for equations (4-52) through (4-55). This may give rise to misinterpretation of system dynamics at high values of ω.

An estimate of the largest value of ω which should be used can be obtained by computing the normalized frequency content, $s(\omega)_n$, of the input and output pulse. The normalized frequency contents, $s(\omega)_{nx}$ amd $s(\omega)_{ny}$ for $X(\theta)$ and $Y(\theta)$ respectively, are given by Schnelle (17) as

$$s(\omega)_{nx} = \frac{\sqrt{C^2 + D^2}\,\Big|_{\omega=\omega}}{\sqrt{C^2 + D^2}\,\Big|_{\omega=0}}$$

$$s(\omega)_{ny} = \frac{\sqrt{A^2 + B^2}\,\Big|_{\omega=\omega}}{\sqrt{A^2 + B^2}\,\Big|_{\omega=0}} \qquad (4\text{-}65)$$

When either output or input normalized frequency content approaches the order of magnitude of the experimental error, the reliability of the calculated values of $R_o(\omega)$, $I_o(\omega)$, amplitude ratio, and the phase angle degenerate. This can be visualized through the results of data processing for experimental data. An irregular fluctuation at high frequency is seen. The largest value of ω to be fitted can be estimated by careful observation of the previous results of data processing. $s(\omega)_n$ is around 4%, which is roughly the magnitude of experimental error in this work.

The frequency response analysis actually fits the model along the purely imaginary axis, $j\omega$, instead of the real positive axis, s, as used in the s-plane analysis. The criterion of fit is the same as that used in the s-plane analysis. The advantage of this method is as follows. Parseval's theorem (18,28),

$$\int_0^\infty \left| Y_p(t) - Y_o(t) \right|^2 dt = \frac{1}{\pi} \int_0^\infty \left| Y_p(j\omega) - Y_o(j\omega) \right|^2 d\omega \quad , \qquad (4\text{-}66)$$

implies that a minimization of response deviations in the frequency domain also leads to a minimization of response deviations in the time domain. The r.h.s. of equation (4-66) can be rewritten as

$$\frac{1}{\pi} \int_0^\infty \left| Y_p(j\omega) - Y_o(j\omega) \right|^2 d\omega = \frac{1}{\pi} \int_0^\infty \left| X(j\omega) \right|^2 \left| H_p(j\omega) - H_o(j\omega) \right|^2 d\omega \quad .$$

This means that the minimization of the deviations between the predicted and observed transfer functions in the frequency domain with respect to a given pulse input gives rise to the minimization of the deviations of response in the time domain. The disadvantages arise from the fact that the expression for $H_p(j\omega)$ must be obtained by substituting $j\omega$ for s in $H_p(s)$ and separating it into the real and imaginary parts. This in itself is a formidable task for a complicated expression representing the model transfer function. Moreover, the least squares error criterion requires the consideration of both the real and imaginary parts for each ω, which, of course, leads to more computational time as compared to that of the s-plane analysis.

An illustration using GDMMB. In this case the predicted transfer

function of the model, expressed in the frequency domain, is given by equation (3-26) as

$$H_p(j\omega) = R_p(\omega) + j\, I_p(\omega) \quad , \tag{4-67}$$

where the real part is

$$R_p(\omega) = \beta \left\{ 1 + \left[\frac{(1-\tau)\omega}{p\beta} \right]^2 \right\}^{-\frac{p}{2}} \cos(pZ-\tau\omega) + (1-\beta)\cos \tau\omega$$

and the imaginary part is

$$I_p(\omega) = \beta \left\{ 1 + \left[\frac{(1-\tau)\omega}{p\beta} \right]^2 \right\}^{-\frac{p}{2}} \sin(pZ-\tau\omega) - (1-\beta)\sin \tau\omega$$

and

$$j = \sqrt{-1} \quad ,$$

ω = frequency, rad./unit dimensionless time ,

$$Z = \tan^{-1} \left(- \frac{1-\tau}{p\beta} \omega \right) \quad .$$

Again the criterion of fitting the model to the experimental data is then to minimize

$$\varphi = \sum_{i=1}^{N} \left[H_p(j\omega_i) - H_o(j\omega_i) \right]^2$$

$$= \sum_{i=1}^{N} \left\{ \left[R_p(\omega_i) - R_o(\omega_i) \right]^2 + \left[I_p(\omega_i) - I_o(\omega_i) \right]^2 \right\} \tag{4-68}$$

$$= \varphi(p,\beta) \quad ,$$

where

N = number of ω values fitted.

As τ is the observed dimensionless dead time and $H_o(j\omega_i)$ are obtained from the experimental data by using equation (4-51), p and β are the

two parameters to be determined from equation (4-68). Again we should seek an unrestricted minimum of the error function, φ. This requires that

$$\frac{\partial \varphi}{\partial p} = 0 \quad , \quad \frac{\partial \varphi}{\partial \beta} = 0$$

or

$$\sum_{i=1}^{N} \left\{ \left[R_p(\omega_i) - R_o(\omega_i) \right] \frac{\partial R_p(\omega_i)}{\partial p} + \left[I_p(\omega_i) - I_o(\omega_i) \right] \frac{\partial I_p(\omega_i)}{\partial p} \right\} = 0 \qquad (4\text{-}69)$$

and

$$\sum_{i=1}^{N} \left\{ \left[R_p(\omega_i) - R_o(\omega_i) \right] \frac{\partial R_p(\omega_i)}{\partial \beta} + \left[I_p(\omega_i) - I_o(\omega_i) \right] \frac{\partial I_p(\omega_i)}{\partial \beta} \right\} = 0 \quad . \qquad (4\text{-}70)$$

If the l.h.s. of equation (4-69) is represented by $\sum_{i=1}^{N} G_i(p,\beta)$ and the l.h.s. of equation (4-70) is represented by $\sum_{i=1}^{N} F_i(p,\beta)$, we have two simultaneous equations given as

$$\sum_{i=1}^{N} G_i(p,\beta) = 0 \quad , \qquad (4\text{-}71)$$

$$\sum_{i=1}^{N} F_i(p,\beta) = 0 \quad . \qquad (4\text{-}72)$$

We thus again face the problem of solving two simultaneous non-linear algebraic equations. As in the previous two methods, a relaxation procedure using only the first order terms of Taylor series expansion was employed. Expanding equations (4-71) and (4-72) in the Taylor series around the initial guess, p_o and β_o, and truncating all but the linear terms yields

$$\sum_{i=1}^{N} G_i(p,\beta) = \sum_{i=1}^{N} G_i(p_o,\beta_o) + \Delta p \sum_{i=1}^{N} \frac{\partial G_i}{\partial p}\bigg|_{p_o,\beta_o} + \Delta\beta \sum_{i=1}^{N} \frac{\partial G_i}{\partial \beta}\bigg|_{p_o,\beta_o}$$

$$= 0 \quad , \tag{4-73}$$

$$\sum_{i=1}^{N} F_i(p,\beta) = \sum_{i=1}^{N} F_i(p_o,\beta_o) + \Delta p \sum_{i=1}^{N} \frac{\partial F_i}{\partial p}\bigg|_{p_o,\beta_o} + \Delta\beta \sum_{i=1}^{N} \frac{\partial F_i}{\partial \beta}\bigg|_{p_o,\beta_o}$$

$$= 0 \quad , \tag{4-74}$$

where

$$\Delta p = p - p_o \quad \text{and} \quad \Delta\beta = \beta - \beta_o \quad .$$

Solving equations (4-73) and (4-74) gives increments Δp and $\Delta\beta$ for improving initial guesses as follows:

$$\Delta p = \left. \frac{\sum_{i=1}^{N} G_i \sum_{i=1}^{N} \frac{\partial F_i}{\partial \beta} - \sum_{i=1}^{N} F_i \sum_{i=1}^{N} \frac{\partial G_i}{\partial \beta}}{\sum_{i=1}^{N} \frac{\partial F_i}{\partial p} \sum_{i=1}^{N} \frac{\partial G_i}{\partial \beta} - \sum_{i=1}^{N} \frac{\partial F_i}{\partial \beta} \sum_{i=1}^{N} \frac{\partial G_i}{\partial p}} \right|_{p_o,\beta_o} , \tag{4-75}$$

$$\Delta\beta = \left. \frac{\sum_{i=1}^{N} F_i \sum_{i=1}^{N} \frac{\partial G_i}{\partial p} - \sum_{i=1}^{N} G_i \sum_{i=1}^{N} \frac{\partial F_i}{\partial p}}{\sum_{i=1}^{N} \frac{\partial F_i}{\partial p} \sum_{i=1}^{N} \frac{\partial G_i}{\partial \beta} - \sum_{i=1}^{N} \frac{\partial F_i}{\partial \beta} \sum_{i=1}^{N} \frac{\partial G_i}{\partial p}} \right|_{p_o,\beta_o} . \tag{4-76}$$

Again the computing logic is the same as the previous methods. An iterative computation is performed until no further significant improvement is achieved. The fitted parameters, p and β, are then used to evaluate the frequency response information predicted from the model by using equations (3-23) through (3-25). The predicted frequency responses are compared with those computed from the experimental data by using the Bode diagram, which indicates the goodness of fit.

Furthermore, the goodness of fit also quantitatively appears in the value of the error function, φ, corresponding to each pair of the fitted parameters, p and β.

Now a difficulty arises in that many terms are required in the r.h.s. of equations (4-75) and (4-76) for the calculation of Δp and $\Delta\beta$. Deriving them is a tedious task. For convenience in the final computer programming, additional notations are introduced to represent terms which appear frequently as groups. All of them will be derived in order and given as follows:

Let

$$H = \frac{1 - \tau}{p\beta}\omega \quad ,$$

$$Y = 1 + H^2 \quad ,$$

$$X = Y^{-\frac{p}{2}} = (1 + H^2)^{-\frac{p}{2}} \quad ,$$

then we have

$$Z = \tan^{-1}(-H) \quad .$$

Setting

$$U = \cos(pZ - \tau\omega) \quad ,$$

$$V = \sin(pZ - \tau\omega) \quad ,$$

we obtain

$$R_p = \beta XU + (1 - \beta)\cos\tau\omega \quad ,$$

$$I_p = \beta XU - (1 - \beta)\sin\tau\omega \quad .$$

The partial differentiation of H with respect to p and β are

$$\frac{\partial H}{\partial p} = \frac{-(1 - \tau)\omega}{p^2\beta} = -\frac{H}{p} \quad ,$$

$$\frac{\partial H}{\partial \beta} = \frac{-(1-\tau)\omega}{p\beta^2} = -\frac{H}{\beta} \quad .$$

The partial differentiation of Y with respect to p and β are

$$\frac{\partial Y}{\partial p} = 2H\frac{\partial H}{\partial p} = -\frac{2H^2}{p} \quad ,$$

$$\frac{\partial Y}{\partial \beta} = 2H\frac{\partial H}{\partial \beta} = -\frac{2H^2}{\beta} \quad .$$

The first and second order partial differentiation of Z with respect to p and β are

$$\frac{\partial Z}{\partial p} = \frac{-1}{1+H^2}\frac{\partial H}{\partial p} = \frac{H}{Yp} \quad ,$$

$$\frac{\partial Z}{\partial \beta} = \frac{-1}{1+H^2}\frac{\partial H}{\partial \beta} = \frac{H}{Y\beta} \quad ,$$

$$\frac{\partial^2 Z}{\partial p^2} = \frac{Yp\frac{\partial H}{\partial p} - H\left(p\frac{\partial Y}{\partial p} + Y\right)}{Y^2 p^2} \quad ,$$

$$\frac{\partial^2 Z}{\partial p \partial \beta} = \frac{Y\frac{\partial H}{\partial p} - H\frac{\partial Y}{\partial p}}{\beta Y^2} \quad ,$$

$$\frac{\partial^2 Z}{\partial \beta^2} = \frac{Y\beta\frac{\partial H}{\partial \beta} - H\left(\beta\frac{\partial Y}{\partial \beta} + Y\right)}{Y^2\beta^2} \quad .$$

The partial differentiation of X with respect to p and β are

$$\frac{\partial X}{\partial p} = \frac{H^2 X}{Y} - \frac{1}{2}X \ln Y \quad ,$$

$$\frac{\partial X}{\partial \beta} = \frac{pH^2 X}{\beta Y} \quad .$$

The partial differentiation of U and V with respect to p and β are

$$\frac{\partial U}{\partial p} = -V\left(Z + p\frac{\partial Z}{\partial p}\right) \quad ,$$

$$\frac{\partial U}{\partial \beta} = -Vp\frac{\partial Z}{\partial \beta} \quad ,$$

$$\frac{\partial V}{\partial p} = U(Z + p\frac{\partial Z}{\partial p}) \quad ,$$

$$\frac{\partial V}{\partial \beta} = Up\frac{\partial Z}{\partial \beta} \quad .$$

The second order partial differentiation of X, U and V with respect to p and β are

$$\frac{\partial^2 X}{\partial p^2} = \frac{Y(2HX\frac{\partial H}{\partial \beta} + H^2\frac{\partial X}{\partial p}) - H^2X\frac{\partial Y}{\partial p}}{Y^2} - \frac{1}{2}(\frac{\partial X}{\partial p}\ln Y + \frac{X\frac{\partial Y}{\partial p}}{Y}) \quad ,$$

$$\frac{\partial^2 X}{\partial p\partial \beta} = \frac{Y(H^2X + 2pHX\frac{\partial H}{\partial p} + pH^2\frac{\partial X}{\partial p} + pH^2\frac{\partial X}{\partial p}) - pH^2X\frac{\partial Y}{\partial p}}{\beta Y^2} \quad ,$$

$$\frac{\partial^2 X}{\partial \beta^2} = \frac{p[(2HX\frac{\partial H}{\partial \beta} + H^2\frac{\partial X}{\partial \beta})\beta Y - H^2X(Y + \beta\frac{\partial Y}{\partial \beta})]}{\beta^2 Y^2} \quad ,$$

$$\frac{\partial^2 U}{\partial p^2} = -\frac{\partial V}{\partial p}(Z + p\frac{\partial Z}{\partial p}) - V(2\frac{\partial Z}{\partial p} + p\frac{\partial^2 Z}{\partial p^2}) \quad ,$$

$$\frac{\partial^2 U}{\partial p\partial \beta} = -(p\frac{\partial V}{\partial p}\frac{\partial Z}{\partial \beta} + V\frac{\partial Z}{\partial \beta} + pV\frac{\partial^2 Z}{\partial p\partial \beta}) \quad ,$$

$$\frac{\partial^2 U}{\partial \beta^2} = -p(\frac{\partial Z}{\partial \beta}\frac{\partial V}{\partial \beta} + V\frac{\partial^2 Z}{\partial \beta^2}) \quad ,$$

$$\frac{\partial^2 V}{\partial p^2} = \frac{\partial U}{\partial p}(Z + p\frac{\partial Z}{\partial p}) + U(2\frac{\partial Z}{\partial p} + p\frac{\partial^2 Z}{\partial p^2}) \quad ,$$

$$\frac{\partial^2 V}{\partial p\partial \beta} = p\frac{\partial U}{\partial p}\frac{\partial Z}{\partial \beta} + U\frac{\partial Z}{\partial \beta} + pU\frac{\partial^2 Z}{\partial p\partial \beta} \quad ,$$

$$\frac{\partial^2 V}{\partial \beta^2} = p(\frac{\partial U}{\partial \beta}\frac{\partial Z}{\partial \beta} + U\frac{\partial^2 Z}{\partial \beta^2}) \quad .$$

With all of the above equations ready, we can now carry out the first and second order of partial differentiation of R_p and I_p with respect to p and β as follows:

$$\frac{\partial R_p}{\partial p} = \beta\left(U \frac{\partial X}{\partial p} + X \frac{\partial U}{\partial p}\right) \quad ,$$

$$\frac{\partial R_p}{\partial \beta} = XU + \beta\left(U \frac{\partial X}{\partial \beta} + X \frac{\partial U}{\partial \beta}\right) - \cos \tau\omega \quad ,$$

$$\frac{\partial I_p}{\partial p} = \beta\left(V \frac{\partial X}{\partial p} + X \frac{\partial V}{\partial p}\right) \quad ,$$

$$\frac{\partial I_p}{\partial \beta} = XV + \beta\left(V \frac{\partial X}{\partial \beta} + X \frac{\partial V}{\partial \beta}\right) + \sin \tau\omega \quad ,$$

$$\frac{\partial^2 R_p}{\partial p^2} = \beta\left(2 \frac{\partial U}{\partial p} \frac{\partial X}{\partial p} + U \frac{\partial^2 X}{\partial p^2} + X \frac{\partial^2 U}{\partial p^2}\right) \quad ,$$

$$\frac{\partial^2 R_p}{\partial p \partial \beta} = U \frac{\partial X}{\partial p} + X \frac{\partial U}{\partial p} + \beta\left(\frac{\partial U}{\partial p} \frac{\partial X}{\partial \beta} + U \frac{\partial^2 X}{\partial p \partial \beta}\right) + \beta\left(\frac{\partial X}{\partial p} \frac{\partial U}{\partial \beta} + X \frac{\partial^2 U}{\partial p \partial \beta}\right) \quad ,$$

$$\frac{\partial^2 R_p}{\partial \beta^2} = 2\left(U \frac{\partial X}{\partial \beta} + X \frac{\partial U}{\partial \beta} + \beta \frac{\partial U}{\partial \beta} \frac{\partial X}{\partial \beta}\right) + \beta\left(U \frac{\partial^2 X}{\partial \beta^2} + X \frac{\partial^2 U}{\partial \beta^2}\right) \quad ,$$

$$\frac{\partial^2 I_p}{\partial p^2} = \beta\left(2 \frac{\partial V}{\partial p} \frac{\partial X}{\partial p} + V \frac{\partial^2 X}{\partial p^2} + X \frac{\partial^2 V}{\partial p^2}\right) \quad ,$$

$$\frac{\partial^2 I_p}{\partial p \partial \beta} = V \frac{\partial X}{\partial p} + X \frac{\partial V}{\partial p} + \beta\left(\frac{\partial V}{\partial p} \frac{\partial X}{\partial \beta} + \frac{\partial X}{\partial p} \frac{\partial V}{\partial \beta}\right) + \beta\left(V \frac{\partial^2 X}{\partial p \partial \beta} + X \frac{\partial^2 V}{\partial p \partial \beta}\right) \quad ,$$

$$\frac{\partial^2 I_p}{\partial \beta^2} = 2\left(V \frac{\partial X}{\partial \beta} + X \frac{\partial V}{\partial \beta} + \beta \frac{\partial V}{\partial \beta} \frac{\partial X}{\partial \beta}\right) + \beta\left(V \frac{\partial^2 X}{\partial \beta^2} + X \frac{\partial^2 V}{\partial \beta^2}\right) \quad .$$

The various terms appearing in the r.h.s. of equations (4-75) and (4-76) can then be evaluated. Again the evaluation corresponding to a single frequency is illustrated as follows:

$$F_i = \left[R_p(\omega_i) - R_o(\omega_i)\right] \frac{\partial R_p(\omega_i)}{\partial \beta} + \left[I_p(\omega_i) - I_o(\omega_i)\right] \frac{\partial I_p(\omega_i)}{\partial \beta} \quad ,$$

$$G_i = \left[R_p(\omega_i) - R_o(\omega_i)\right] \frac{\partial R_p(\omega_i)}{\partial p} + \left[I_p(\omega_i) - I_o(\omega_i)\right] \frac{\partial I_p(\omega_i)}{\partial p} ,$$

$$\frac{\partial F_i}{\partial \beta} = \left[\frac{\partial R_p(\omega_i)}{\partial \beta}\right]^2 + \left[R_p(\omega_i) - R_o(\omega_i)\right] \frac{\partial^2 R_p(\omega_i)}{\partial \beta^2}$$

$$+ \left[\frac{\partial I_p(\omega_i)}{\partial \beta}\right]^2 + \left[I_p(\omega_i) - I_o(\omega_i)\right] \frac{\partial^2 I_p(\omega_i)}{\partial \beta^2} ,$$

$$\frac{\partial F_i}{\partial p} = \frac{\partial R_p(\omega_i)}{\partial p} \frac{\partial R_p(\omega_i)}{\partial \beta} + \left[R_p(\omega_i) - R_o(\omega_i)\right] \frac{\partial^2 R_p(\omega_i)}{\partial p \partial \beta}$$

$$+ \frac{\partial I_p(\omega_i)}{\partial p} \frac{\partial I_p(\omega_i)}{\partial \beta} + \left[I_p(\omega_i) - I_o(\omega_i)\right] \frac{\partial^2 I_p(\omega_i)}{\partial p \partial \beta} ,$$

$$\frac{\partial G_i}{\partial \beta} = \frac{\partial R_p(\omega_i)}{\partial \beta} \frac{\partial R_p(\omega_i)}{\partial p} + \left[R_p(\omega_i) - R_o(\omega_i)\right] \frac{\partial^2 R_p(\omega_i)}{\partial \beta \partial p}$$

$$+ \frac{\partial I_p(\omega_i)}{\partial \beta} \frac{\partial I_p(\omega_i)}{\partial p} + \left[I_p(\omega_i) - I_o(\omega_i)\right] \frac{\partial^2 I_p(\omega_i)}{\partial \beta \partial p} ,$$

$$\frac{\partial G_i}{\partial p} = \left[\frac{\partial R_p(\omega_i)}{\partial p}\right]^2 + \left[R_p(\omega_i) - R_o(\omega_i)\right] \frac{\partial^2 R_p(\omega_i)}{\partial p^2}$$

$$+ \left[\frac{\partial I_p(\omega_i)}{\partial p}\right]^2 + \left[I_p(\omega_i) - I_o(\omega_i)\right] \frac{\partial^2 I_p(\omega_i)}{\partial p^2}$$

If we evaluate the above terms over the entire range of ω fitted, we obtain the summation terms through iterative summation and the increments for improvement, Δp and $\Delta \beta$, are then easily determined by using equations (4-75) and (4-76).

Discussion of some of the computational techniques involved in the curve fitting (9,20,21). In general, the model selected and formulated for a practical system is often non-linear. The model tends

to increase its complexity with the increase of the number of parameters contained in it. We thus face the problem of non-linear regression. Consider now a general case, that of a model containing n parameters. Using the moments method gives rise to n simultaneous non-linear algebraic equations to be solved. Linearization of the equations by using the Taylor series expansion and truncating all but the linear terms yields, in general, the following matrix representation:

$$\underset{\sim}{Z}\,\underset{\sim}{\Delta\alpha} = \underset{\sim}{b} \quad ,$$

where

$\underset{\sim}{Z}$ = an n x n matrix

$\underset{\sim}{\Delta\alpha}$ = an n x 1 matrix, step sizes of improvement for n parameters

$\underset{\sim}{b}$ = an n x 1 matrix.

The step sizes of improvement for n parameters are then given by

$$\underset{\sim}{\Delta\alpha} = \underset{\sim}{Z}^{-1}\,\underset{\sim}{b} \quad , \tag{4-77}$$

where

$\underset{\sim}{Z}^{-1}$ = the inverse matrix of $\underset{\sim}{Z}$.

The improved values of the parameters are thus given by the recurrence relation of the following form.

$$\underset{\sim}{\alpha}^{i+1} = \underset{\sim}{\alpha}^{i} + \underset{\sim}{\Delta\alpha}^{i} \quad , \tag{4-78}$$

where

$\underset{\sim}{\alpha}^{i}$ = vector of parameter values at the ith step,

$\underset{\sim}{\Delta\alpha}^{i}$ = step sizes vector for correction at the ith step,

$\underset{\sim}{\alpha}^{i+1}$ = improved vector of parameter values at the (i+1)th step.

The relaxation procedure is as follows:

1. Guess an initial vector of parameter values as $\underline{\alpha}^i$.
2. Calculate $(\underline{Z}^{-1})^i$, $\underline{b}^i$ and then obtain $\underline{\Delta\alpha}^i$ by using equation (4-77).
3. Obtain the improved vector of parameter values, $\underline{\alpha}^{i+1}$, by using equation (4-78).
4. Repeat 2 and 3 until no further significant improvement is achieved.

In using the s-plane or frequency response analysis, a criterion for evaluating the values of model parameter is to minimize an error function, φ, i.e.

$$\varphi = \varphi(\underline{\alpha}) = \text{minimum},$$

where

$\underline{\alpha}$ = vector of parameter values.

The necessary conditions for an unrestricted minimum require that

$$\frac{\partial \varphi}{\partial \alpha_j} = 0 \quad , \quad j = 1, 2, \ldots, n \quad .$$

This again is a problem of solving n simultaneous non-linear equations. In a similar manner, the previous relaxation procedure may be applied. The use of the Taylor series expansion for linearization yields extremely rapid convergence once it converges. Nevertheless, this method has its practical limitations when the number of parameters contained in the model becomes larger. The evaluation of the inverse matrix of $\underline{Z}$ becomes very cumbersome. The so-called gradient technique may also be used (30). The iterative algorithm for this technique can be written as

$$\underline{\alpha}^{i+1} = \underline{\alpha}^i + k^i \nabla\varphi^i$$

where

$\underset{\sim}{\alpha}^i$ = vector of parameter values at the ith step in the search,

k^i = step size factor at the ith step, a negative value for searching the minimum,

$\nabla\varphi^i$ = gradient vector of the error function at the ith step in the search.

The number of iterations required for converging towards the minimum is, in general, more than the preceding method.

In case the calculation of derivatives involved in the above methods becomes very tedious, the direct search techniques currently developed may be applied. However, it is expected that a much greater number of iterations are required than the two methods described above.

The curve fitting procedure is, in general, carried out by the digital computer. The analog computer may help with part of the data processing from an on-line viewpoint (4) but has its practical limitations in the final curve fitting. In case the parameters contained in the model are more than two, a direct search on the analog computer by adjusting the potentiometer setting is a formidable task. It is especially true in this work in which the fitting is not restricted to boundary point fitting. Moreover, difficulties arise in scaling and programming when the model is highly non-linear.

CHAPTER 5

APPLICATION TO LIQUID MIXING ON DISTILLATION TRAYS

Experimental work was carried out by Johnson for studying the characteristics of liquid mixing on distillation trays (5). In his investigation, the air-water system and sieve plates with circular down-pipes were employed. Radioactive phosphorus, P^{32}, was used as the tracer. The investigation included the effect of five variables. They were the liquid flow rate (L), the air velocity (V), the weir height (H), the number of holes (N), and the hole diameter (D). Each variable was allowed to take on two different values, i.e. level 1 (lower value) and level 2 (higher value). Data were then taken for each possible combination of the five variables at both levels (values), that is, for 32 different combinations. Two replicate runs (R) were made for each combination, giving a total of 64 experimental runs. The (LVH NDR) notations used to indicate the experimental conditions are explained in Table 5-1. For example, the experimental condition denoted by 112111 means

liquid flow rate (L)	3.29 gpm.
air velocity (V)	21.76 ft./sec.
weir height (H)	2.25 inches
number of holes (N)	one
hole diameter (D)	3/16 inches
replicate (R)	first

The gamma distribution model with bypassing (GDMMB) described in Chapter 3 was selected to fit the experimental data according to the

Table 5-1. Levels of the experimental condition.

Variable	Level 1	Level 2
liquid flow rate (L)	3.29 gpm.	8.00 gpm.
air velocity (V)	21.76 ft./sec.	36.18 ft./sec.
weir height (H)	1.51 inches	2.25 inches
number of holes (N)	1	9
hole diameter (D)	3/16 inches	1/4 inches
replicate (R)	first	second

s-plane analysis by Johnson (5). In this work, two other methods of response data analysis are applied to his experimental data by using the same model (GDMMB). The results of fitting the model by using the moments method of analysis are presented in Table 5-2. The results of fitting the model by using the s-plane analysis by Johnson (5) are reproduced in Table 5-3. The results of fitting the model by using the frequency response analysis are presented in Table 5-4.

In order to illustrate the goodness of curve fitting by using the frequency response analysis, the data and results of analysis for run 31 are plotted in the form of a Bode diagram as shown in Fig. 5-1.

Since each method of analysis was based on the same 64 runs of experimental data, the characteristics of the analysis can be visualized through the distributions of the fitted parameters, p and β, resulting from the use of each method. For the purposes of comparing the distribution of the fitted parameters by the three methods of response data analysis, the mean (μ), variance (σ^2) and standard deviation (σ) of the fitted model parameters from each method are calculated as follows (29):

$$\mu_\beta = \frac{\sum_{i=1}^{N} \beta_i}{N} \quad , \quad \mu_p = \frac{\sum_{i=1}^{N} p_i}{N} \quad ,$$

$$\sigma_\beta^2 = \frac{\sum_{i=1}^{N} (\beta_i - \mu_\beta)^2}{N} \quad , \quad \sigma_p^2 = \frac{\sum_{i=1}^{N} (p_i - \mu_p)^2}{N} \quad ,$$

$$\sigma_\beta = \sqrt{\sigma_\beta^2} \quad , \quad \sigma_p = \sqrt{\sigma_p^2} \quad ,$$

where

N = total number of data sampled.

The results are presented in Table 5-5.

Table 5-2. Results of fitting the model (C.M.M.B) by using the moments method of analysis.

Run Number	Experimental Conditions	τ Observed	$\Delta\sigma^2_{\theta yx}$	$\Delta\sigma^3_{\theta yx}$	β	p
26	111111	0.275	0.543	0.751	0.72	1.14
31	111112	0.226	0.515	0.624	0.93	1.96
42	112111	0.170	0.467	0.445	0.87	2.02
44	112112	0.183	0.514	0.521	0.88	1.77
34	121111	0.372	0.512	0.585	0.70	1.67
38	121112	0.314	0.537	0.632	0.78	1.53
30	122111	0.136	0.477	0.465	0.89	2.13
44	122112	0.184	0.556	0.515	0.80	2.10
32	211111	0.320	0.553	0.577	0.68	2.02
34	211112	0.368	0.566	0.703	0.56	1.67
46	212111	0.189	0.652	1.510	0.82	1.15
45	212112	0.212	0.764	1.114	0.75	1.49
31	221111	0.282	0.544	0.642	0.81	1.52
36	221112	0.341	0.646	0.935	0.68	1.43
4	222111	0.242	0.710	0.924	0.71	1.73
41	222112	0.212	0.757	1.165	0.79	1.33
56	111121	0.316	0.537	0.728	0.86	1.19
61	111122	0.313	0.319	0.249	0.93	1.96
52	112121	0.181	0.543	0.524	0.83	1.96
49	112122	0.222	0.546	0.622	0.86	1.57
57	121121	0.316	0.540	0.997	1.29	0.56
50	121122	0.217	0.302	0.255	0.80	2.42
48	122121	0.141	0.439	0.388	0.94	2.01
55	122122	0.204	0.481	0.484	0.90	1.71
62	211121	0.262	0.514	0.538	0.79	1.74
63	211122	0.292	0.596	0.835	0.82	1.25
53	212121	0.223	0.660	0.761	0.70	2.06
51	212122	0.227	0.695	0.954	0.77	1.49
60	221121	0.324	0.481	0.446	0.73	2.08
58	221122	0.244	0.506	0.523	0.70	1.88
54	222121	0.188	0.600	0.713	0.85	1.58
5	222122	0.244	0.723	1.050	0.75	1.45
65	111211	0.196	0.472	0.327	0.88	2.60
69	111212	0.153	0.556	0.500	0.82	2.16
73	112211	0.151	0.434	0.154	0.78	2.19
79	112212	0.120	0.533	0.438	0.84	1.92
8	121211	0.162	0.630	0.728	0.82	1.70
64	121212	0.135	0.686	0.826	0.85	1.70
77	122211	0.128	0.526	0.357	0.80	2.60
76	122212	0.163	0.544	0.466	0.78	2.65

Table D-2. (Continued)

Run Number	Experimental Conditions	τ Observed	$\Delta\sigma^2_{\theta yx}$	$\Delta\sigma^3_{\theta yx}$	β	p
[illegible]	211211	[illegible]	[illegible]	[illegible]	[illegible]	[illegible]
[illegible]	211212	[illegible]	[illegible]	[illegible]	[illegible]	[illegible]
[illegible]	212211	[illegible]	[illegible]	[illegible]	[illegible]	[illegible]
[illegible]	212212	[illegible]	[illegible]	[illegible]	[illegible]	[illegible]
[illegible]	221211	[illegible]	[illegible]	[illegible]	[illegible]	[illegible]
[illegible]	221212	[illegible]	[illegible]	[illegible]	[illegible]	[illegible]
[illegible]	222211	[illegible]	[illegible]	[illegible]	[illegible]	[illegible]
[illegible]	222212	[illegible]	[illegible]	[illegible]	[illegible]	[illegible]
[illegible]	111221	[illegible]	[illegible]	[illegible]	[illegible]	[illegible]
[illegible]	111222	[illegible]	[illegible]	[illegible]	[illegible]	[illegible]
[illegible]	112221	[illegible]	[illegible]	[illegible]	[illegible]	[illegible]
[illegible]	112222	[illegible]	[illegible]	[illegible]	[illegible]	[illegible]
[illegible]	121221	[illegible]	[illegible]	[illegible]	[illegible]	[illegible]
[illegible]	121222	[illegible]	[illegible]	[illegible]	[illegible]	[illegible]
[illegible]	122221	[illegible]	[illegible]	[illegible]	[illegible]	[illegible]
[illegible]	122222	[illegible]	[illegible]	[illegible]	[illegible]	[illegible]
[illegible]	211221	[illegible]	[illegible]	[illegible]	[illegible]	[illegible]
[illegible]	211222	[illegible]	[illegible]	[illegible]	[illegible]	[illegible]
[illegible]	212221	[illegible]	[illegible]	[illegible]	[illegible]	[illegible]
[illegible]	212222	[illegible]	[illegible]	[illegible]	[illegible]	[illegible]
[illegible]	221221	[illegible]	[illegible]	[illegible]	[illegible]	[illegible]
[illegible]	221222	[illegible]	[illegible]	[illegible]	[illegible]	[illegible]
[illegible]	222221	[illegible]	[illegible]	[illegible]	[illegible]	[illegible]
[illegible]	222222	[illegible]	[illegible]	[illegible]	[illegible]	[illegible]

Table 5-3. Results of fitting the model (CDAMB) by using the s-plane analysis.

Run Number	Experimental Conditions	τ Observed	β	p	Error Squared X 10^6
25	111111	.275	1.[illegible]2	[illegible].92	0.14
27	111112	.224	1.[illegible]3	1.06	[illegible].03
43	112111	.170	1.00	1.29	1.22
46	112112	.193	1.00	1.24	0.31
33	121111	.372	0.75	1.36	2.77
38	121112	.334	0.92	1.01	0.15
30	122111	.138	1.01	1.43	[illegible].46
44	122112	.184	0.85	1.21	2.32
29	211111	.320	0.56	2[illegible].38	1252.00
34	211112	.368	0.62	2.23	13.42
42	212111	.180	[illegible].80	[illegible].84	0.74
45	212112	.212	[illegible].92	[illegible].80	[illegible].00
31	221111	.282	0.85	1.32	0.24
36	221112	.341	0.67	1.74	11.92
5	222111	.242	0.77	1.37	2.26
41	222112	.212	0.90	0.97	[illegible].66
56	111121	.316	0.97	0.91	0.25
61	111122	.303	1.02	1.40	[illegible].42
59	112121	.181	0.99	1.16	2.63
60	112122	.222	0.90	1.46	15.35
57	121121	.[illegible]26	1.[illegible]8	[illegible].84	[illegible].80
58	121122	.297	0.96	1.28	2.[illegible]2
48	122121	.141	[illegible].99	1.74	6.65
55	122122	.2[illegible]4	[illegible].99	1.29	0.29
62	211121	.282	0.89	1.20	[illegible].41
63	211122	.2[illegible]2	0.80	1.44	5.71
53	212121	.223	0.84	1.[illegible]3	[illegible].[illegible]6
51	212122	.227	0.84	1.21	0.80
54	221121	.324	[illegible].90	1.4[illegible]	0.1[illegible]
50	221122	.344	0.72	1.84	4.02
64	222121	.[illegible]68	[illegible].96	1.11	2.72
52	222122	.244	0.80	1.20	0.34
65	111211	0.156	0.94	1.62	1.84
69	111212	.[illegible]63	[illegible].93	1.41	2.64
75	112211	.[illegible]31	[illegible].91	1.09	[illegible].[illegible]
78	112212	.[illegible]24	[illegible].96	1.46	[illegible].28
71	121211	.[illegible]62	[illegible].91	1.3[illegible]	1.01
66	121212	.[illegible]15	[illegible].98	1.16	[illegible].41
70	122211	.128	0.90	1.72	[illegible].64
74	122212	.163	0.93	1.39	2.14

Table 5-3. (Continued)

Run Number	Experimental Conditions	τ Observed	β	p	Error Squared X 10^6
1					
[illegible]	211211	.21[illegible]	0.9[illegible]	1.37	[illegible].43
71	211212	.264	1.04	1.17	2.27
74	212211	.218	0.[illegible]5	1.50	[illegible].45
78	212212	.214	[illegible].01	0.[illegible]8	[illegible].54
67	221211	.[illegible]9	0.96	1.[illegible]	2.02
64	221212	.255	0.92	1.72	2.78
70	222211	.269	0.93	1.25	2.00
77	222212	.230	1.14	0.82	4.00
63	111221	.114	[illegible].99	1.67	[illegible].00
81	111222	.155	1.[illegible]5	[illegible].02	0.[illegible]9
61	112221	.[illegible]03	1.[illegible]0	1.16	0.81
80	112222	0.106	0.97	1.23	0.50
83	121221	.146	0.[illegible]0	1.[illegible]0	[illegible].01
67	121222	.110	0.97	1.24	0.63
[illegible]3	[illegible]22221	.1[illegible]3	0.97	1.14	1.36
43	122222	.1[illegible]4	0.98	1.1[illegible]	[illegible].95
[illegible]5	211221	.233	0.94	1.51	0.61
80	211222	.250	0.97	1.42	4.39
88	212221	.129	[illegible].96	0.99	1.01
[illegible]4	212222	.121	.97	1.[illegible]2	0.59
87	221221	.148	1.01	1.62	3.17
86	221222	.243	1.[illegible]3	0.90	1.10
65	222221	.173	0.94	1.54	[illegible].54
80	222222	.151	0.99	1.25	3.50

Table 5-4. Results of fitting the model (GDMMB) by using the frequency response analysis.

Run Number	Experimental Conditions	τ Observed	β	p	Error Squared X 10
[illegible]	111111	.275	1.10	.96	0.95
[illegible]	111112	.226	1.05	[illegible]	2.14
[illegible]	112111	.170	1.11	1.10	0.42
[illegible]	112112	.143	1.06	1.22	0.21
[illegible]	121111	.372	0.90	1.01	0.91
[illegible]	121112	.324	0.90	1.10	2.49
[illegible]	122111	.139	1.01	1.39	0.52
[illegible]	122112	.184	1.02	0.93	0.70
33	211111	.320	0.92	1.06	2.36
[illegible]	211112	.368	0.88	1.08	4.71
[illegible]	212111	.189	0.95	0.79	1.91
[illegible]	212112	.212	0.98	0.82	2.88
37	221111	.289	0.87	1.22	0.43
38	221112	.341	0.79	1.35	6.13
40	222111	.242	0.84	1.03	2.64
41	222112	.212	0.95	0.79	6.35
56	111121	.316	0.97	0.96	2.05
61	111122	.306	1.03	1.26	0.56
59	112121	.161	0.99	1.09	0.82
60	112122	.222	0.97	1.14	1.50
57	121121	.316	1.00	1.13	0.78
58	121122	.297	0.97	1.11	1.53
49	122121	.141	1.01	1.57	1.02
55	122122	.204	1.00	1.27	0.20
62	211121	.282	0.95	1.05	0.87
63	211122	0.292	0.91	1.14	0.71
53	212121	.223	0.86	0.99	0.73
51	212122	.227	0.97	0.86	1.52
47	221121	.324	0.80	1.11	0.86
48	221122	.344	0.80	1.18	1.54
54	222121	.156	1.01	0.91	0.41
50	222122	.244	0.90	0.92	1.35
45	111211	.156	0.96	1.46	0.49
69	111212	.153	1.00	1.09	1.10
75	112211	.121	0.97	1.42	2.23
78	112212	.126	0.99	1.28	2.04
70	121211	.162	0.96	1.16	0.19
66	121212	.175	1.00	1.09	0.39
72	122211	.128	0.95	1.29	1.25
76	122212	.162	1.00	1.07	1.78

Table 5-4. (Continued)

Run Number	Experimental Conditions	τ Observed	β	p	Error Squared X 10
[illegible]	211211	.259	[illegible]	1.41	[illegible]
71	211212	.268	0.90	1.71	0.57
74	212211	.218	0.92	1.51	0.09
78	212212	.234	0.96	1.45	0.45
67	221211	.309	0.74	1.95	27.40
80	221212	.225	0.96	2.21	1.99
70	222211	.260	0.95	1.75	0.81
77	222212	.230	0.97	1.12	5.46
69	111221	.114	0.96	2.19	21.14
81	111222	.155	0.99	1.11	4.09
61	112221	.088	0.97	1.27	1.74
84	112222	.106	0.94	1.59	25.84
89	121221	.146	0.92	1.19	5.15
87	121222	.110	0.96	1.23	1.16
72	122221	.103	0.97	1.24	2.67
93	122222	0.134	0.96	1.38	16.20
68	211221	.239	0.94	1.42	3.73
83	211222	.250	0.94	1.44	0.20
88	212221	.129	0.96	1.02	2.74
94	212222	0.121	0.94	1.16	5.11
82	221221	0.148	0.92	2.62	0.89
86	221222	.243	0.90	1.26	0.77
95	222221	.173	0.90	1.06	3.23
90	222222	.151	0.95	1.48	2.31

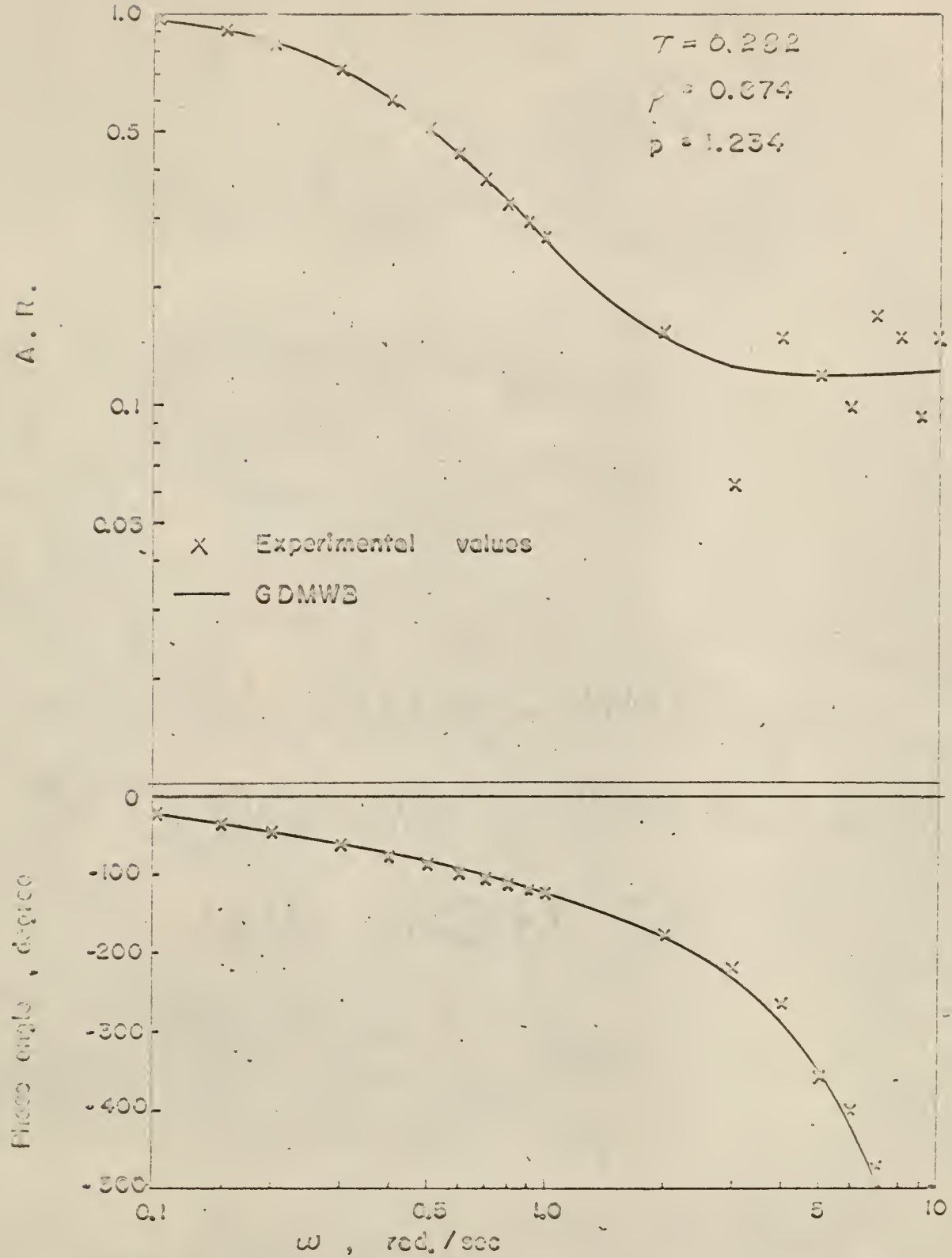

Fig. 5-1. Curve fitting to the experimental data from Run 31 by the frequency response analysis.

Table 3-5. The mean (μ), variance (σ^2) and standard deviation (σ) of the fitted parameters by three methods of response data analysis

	Number of data sampled	μ_β	σ_β^2	σ_β	μ_p	σ_p^2	σ_p
Moments method of analysis	64	0.82	0.0079	0.0887	2.02	0.478	0.692
s-plane analysis	63*	0.91	0.0077	0.0875	1.40	0.128	0.357
Frequency response analysis	64	0.97	0.0032	0.0566	1.16	0.050	0.225

*Run number 32, which showed an unusually large value of p in the s-plane analysis, is not included.

Discussion.

1. Using the moments method of analysis, all cases except run 57 give values of p greater than unity and values of β less than unity. Run 57 gives (see Table 5-2)

$$\tau = 0.306 \ , \ \Delta\sigma^2_{\theta yx} = 0.540 \ , \ \Delta\sigma^3_{\theta yx} = 0.997$$

and the fitted parameters

$$\beta = 1.29 > 1 \quad , \quad p = 0.58 < 1 \quad .$$

The unusually large value of $\Delta\sigma^3_{\theta yx}$ (high skewness to right) with respect to given τ (fraction of plug flow) and $\Delta\sigma^2_{\theta yx}$ (degree of spread or dispersion) means a very slow decay in the response curve. This is why the computed parameters show a value of β greater than unity (corresponding to the effect of recycle) and a value of p less than unity (the order of the transfer function is less than one which is the limit case of completely mixed system). In general, curve fitting by the moments method gives rise to results indicating a higher degree of bypassing and a lesser degree of mixing. In other words, this method leads to higher values of (1-β) and p as compared to the values given by two other methods of analysis. The mean values of (1-β) and p for the moments method of analysis are given in Table 5-5 as

$$\mu_{1-\beta} = 1 - \mu_\beta = 1 - 0.82 = 0.18 = 18\%$$

$$\mu_p = 2.02 \quad .$$

This can be interpreted as the introduction of truncating error, which means the response curves were read prematurely. In other words, we have neglected the effect of slow decay (the tail part). We thus obtain small $\Delta\sigma^2_{\theta yx}$ and $\Delta\sigma^3_{\theta yx}$, which in turn leads to the higher values

of (1-β) and p as compared to the values obtained by the s-plane analysis or the frequency response analysis (Table 5-5).

2. Using the s-plane analysis (5), values of p greater than unity and values of β less than unity are obtained in almost all cases except a few runs (Table 5-3). Integer values of s ranging from 1 to 10 are fitted. The least squares errors are around the order of 10^{-6}. Run 32 which is omitted in computation for constructing Table 5-5 gives (Table 5-3)

$$\beta = 0.56 \quad , \quad p = 20.38$$

while the corresponding replicate run 34 (under the same condition of operation) gives

$$\beta = 0.62 \quad , \quad p = 2.23 \quad .$$

The unusually high deviation of the p value in run 32 from the p value in run 34 can be attributed partly to random experimental error and partly to the inherent error in the data processing procedure (5). In general, the curve fitting by the s-plane analysis gives rise to results indicating a lower degree of bypassing but a higher degree of mixing compared to the values given by the moments method of analysis. The mean values of (1-β) and p for the s-plane analysis are given in Table 5-5 as

$$\mu_{1-\beta} = 1 - \mu_{\beta} = 1 - 0.91 = 0.09 = 9\% \quad ,$$

$$\mu_p = 1.40 \quad .$$

3. Using the frequency response analysis, values of p greater than unity and values of β less than unity are also obtained in almost all cases except a few runs (Table 5-4). The range of the frequency

fitted depends on the magnitude of experimental error in each run, which can be visualized through the calculation of $S(\omega)_n$ (see Chapter 4). In this work, a maximum of 22 points, ranging from ω = 0.01 rad./sec. to ω = 10 rad./sec., were fitted and a minimum of 17 points, ranging from ω = 0.01 rad./sec. to ω = 5 rad./sec., were fitted. The range of frequency fitted differed from run to run, ranging from 17 points to 22 points. The least squares errors given in Table 5-4 are around the order of 10^{-1}, which is higher than that of the s-plane analysis. This does not mean that the accuracy of curve fitting by the frequency response analysis is poorer than that of the s-plane analysis. The comparison can become meaningful only if we return to the time domain. In general, results of the curve fitting by the frequency response analysis shows the least bypassing (1-β) but the highest degree of mixing as compared to those by the other two methods. The mean values of (1-β) and p for the frequency response analysis are given in Table 5-5 as

$$\mu_{1-\beta} = 1 - \mu_\beta = 1 - 0.97 = 0.03 = 3\% \quad ,$$

$$\mu_p = 1.16 \quad .$$

Comparison.

1. The mean (μ), variance (σ^2) and standard deviation (σ) of the fitted parameters given by each method as shown in Table 5-5 reveals that

$$(\mu_\beta)_m = 0.82 < (\mu_\beta)_s = 0.91 < (\mu_\beta)_f = 0.97$$

$$(\sigma^2_\beta)_m = 0.0079 > (\sigma^2_\beta)_s = 0.0077 > (\sigma^2_\beta)_f = 0.0032$$

$$(\sigma_\beta)_m = 0.0807 > (\sigma_\beta)_s = 0.0875 > (\sigma_\beta)_f = 0.0936$$

$$(\mu_p)_m = 2.02 > (\mu_p)_s = 1.30 > (\mu_p)_f = 1.16$$

$$(\sigma_p^2)_m = 0.478 > (\sigma_p^2)_s = 0.128 > (\sigma_p^2)_f = 0.050$$

$$(\sigma_p)_m = 0.692 > (\sigma_p)_s = 0.357 > (\sigma_p)_f = 0.225 \quad ,$$

where the subscripts m, s and f refer respectively to the moments method, s-plane and frequency response analyses. The above statistical data implies that using the moments method of analysis leads to the highest degree of bypassing but the lowest degree of mixing, while using the frequency response analysis shows the least bypassing and the highest degree of mixing. For example, the parameters determined by three methods for run 31 are

$$\beta_m = 0.81 < \beta_s = 0.85 < \beta_f = 0.87$$

$$p_m = 1.52 > p_s = 1.32 > p_f = 1.23 \quad ,$$

where the subscripts m, s and f have the same meanings as described previously.

2. The computational times involved are roughly in the ratio of

$$t_m : t_s : t_f = 1 : 3 : 10$$

where the subscripts m, s and f have the same meanings as described above.

Conclusion.

1. The data given in Tables 5-2 through 5-5 demonstrate the reliability of the experimental work, the model selected and the data processing procedure.

2. For each method of the corresponding replicate runs, values

of the parameters fitted by any method differ a certain degree from each of the first runs. This could be attributed partly to random experimental error or the inherent error in the data processing (5). Another reason might be fluctuation of the flow pattern (a stationary process can not be assumed).

3. Values of β greater than unity appear in the results of the three methods of response data analyses, which implies the occurrence of recycle in the experimental system. This may mean that oscillation phenomenon was caused in some of the experimental runs. Nevertheless, the model (GDMMB) can take this effect into consideration.

4. The moments method requires the least amount of computational time. Yet it may give rise to serious error of fitting if higher moments are used. The s-plane analysis gives a satisfactory fitting with respect to computational time and reliability. The disadvantage is that the fit obtained does not guarantee the best in the least squares sense in the time domain. The frequency response analysis needs a much greater computational time than the other two methods. The advantage is that the fit based in the frequency domain also leads to the best in the least squares sense in the time domain.

5. The computed parameters, p and β, and the computational time associated with the s-plane analysis lie between the values given by the other two methods. The s-plane analysis may be recommended as the best way of data processing with respect to rapidity, reliability and simplicity for this work (procuring knowledge of the flow pattern in liquid mixing on distillation trays).

ACKNOWLEDGMENTS

The author wishes to express his sincere gratitude to:

Dr. Liang-tseng Fan, his adviser, for his interest and helpful suggestions on this work, his patience and constant help in correcting the manuscript;

Dr. J.L. Johnson, for his suggestions and help on this work;

the Computing Center of Kansas State University whose staff always found time to be of assistance;

the National Science Foundation for its financial support under NSF Grant GK67.

NOTATION

Independent Variables.

t	Time
θ	Dimensionless time
s	Laplace variable
ω	Frequency variable
i, j, k, m, n	Dummy variable

Functions.

$C_i(t)$, $C_e(t)$	Tracer concentrations in the inlet and exit streams respectively
$C(\theta)$	C-curve, impulse response
$\delta(t)$, $\delta(\theta)$	Delta functions in the real time domain and dimensionless time domain respectively
$E(t)$, $E(\theta)$	Dimensional and dimensionless exit age distributions
$E(s)$	Laplace transform of $E(\theta)$
$f(t)$	Probability density function of the gamma distribution model in the real time domain
$F(\theta)$	F-curve, step response
$H(s)$	Transfer function in the Laplace s-domain
$H_o(s)$	Observed transfer function from the experimental data
$H_p(s)$	Predicted transfer function from the model
$H(j\omega)$	Transfer function in the frequency ω-domain
$H_o(j\omega)$	Observed transfer function
$H_p(j\omega)$	Predicted transfer function
$R(\omega)$, $I(\omega)$	Real and Imaginary parts of $H(j\omega)$

$R_o(\omega)$, $I_o(\omega)$	Observed real and imaginary parts of $H_o(j\omega)$
$R_p(\omega)$, $I_p(\omega)$	Predicted real and imaginary parts of $H_p(j\omega)$
$R_i(t)$, $R_o(t)$	The inlet and exit recordings of the concentration signals
$S(\omega)_n$	Normalized frequency content
$U(\theta)$	Step function
$X(t)$, $Y(t)$	Probability density functions of the inlet and exit pulses in the real time domain
$X(\theta)$, $Y(\theta)$	Probability density functions of the inlet and exit pulses in the dimensionless time domain
$\overline{X}(\theta)_n$, $\overline{Y}(\theta)_n$	Staircase approximations for $X(\theta)$ and $Y(\theta)$
$X(s)$, $Y(s)$	Lapalce transforms of $X(\theta)$ and $Y(\theta)$
$Y_c(t)$, $Y_c(\theta)$	Adjusted data for $Y(t)$ and $Y(\theta)$
φ	Error function
$\Gamma(p)$	Gamma function

Model Variables.

ν	A parameter of the gamma distribution
D	Dimensional dead time
τ	Dimensionless dead time, fraction of plug flow section
p	Order of the transfer function of the model
β	Fraction of the flow into the gamma-mixing section

Other Symbols.

$\langle C \rangle$	Average concentration of the tracer if it were uniformly distributed throughout the system
A_c	Area under the concentration distribution
M	Amount of the tracer

V	Fluid volume contained in the system
Q	Steady flow rate
$\bar{t}$, μ_t	Mean residence time
K_i, K_e	Proportionality factors in the inlet and exit concentration recordings
m_{txk}, m_{tyk}	The kth moments of $X(t)$ and $Y(t)$
$m_{\theta xk}$, $m_{\theta yk}$	The kth moments of $X(\theta)$ and $Y(\theta)$
μ_{tx}, μ_{ty}	The means or the first moments of $X(t)$ and $Y(t)$
σ^2_{tx}, σ^2_{ty}	The variances of $X(t)$ and $Y(t)$
σ^3_{tx}, σ^3_{ty}	The skewnesses of $X(t)$ and $Y(t)$
$\Delta\mu_{tyx}$	Difference between the means of $Y(t)$ and $X(t)$
$\Delta\sigma^2_{tyx}$	Difference between the variances of $Y(t)$ and $X(t)$
$\Delta\sigma^3_{tyx}$	Difference between the skewnesses of $Y(t)$ and $X(t)$
$\mu_{\theta x}$, $\mu_{\theta y}$	The means or the first moments of $X(\theta)$ and $Y(\theta)$
$\sigma^2_{\theta x}$, $\sigma^2_{\theta y}$	The variances of $X(\theta)$ and $Y(\theta)$
$\sigma^3_{\theta x}$, $\sigma^3_{\theta y}$	The skewnesses of $X(\theta)$ and $Y(\theta)$
$\Delta\mu_{\theta yx}$	Difference between the means of $Y(\theta)$ and $X(\theta)$
$\Delta\sigma^2_{\theta yx}$	Difference between the variances of $Y(\theta)$ and $X(\theta)$
$\Delta\sigma^3_{\theta yx}$	Difference between the skewnesses of $Y(\theta)$ and $X(\theta)$
P, Q	Correction factors
M, N, J	Some constants
μ_β, σ^2_β, σ_β	Mean, variance and standard deviation of the distribution of β in each method of response data analysis

μ_p, σ_p^2, σ_p	Mean, variance and standard deviation of the distribution of p in each method of response data analysis

Subscripts.

k	kth
t	Real time domain
θ	Dimensionless time domain
Γ	Gamma-mixing property
p	Plug flow property, predicted property
o	Observed property
T	Total property
m	By moments method of analysis
s	By s-plane analysis
f	By frequency response analysis
x	Inlet property
y	Exit property

LITERATURE CITED

1. Danckwerts, P.V., Chem. Eng. Sci., 1, 1 (1953).

2. Zwietering, Th.N., Chem. Eng. Sci., 11, 1 (1959).

3. Bischoff, K.B. and McCracken, E.A., I&EC, 58, 7 (1966).

4. Hyman, D. and Corson, W.B., CEP, 61, 6 (1965).

5. Johnson, J.L., Ph.D. Dissertation, Kansas State University (1966).

6. Cha, L.C., Ph.D. Dissertation, Kansas State University (1965).

7. Hougen, J.O. and Walsh, R.A., CEP Symp. Series, Proc. Dyn. and Control, 36, 57 (1961).

8. Otto, R.E. and Stout, L.E., JR., CEP Symp. Series, Proc. Dyn. and Control, 36, 57 (1961).

9. Williams, J.A., Bulletin SRC 60-C-64-22, Systems Research Center, Case Inst. of Tech. (1967).

10. Kendall, M.G., "The Advanced Theory of Statistics" Vol. I & II, Griffin & Co., London (1947).

11. Churchill, R.V., "Operational Mathematics," McGraw-Hill Book Company, Inc., New York (1958).

12. Stater, V.E., Ph. D. Dissertation, Illi. Inst. of Tech. (1963).

13. Rooze, J.W., Bulletin SRC 20-C-62-6, Systems Research Center, Case, Inst. of Tech. (1962).

14. Aris, R., "Intracellular Transport," Academic Press Inc., New York (1966).

15. Ahn, Y.K., Ph.D. Dissertation, Kansas State University (1966).

16. Huss, C.R., and Donegan, J.J., NACA Tech. Note 3598 (1956).

17. Schnelle, K.B. and Clements, W.C., Jr., "Pulse Testing for Dynamic Analysis," Vanderbilt University (1963).

18. Newton, G.C., Jr., Gould, L.A. and Kaiser, J.F., "Analytical Design of Linear Feedback Controls," John Wiley and Sons, Inc., New York (1961).

19. Levenspiel, O. and Bischoff, K.B., "Advances in Chemical Engineering," Vol. 4 (1963).

20. Law, V.J. and Bailoy, R.V., Chem. Eng. Sci., 18, 189 (1963).

21. Fine, F.A. and Bankoff, S.G., I&EC, May (1967).

22. Nakanishi, K., "Chemical Engineering Study of the Fluid Mixing in the Reactors," Japan (1967).

23. van der Laan, E.T., Chem. Eng. Sci., 7, 187 (1958).

24. Coughanowr, D.R. and Koppel, L.B., "Process Systems Analysis and Control," McGraw-Hill Book Company, Inc., New York (1965).

25. Shinsky, F.G., "Process Control Systems," McGraw-Hill Book Company, Inc., New York (1967).

26. Roemer, M.H. and Durbin, L.D., I&EC Fundamentals, 6, 1 (1967).

27. Adler, R.J., "Finite Stage Modeling," 4th National Chem. & Petro. Symp. of the Inst. Soc. of America, April 9-10 (1962).

28. Hays, J.R., Clements, W.C., Jr. and Harris, T.R., A.I.Ch.E. Journal, March (1967).

29. Johnson, N.L. and Leone, F.C., "Statistics and Experimental Design" Vol. 1, John Wiley & Sons, Inc., New York (1964).

30. Fan, L.T., "The Continuous Maximum Principle," John Wiley & Sons, Inc., New York (1966).

APPENDICES

COMPUTER PROGRAMS

(IBM 1410)

TABLE A-1 FORTRAN PROGRAM FOR COMPUTING IMPULSE RESPONSE OF GDMWB.

```
C       IMPULSE RESPONSE OF GAMMA MIXER WITH BYPASSING  BY Y S WU
      1 FORMAT(I3)
      2 FORMAT(3F6.2)
      3 FORMAT(5H1TAU=,F4.2,5X,2HB=,F5.2,5X,2HP=,F6.2)
      4 FORMAT(14HL  Z       Y(Z))
      5 FORMAT(F6.2,F8.3)
        READ(1,1)L
        DO 100 M=1,L
        READ(1,2)T,B,P
        WRITE(3,3)T,B,P
        FP=1.
        NP=P
        DO 10 J=1,NP
        FJ=J
     10 FP=FP*FJ
        C=(B*P)**(P+1.)/(1.-T)**P/FP
        A=P*B/(1.-T)
        Z=T
        WRITE(3,4)
        DO 20 I=1,30
        ZT=Z-T
        Y=C*ZT**(P-1.)*EXP(-A*ZT)
        WRITE(3,5)Z,Y
     20 Z=Z+0.1
    100 CONTINUE
        STOP
        END
```

TABLE A-1-1. LIST OF IMPORTANT PROGRAM VARIABLES OF TABLE A-1.

Computer Designation.	Comments.
L	Number of runs to be processed
T	τ
B	β
P	p
FP	$p!$
C	$\frac{(\beta p)^{p+1}}{(1-\tau)^{p}\ p!}$
A	$\frac{\beta p}{1-\tau}$
Z	θ
ZT	$\theta - \tau$
Y	$Y(\theta)$, $E(\theta)$

TABLE A-2 FORTRAN PROGRAM FOR COMPUTING STEP RESPONSE OF GDMWB.

```
C       STEP RESPONSE OF GDMWB BY NUMERICAL INTEGRATION
        DIMENSION F(30)
    1   FORMAT(I3)
    2   FORMAT(3F6.2)
    3   FORMAT(5H1TAU=,F4.2,5X,2HB=,F5.2,5X,2HP=,F6.2)
    4   FORMAT(14HL  Z       Y(Z))
    5   FORMAT(F6.2,F8.3)
        READ(1,1)L
        DO 100 M=1,L
        READ(1,2)T,B,P
        WRITE(3,3)T,B,P
        A=P*B/(1.-T)
        D=B**(P+1.)*P**P/(1.-T)**P
        B1=1.-B
        Z=T
        NP=P-1.
        DZ=0.1
        FP=1.
        F(1)=0.
        Y=B1
        IF(NP)15,15,9
    9   DO 10 I=1,NP
        FI=I
   10   FP=FP*FI
   15   C=D*DZ/FP
        WRITE(3,4)
        DO 20 J=2,26
        ZT=Z-T
        IF(NP)18,18,16
   16   F(J)=ZT**(P-1.)*EXP(-A*ZT)
        AF=.5*(F(J)+F(J-1))
        Y=Y+AF*C
        GO TO 19
   18   Y=D*(1./A-1./A*EXP(-A*ZT))+B1
   19   WRITE(3,5)Z,Y
   20   Z=Z+0.1
  100   CONTINUE
        STOP
        END
```

TABLE A-2-1. LIST OF IMPORTANT PROGRAM VARIABLES OF TABLE A-2.

Computer Designation.	Comments.
L, T, B, P, A, Z, ZT	See TABLE A-1-1.
D	$\frac{\beta^{p+1}\ {}_{p}p}{(1-\tau)^{p}}$
B1	$1 - \beta$
FP	$(p - 1)!$
Y	$Y(\theta)$, $F(\theta)$

TABLE A-3 FORTRAN PROGRAM FOR COMPUTING FREQUENCY RESPONSE OF GDMWB.

```
C       FREQUENCY RESPONSE FOR GAMMA MIXER WITH BYPASSING
        DIMENSIONW(22)
    1   FORMAT(2I3)
    2   FORMAT(3F6.2)
    3   FORMAT(6F7.3)
    4   FORMAT(5H1TAU=,F4.2,5X,2HB=,F5.2,5X,2HP=,F6.2)
    8   FORMAT(14HL     DIML FREQ,5X,9HMAG RATIO,5X,4HREAL,10X,9HIMAGINARY,
       15X,9HANGLE RAD,5X,9HANGLE DEG)
    9   FORMAT(6E14.6)
        READ(1,1)K,L
        READ(1,3)(W(I),I=1,K)
        DO10I=1,K
   10   W(I)=W(I)*10.
        DO 20J=1,L
        READ(1,2)T,B,P
        WRITE(3,4)T,B,P
        WRITE(3,8)
        DO30I=1,K
        H=(1.-T)*W(I)/P/B
        Z=ATAN(-H)
        Y=1.+H*H
        X=Y**(-.5*P)
        U=COS(P*Z-T*W(I))
        V=SIN(P*Z-T*W(I))
        PR=B*X*U+(1.-P)*COS(T*W(I))
        PI=B*X*V-(1.-P)*SIN(T*W(I))
        AM=(PR*PR+PI*PI)**.5
        ZR=ATAN(PI/PR)
        ZD=57.296*ZR
   30   WRITE(3,9)W(I),AM,PR,PI,ZR,ZD
   20   CONTINUE
        STOP
        END
```

TABLE A-3-1. LIST OF IMPORTANT PROGRAM VARIABLES OF TABLE A-3.

Computer Designation.	Comments.
L, T, B, P	See TABLE A-1-1
K	Number of frequencies to be used
W(I)	ith value of the frequency, ω_i, read in rad./sec. but transformed to rad./unit dimensionless time
PR	Real part of $H(j\omega)$ in equation (3-26)
PI	Imaginary part of $H(j\omega)$ in equation (3-26)
AM	Amplitude ratio, given by equation (3-27)
ZR	Phase angle in radians, given by equation (3-28)
ZD	Phase angle in degrees

TABLE A-4 FORTRAN PROGRAM FOR COMPUTING FIRST, SECOND AND THIRD MOMENTS FROM PULSE TESTING DATA.

```
C      FIRST, SECOND AND THIRD MOMENTS FROM INPUT AND OUTPUT CURVES
C      N=NN-1, M=M-1, WHERE NN AND MM ARE FROM FREQ RESPONSE DATA
C      REVISED OCTOBER 10, 1966
       DIMENSIONX(200),Y(300)
     1 FORMAT(12HL     RUN NO=,I3)
     2 FORMAT(21HK     FIRST Y MOMENT =,F10.4,21H     SECOND Y MOMENT =,F10
      1.4,20H     THIRD Y MOMENT =,F10.4)
     3 FORMAT(21HK     FIRST X MOMENT =,F10.4,21H     SECOND X MOMENT =,F10
      1.4,20H     THIRD X MOMENT =,F10.4)
     4 FORMAT(34HK     DIFFERENCE IN FIRST MOMENTS =,F10.4,30H     DIMENSIO
      1NLESS DIFFERENCE =,F10.4)
     5 FORMAT(35HK     DIFFERENCE IN SECOND MOMENTS =,F10.4,30H     DIMENSI
      1ONLESS DIFFERENCE =,F10.4)
    11 FORMAT(34HK     DIFFERENCE IN THIRD MOMENTS =,F10.4,30H     DIMENSIO
      1NLESS DIFFERENCE =,F10.4)
     6 FORMAT(6F9.2)
     7 FORMAT(I3)
     8 FORMAT(3I3,3F8.3)
     9 FORMAT(3F8.4,F6.4,I3,F8.4)
    10 FORMAT(12HKRES TIME = ,F8.4,11HLIQ RATE = ,F8.4,11HAIR RATE = ,F8.
      14,10HWEIR HT = ,F8.4,11HHOLE DIA = ,F6.4,14HNO OF HOLES = ,I3,9HLI
      2Q HT = ,F8.4)
       READ(1,7)L
       DO100IL=1,L
       READ(1,8)KUN,N,M,DEL1,DEL2,RTIME
       READ(1,9)RATE1,RATE2,WEIR,DIA,HOLES,DEPT
       WRITE(3,1)KUN
       WRITE(3,10)RTIME,RATE1,RATE2,WEIR,DIA,HOLES,DEPT
```

TABLE A-4 (CONT.)

```
      READ(1,6)(Y(I),I=1,N)
      READ(1,6)(X(J),J=1,M)
      SUMY1=0.0
      SUMY2=0.0
      SUMY3=0.0
      SUMY4=0.0
      SUMX1=0.0
      SUMX2=0.0
      SUMX3=0.0
      SUMX4=0.0
      NN=N-1
      DO 50 I=1,NN
      SI=I-1
      TIME=DEL1*SI
      A=TIME*Y(I)
      B=TIME*A
      R=TIME*B
      SUMY1=SUMY1+A
      SUMY2=SUMY2+B
      SUMY4=SUMY4+R
   50 SUMY3=SUMY3+Y(I)
      CONTINUE
      C=SUMY1/SUMY3
      D=(SUMY2/SUMY3)-C**2.0
      S=(SUMY4/SUMY3)-3.0*C*D-C**3.0
      MM=M-1
      DO 60 J=1,MM
```

TABLE A-4 (CONCL.)

```
      RJ=J-1
      TIME=DEL2*RJ
      E=TIME*X(J)
      F=TIME*E
      T=TIME*F
      SUMX1=SUMX1+E
      SUMX2=SUMX2+F
      SUMX4=SUMX4+T
   60 SUMX3=SUMX3+X(J)
      CONTINUE
      G=SUMX1/SUMX3
      H=(SUMX2/SUMX3)-G**2.0
      U=(SUMX4/SUMX3)-3.0*G*H-G**3.0
      DELM=C-G
      DELMD=DELM/RTIME
      DELV=D-H
      DELVD=DELV/(RTIME*RTIME)
      DELS=S-U
      DELSD=DELS/(RTIME**3.0)
      WRITE(3,2)C,D,S
      WRITE(3,3)G,H,U
      WRITE(3,4)DELM,DELMD
      WRITE(3,5)DELV,DELVD
      WRITE(3,11)DELS,DELSD
  100 CONTINUE
      STOP
      END
```

TABLE A-4-1. LIST OF IMPORTANT PROGRAM VARIABLES OF TABLE A-4.

Computer Designation.	Comments.
L	Number of runs to be processed
KUN	Run number
N	Number of values of the output pulse, Y(t)
M	Number of values of the input pulse, X(t)
DEL1	Time increment used to read Y(t)
DEL2	Time increment used to read X(t)
RTIME	The mean residence time
RATE1	Liquid flow rate
RATE2	Vapor flow rate
WEIR	Weir height
DIA	Hole diameter
HOLES	Number of holes on tray
DEPT	Measured liquid depth
Y(I)	ith value of output pulse, Y(t)
X(I)	ith value of input pulse, X(t)
TIME	Time, t, sec.
SUMY1	$\Sigma tY(t)$
SUMY2	$\Sigma t^2Y(t)$
SUMY4	$\Sigma t^3Y(t)$
SUMY3	$\Sigma Y(t)$
C	Mean of Y(t), μ_{ty}
D	Variance of Y(t), σ^2_{ty}
S	Skewness of Y(t), σ^3_{ty}

TABLE A-4-1. (CONT.)

Computer Designation.	Comments.
SUMX1	$\Sigma tX(t)$
SUMX2	$\Sigma t^2X(t)$
SUMX4	$\Sigma t^3X(t)$
SUMX3	$\Sigma X(t)$
G	Mean of $X(t)$, μ_{tx}
H	Variance of $X(t)$, σ^2_{tx}
U	Skewness of $X(t)$, σ^3_{tx}
DELM	$\mu_{ty} - \mu_{tx}$
DELMD	$\Delta\mu_{\theta yx}$
DELV	$\sigma^2_{ty} - \sigma^2_{tx}$
DELVD	$\Delta\sigma^2_{\theta yx}$
DELS	$\sigma^3_{ty} - \sigma^3_{tx}$
DELSD	$\Delta\sigma^3_{\theta yx}$

TABLE A-5 FORTRAN PROGRAM FOR FITTING B AND P OF GDMWB BY MOMENT METHOD ANALYSIS.

```
C      FITTING B,P OF GAMMA MIXER WITH BY PASSING BY MOMENT METHOD
     1 FORMAT(I3)
     2 FORMAT(I3,F5.3,2F6.4,2F5.2)
     3 FORMAT(12H1RUN NUMBER ,I3)
     4 FORMAT(10HL TRIAL NO,10X,1HB,10X,1HP,10X,3HTAU,10X,4HTEST)
     5 FORMAT(1HL,6X,I3,4X,F7.3,4X,F7.3,6X,F7.3,4X,E10.4)
       READ(1,1)L
       DO40I=1,L
       READ(1,2)KUN,T,DV,DS,B,P
       WRITE(3,3)KUN
       WRITE(3,4)
       K=1
    10 F=(1.-T)**2.*(-1.+(P+1.)/(P*B))-DV
       G=(1.-T)**3.*(2.-3.*(P+1.)/(P*B)+(P+2.)*(P+1.)/(P*P*B*B))-DS
       FP=-(1.-T)**2./(B*P*P)
       FB=-(1.-T)**2.*(P+1.)/(P*B*B)
       GP=(1.-T)**3.*(3.*P*(B-1.)-4.)/(B*B*P*P*P)
       GB=(1.-T)**3.*(3.*(P+1.)/(P*B*B)-2.*(P+2.)*(P+1.)/(B*B*B*P*P))
       D=FP*GB-FB*GP
       DP=(G*FB-F*GB)/D
       DB=(F*GP-G*FP)/D
       TEST=ABS(DB/B)+ABS(DP/P)
       WRITE(3,5)K,B,P,T,TEST
       IF(K-3)20,20,30
    20 DB=DB/4.
       DP=DP/4.
    30 B=B+DB
       P=P+DP
       K=K+1
       IF(TEST-0.0001)40,40,10
    40 CONTINUE
       STOP
       END
```

TABLE A-5-1. LIST OF IMPORTANT PROGRAM VARIABLES OF TABLE A-5.

Computer Designation.	Comments.
L, KUN	See TABLE A-4-1
T, B, P	See TABLE A-1-1
DV	$\Delta\sigma^2_{\theta yx}$
DS	$\Delta\sigma^3_{\theta yx}$
DP	Δp
DB	$\Delta\beta$
F	$F(p,\beta)$
G	$G(p,\beta)$
FP	$\frac{\partial F}{\partial p}$
FB	$\frac{\partial F}{\partial \beta}$
GP	$\frac{\partial G}{\partial p}$
GB	$\frac{\partial G}{\partial \beta}$
D	$\frac{\partial F}{\partial p}\frac{\partial G}{\partial \beta} - \frac{\partial F}{\partial \beta}\frac{\partial G}{\partial p}$

TABLE A-6 FORTRAN PROGRAM FOR COMPUTING FREQUENCY RESPONSE FROM PULSE TESTING DATA (PARABOLIC APPROXIMATION).

```
C      FREQUENCY RESPONSE STAIRCASE METHOD NORMALIZED NOVEMBER 25, 1966
       DIMENSION W(30),Y(300),X(100),Y1(300),X1(100)
     1 FORMAT(3I3,3F8.3)
     2 FORMAT(3E13.6)
     3 FORMAT(6F7.3)
     5 FORMAT(12H1     RUN NO=,I3)
     7 FORMAT(14HS     FREQUENCY,7X,9HDIML FREQ,7X,9HMAG RATIO,7X,11HANGLE
      1 RAD  ,5X,11HANGLE DEG  ,5X,4HREAL,12X,9HIMAGINARY,7X,7HCONTENT)
     9 FORMAT(8E16.8)
    11 FORMAT (2I3)
    13 FORMAT(6F9.2)
    15 FORMAT(25H AREA UNDER INPUT CURVE = ,E14.8,25HAREA UNDER OUTPUT CU
      1RVE = ,E14.8)
    17 FORMAT(12H RES TIME = ,F8.4,11HLIQ RATE = ,F8.4,11HAIR RATE = ,F8.
      14,10HWEIR HT = ,F8.4,11HHOLE DIA = ,F6.4,14HNO OF HOLES = ,I3,9HLI
      2Q HT = ,F8.4)
    19 FORMAT(3F8.4,F6.4,I3,F8.4)
       READ(1,11)K,L
       READ(1,3)(W(IJ),IJ=1,K)
       DO 160 IL=1,L
       READ(1,1) KUN,NN,MM,DEL1,DEL2,RTIME
       READ(1,19)RATE1,RATE2,WEIR,DIA,HOLES,DEPT
       NN=NN+1
       MM=MM+1
       READ(1,13)(Y1(II),II=2,NN)
       READ(1,13)(X1(JJ),JJ=2,MM)
       WRITE(2,11)KUN,K
       WRITE(3,5)KUN
       WRITE(3,17)RTIME,RATE1,RATE2,WEIR,DIA,HOLES,DEPT
```

TABLE A-6 (CONT.)

```
      SUMY=0.0
      SUMX=0.0
      NNN=NN-2
      DO 200 II=3,NNN
  200 SUMY=SUMY+Y1(II)
      AREAY=DEL1*SUMY
      DO 250 II=3,NNN
  250 Y1(II)=Y1(II)*RTIME/AREAY
      NNL=NN-1
      DO 300 II=3,NNL
      I=II-2
  300 Y(I)=(5.0*Y1(II-1)+8.0*Y1(II)-Y1(II+1))/12.0
      MMM=MM-2
      DO 500 JJ=3,MMM
  500 SUMX=SUMX+X1(JJ)
      AREAX=DEL2*SUMX
      DO 550 JJ=3,MMM
  550 X1(JJ)=X1(JJ)*RTIME/AREAX
      MML=MM-1
      DO 600 JJ=3,MML
      J=JJ-2
  600 X(J)=(5.0*X1(JJ-1)+8.0*X1(JJ)-X1(JJ+1))/12.0
      N=NN-3
      M=MM-3
      WRITE(3,15)AREAX,AREAY
      WRITE(3,7)
      DO 140 IJ=1,K
      A=0.0
      B=0.0
      C=0.0
      D=0.0
```

TABLE A-6 (CONCL.)

```
      W1=2./W(IJ)
      W2=W(IJ)/2.
      W3=RTIME*W(IJ)
      DO 20 I=1,N
      SI=I
      A1=Y(I)*W1*SIN(DEL1*W2)*COS((2.*SI-1.)*DEL1*W2)
      A=A+A1
      B1=+1.*Y(I)*W1*SIN(DEL1*W2)*SIN((2.*SI-1.)*DEL1*W2)
   20 B=B+B1
      DO 30 J=1,M
      SJ=J
      C1=X(J)*W1*SIN(DEL2*W2)*COS((2.*SJ-1.)*DEL2*W2)
      C=C+C1
      D1=+1.*X(J)*W1*SIN(DEL2*W2)*SIN((2.*SJ-1.)*DEL2*W2)
   30 D=D+D1
      DENOM=C*C+D*D.
      UR=A*C+B*D
      UI=A*D-B*C
      PFR=UR/DENOM
      PFI=UI/DENOM
      RATIO=(PFR*PFR+PFI*PFI)**.5
      ANGL1=ATAN(UI/UR)
      ANGL2=57.296*ANGL1
      CONT=DENOM**.5
      WRITE(2,2)W3,PFR,PFI
  140 WRITE(3,9)W(IJ),W3,RATIO,ANGL1,ANGL2,PFR,PFI,CONT
  160 CONTINUE
      STOP
      END
```

TABLE A-6-1. LIST OF IMPORTANT PROGRAM VARIABLES OF TABLE A-6.

Computer Designation.	Comments.
L, K	See TABLE A-3-1
W(IJ)	ijth value of the frequency, ω_{ij}, rad./sec.
KUN	Run number
NN	Number of values of Y(t) plus one
MM	Number of values of X(t) plus one
DEL1, DEL2, RTIME, RATE1, RATE2, WEIR, DIA, HOLES, DEPT	See TABLE A-4-1
Y1(II)	iith value of output pulse, Y(t)
X1(JJ)	jjth value of input pulse, X(t)
AREAY	Area under Y(t)
Y(I)	ith value of the staircase approximation to Y(t)
AREAX	Area under X(t)
X(J)	jth value of the staircase approximation to X(t)
A, B, C, D	A, B, C, D given in equation (4-50)
W3	Frequency, rad./unit dimensionless time
PFR	Real part of $H_o(j\omega)$, given by equation (4-52)
PFI	Imaginary part of $H_o(j\omega)$, given by equation (4-53)
RATIO	Amplitude ratio, given by equation (4-54)
ANGL1	Phase angle in rad., given by equation (4-55)
ANGL2	Phase angle in degrees
CONT	Frequency content of the input pulse, not normalized, $\sqrt{C^2 + D^2}\,\Big|_{\omega=\omega}$

TABLE A-7 FORTRAN PROGRAM FOR FITTING B AND P OF GDMWB BY FREQUENCY RESPONSE ANAYSIS.

```
C       FITTING B, P OF GAMMA MIXER WITH BY PASSING BY FREQ. RES. METHOD
        DIMENSIONW(22),CR(22),CI(22),FR(22),FI(22),AM(22),ZR(22),ZD(22)
      1 FORMAT(I3)
      2 FORMAT(2I3)
      3 FORMAT(F5.3,2F5.2)
      4 FORMAT(12H1RUN NUMBER ,I3)
      5 FORMAT(3E13.6)
      6 FORMAT(10HL TRIAL NO,10X,1HB,10X,1HP,10X,3HTAU,10X,4HTEST,10X,12HS
       1QUARE ERROR)
      7 FORMAT(1HL,6X,I3,4X,F7.3,4X,F7.3,6X,F7.3,4X,E10.4,12X,E10.4)
      8 FORMAT(14HL    DIML FREQ,5X,9HMAG RATIO,5X,4HREAL,10X,9HIMAGINARY,
       15X,9HANGLE RAD,5X,9HANGLE DEG)
      9 FORMAT(6E14.6)
     10 FORMAT(19HLNO OF FREQ FITTED=,I3)
        READ(1,1)L
        DO100J=1,L
        READ(1,2)KUN,N
        READ(1,3)T,B,P
        WRITE(3,4)KUN
        READ(1,5)(W(I),CR(I),CI(I),I=1,N)
        K=1
        WRITE(3,10)N
        WRITE(3,6)
     20 SE=0.
        SF=0.
        SG=0.
        SFB=0.
        SFP=0.
        SGB=0.
        SGP=0.
```

TABLE A-7 (CONT.)

```
      DO80I=1,N
      H=(1.-T)*W(I)/P/B
      Z=ATAN(-H)
      Y=1.+H*H
      X=Y**(-.5*P)
      U=COS(P*Z-T*W(I))
      V=SIN(P*Z-T*W(I))
      PR=B*X*U+(1.-B)*COS(T*W(I))
      PI=B*X*V-(1.-B)*SIN(T*W(I))
      FR(I)=PR
      FI(I)=PI
      AM(I)=(PR*PR+PI*PI)**.5
      ZR(I)=ATAN(PI/PR)
      ZD(I)=57.296*ZR(I)
      HB=-H/B
      HP=-H/P
      YB=2.*H*HB
      YP=2.*H*HP
      ZB=-HB/Y
      ZP=-HP/Y
      Z2B2=(Y*B*HB-H*(B*YB+Y))/Y/Y/B/B
      Z2BP=(Y*HP-H*YP)/B/Y/Y
      Z2P2=(Y*P*HP-H*(P*YP+Y))/Y/Y/P/P
      XB=P*H*H*X/B/Y
      XP=H*H*X/Y-.5*X*ALOG(Y)
      UB=-V*P*ZB
      UP=-V*(Z+P*ZP)
      VB=U*P*ZB
      VP=U*(Z+P*ZP)
      X2B2=P*((2.*H*X*HB+H*H*XB)*B*Y-H*H*X*(Y+B*YB))/B/B/Y/Y
      X2BP=(Y*(H*H*X+2.*P*H*X*HP+P*H*H*XP)-P*H*H*X*YP)/B/Y/Y
```

TABLE A-7 (CONT.)

```
X2P2=(Y*(2.*H*X*HP+H*H*XP)-H*H*X*YP)/Y/Y-.5*(XP*ALOG(Y)+X*YP/Y)
U2B2=-P*(ZB*VB+V*Z2B2)
U2BP=-(P*VP*ZB+V*ZB+P*V*Z2BP)
U2P2=-VP*(Z+P*ZP)-V*(2.*ZP+P*Z2P2)
V2B2=P*(UB*ZB+U*Z2B2)
V2BP=P*UP*ZB+U*ZB+P*U*Z2BP
V2P2=UP*(Z+P*ZP)+U*(2.*ZP+P*Z2P2)
PRB=X*U+B*U*XB+B*X*UB-COS(T*W(I))
PRP=B*(U*XP+X*UP)
PIB=X*V+B*V*XB+B*X*VB+SIN(T*W(I))
PIP=B*(V*XP+X*VP)
PRB2=2.*(U*XB+X*UB+B*UB*XB)+B*U*X2B2+B*X*U2B2
PRBP=U*XP+X*UP+B*(UP*XB+U*X2BP)+B*(XP*UB+X*U2BP)
PRP2=B*(2.*UP*XP+U*X2P2+X*U2P2)
PIB2=2.*(V*XB+X*VB+B*VB*XB)+B*(V*X2B2+X*V2B2)
PIBP=V*XP+X*VP+B*(VP*XB+V*X2BP+XP*VB+X*V2BP)
PIP2=B*(2.*VP*XP+V*X2P2+X*V2P2)
DRPC=PR-CR(I)
DIPC=PI-CI(I)
F=DRPC*PRB+DIPC*PIB
G=DRPC*PRP+DIPC*PIP
FB=PRB*PRB+DRPC*PRB2+PIB*PIB+DIPC*PIB2
FP=PRP*PRB+DRPC*PRBP+PIP*PIB+DIPC*PIBP
GB=PRB*PRP+DRPC*PRBP+PIB*PIP+DIPC*PIBP
GP=PRP*PRP+DRPC*PRP2+PIP*PIP+DIPC*PIP2
SE=SE+DRPC*DRPC+DIPC*DIPC
SF=SF+F
SG=SG+G
```

TABLE A-7 (CONCL.)

```
      SFB=SFB+FB
      SFP=SFP+FP
      SGB=SGB+GB
      SGP=SGP+GP
   80 CONTINUE
      D=SFP*SGB-SFB*SGP
      DB=(SF*SGP-SG*SFP)/D
      DP=(SG*SFB-SF*SGB)/D
      TEST=ABS(DB/B)+ABS(DP/P)
      WRITE(3,7)K,B,P,T,TEST,SE
      IF(K-5)40,40,50
   40 DB=DB/5.
      DP=DP/5.
   50 B=B+DB
      P=P+DP
      K=K+1
      IF(TEST-0.0001)200,200,20
  200 WRITE(3,8)
      WRITE(3,9)(W(I),AM(I),FR(I),FI(I),ZR(I),ZD(I),I=1,N)
  100 CONTINUE
      STOP
      END
```

TABLE A-7-1. LIST OF IMPORTANT PROGRAM VARIABLES OF TABLE A-7.

Computer Designation.	Comments.
L, KUN	See TABLE A-6-1
N	Number of frequencies to be fitted
T, B, P	See TABLE A-1-1
W(I)	ith value of frequency, rad./unit dimensionless time
OR(I)	Observed real part of $H_o(j\omega)$
OI(I)	Observed imaginary part of $H_o(j\omega)$
DP, DB	Δp, $\Delta\beta$, given by equations (4-75), (4-76)
H, Y, X, Z, U, V	See Chapter 4, page 76
PR	R_p
PI	I_p
HB	$\frac{\partial H}{\partial \beta}$
HP	$\frac{\partial H}{\partial p}$
YB	$\frac{\partial Y}{\partial \beta}$
YP	$\frac{\partial Y}{\partial p}$
ZB	$\frac{\partial Z}{\partial \beta}$
ZP	$\frac{\partial Z}{\partial p}$
Z2B2	$\frac{\partial^2 Z}{\partial \beta^2}$
Z2BP	$\frac{\partial^2 Z}{\partial \beta \partial p}$
Z2P2	$\frac{\partial^2 Z}{\partial p^2}$

TABLE A-7-1. (CONT.)

Computer Designation.	Comments.
XB	$\frac{\partial X}{\partial \beta}$
XP	$\frac{\partial X}{\partial p}$
UB	$\frac{\partial U}{\partial \beta}$
UP	$\frac{\partial U}{\partial p}$
VB	$\frac{\partial V}{\partial \beta}$
VP	$\frac{\partial V}{\partial p}$
X2B2	$\frac{\partial^2 X}{\partial \beta^2}$
X2BP	$\frac{\partial^2 X}{\partial \beta \partial p}$
X2P2	$\frac{\partial^2 X}{\partial p^2}$
U2B2	$\frac{\partial^2 U}{\partial \beta^2}$
U2BP	$\frac{\partial^2 U}{\partial \beta \partial p}$
U2P2	$\frac{\partial^2 U}{\partial p^2}$
V2B2	$\frac{\partial^2 V}{\partial \beta^2}$
V2BP	$\frac{\partial^2 V}{\partial \beta \partial p}$
V2P2	$\frac{\partial^2 V}{\partial p^2}$

TABLE A-7-1. (CONT.)

Computer Designation.	Comments.
PRB	$\frac{\partial R_p}{\partial \beta}$
PRP	$\frac{\partial R_p}{\partial p}$
PIB	$\frac{\partial I_p}{\partial \beta}$
PIP	$\frac{\partial I_p}{\partial p}$
PRB2	$\frac{\partial^2 R_p}{\partial \beta^2}$
PRBP	$\frac{\partial^2 R_p}{\partial \beta \partial p}$
PRP2	$\frac{\partial^2 R_p}{\partial p^2}$
PIB2	$\frac{\partial^2 I_p}{\partial \beta^2}$
PIBP	$\frac{\partial^2 I_p}{\partial \beta \partial p}$
PIP2	$\frac{\partial^2 I_p}{\partial p^2}$
DRPO	$R_p - R_o$
DIPO	$I_p - I_o$
F	F_i
G	G_i
SE	$\Sigma \left[(R_p - R_o)^2 + (I_p - I_o)^2 \right]$
SF	ΣF_i
SG	ΣG_i

TABLE A-7-1. (CONCL.)

Computer Designation.	Comments.
FB	$\frac{\partial F_i}{\partial \beta}$
FP	$\frac{\partial F_i}{\partial p}$
GB	$\frac{\partial G_i}{\partial \beta}$
GP	$\frac{\partial G_i}{\partial p}$
SFB	$\Sigma\frac{\partial F_i}{\partial \beta}$
SFP	$\Sigma\frac{\partial F_i}{\partial p}$
SGB	$\Sigma\frac{\partial G_i}{\partial \beta}$
SGP	$\Sigma\frac{\partial G_i}{\partial p}$
D	$\Sigma\frac{\partial F_i}{\partial p}\ \Sigma\frac{\partial G_i}{\partial \beta} - \Sigma\frac{\partial F_i}{\partial \beta}\Sigma\frac{\partial G_i}{\partial p}$
TEST	$\left\lvert\frac{\Delta\beta}{\beta}\right\rvert + \left\lvert\frac{\Delta p}{p}\right\rvert$
K	Number of iterations

MODEL FITTING AND METHODS OF RESPONSE DATA ANALYSIS FOR LIQUID MIXING ON DISTILLATION TRAYS

by

YIE-SHON WU

B.S., NATIONAL TAIWAN UNIVERSITY, TAIWAN, CHINA, 1963

AN ABSTRACT OF A MASTER'S THESIS

submitted in partial fulfillment of the
requirements for the degree

MASTER OF SCIENCE

DEPARTMENT OF CHEMICAL ENGINEERING

KANSAS STATE UNIVERSITY

Manhattan, Kansas

1968

The experimental data previously obtained by Johnson in his investigation of liquid mixing on distillation trays were analyzed by two other methods of response data analysis, i.e. the moments method of analysis and the frequency response analysis. The same gamma distribution model with bypassing (GDMWB) was again fitted. The resulting parameters in the model fitted by these two methods were compared to the results given in the s-plane analysis by Johnson. In conclusion, the purpose is to obtain what appears to be a rapid, reliable and simple procedure for procuring information about a flow pattern of liquid mixing on distillation trays.